

AISC E&R Library



8504

7 November 1995

DRAFT

**Review of Weldability of Proposed Single Grade 50 Steel for
Structural Shapes**

Prepared by B.A. Graville

for

American Institute of Steel Construction

Report P371/1

RR3045

8504

GRAVILLE ASSOCIATES INC.

P.O.Box 225 Georgetown Ontario L7G 4Y5

Tel (905) 873-1739 FAX (905) 873-0466

Review of Weldability of Proposed Single Grade 50 Steel
for Structural Shapes

DRAFT

Date:

1.0 Introduction

**FOR COMMITTEE USE ONLY
NOT FOR PUBLICATION**

1.1 Background

Structural steel shapes for use in building framing have usually been supplied to meet ASTM A36 or A572, A36 having a minimum specified yield strength of 36 ksi while A572 provides for several strength grades. When these specifications were first written most of the steel supplied was from integrated steel mills where the use of scrap was a relatively small percentage. Over the years there has been a significant trend in the manufacture of structural shapes to electric furnace steelmaking using scrap. The result of this has been a shift in the detailed chemical composition of steels within the broad limits provided by A36 and A572. Shapes supplied to these specifications today are likely to contain significant levels of "residuals" such as copper. The presence of these residuals contributes to strength. Because there is no upper yield strength limit in A36, steels supplied to this specification often meet A572 Grade 50 as well. In fact some suppliers offer a single "multigrade" product that meets the requirements of A36, A572 grade 50 and the corresponding Canadian specifications.

In recognition of the type of steel product currently being supplied to the market, the American Institute of Steel Construction (AISC) Inc. and the Structural Shapes Producers Council have developed a Draft specification for a single Grade 50 steel for structural shapes with the intention of having it issued as an ASTM standard specification.

1.2 Scope

As part of the development process for the new specification, the present study was undertaken to examine the implications of the Draft specification on various weldability issues. Since the study addresses the implications of the specification it deals with hypothetical steels that could theoretically be supplied under the Draft specification and does not

make any judgments on the weldability of materials currently being supplied to the marketplace. In addition, it is emphasized that only weldability issues have been addressed, and the implications of the specification on material properties, such as strength, toughness, ability to be hot or cold formed, and so forth, are beyond the scope of the study. Inadequate toughness, for example, may result in cracking during fabrication under the influence of welding stresses, but where the cracks are not directly associated with the weld, such as heat affected zone cracking or lamellar tearing, such behavior is considered a material property problem rather than a weldability issue. Thermal cutting, however, has been addressed because of its close relation with welding.

The Draft specification is intended to apply to rolled shapes which could be provided in a very wide thickness range, e.g., from 1/8 in. for light angles to over 4 in. for the flange of a heavy group 5 W shape. In typical applications structural shapes are not exposed to very low temperatures and the steel is usually supplied without specified impact requirements. In some cases heavy section tension members may require Charpy V notch impact testing and this is provided for in the Draft specification as an added supplementary requirement.

1.3 Joints and Welding Processes

Most of the common welding processes, including Shielded Metal Arc Welding (SMAW), Flux Cored Arc Welding (FCAW) and Submerged Arc (SAW), could be used on the structural shapes. Gas Tungsten Arc (GTAW) is unlikely to be employed, and therefore welds would normally have filler material added with the effect of diluting any contribution from the base metal to the weld. Heat inputs could cover a wide range from those associated with small fillets or small root passes in groove welds to the very high heat inputs associated with electroslag welding.

A range of joint types could be encountered including fillet welds, groove welded butt splices, and T joints such as are encountered in special moment resisting connections. Four typical welds are illustrated in Fig. 1. The single pass fillet weld is characterized by moderate dilution and heat input of about 30-35 kJ/in. for a typical 1/4 in. fillet. Being a single pass weld, there is no additional thermal cycle on the weld or heat affected zone from subsequent passes.

DRAFT
Date:

**FOR COMMITTEE USE ONLY
NOT FOR PUBLICATION**

00583

At the other extreme of heat input is the electroslag weld which has high dilution and is a single pass. It is characterized by a wide heat affected zone covering the complete section thickness and is subject to slow cooling. Because of possible poor toughness in the as-welded condition, electroslag welds may require a post-weld heat treatment or be restricted to members acting only in compression (AWS D1.1).

Typical groove welds are multipass and therefore each pass provides an additional thermal cycle to previous passes. This may result in complex metallurgical changes which affect the weld metal and heat affected zone properties. In the beam flange-to-column connection the weld is made from one side on to a backing bar. This creates a stress concentration and a likely source of crack initiation. In addition, T joints in heavy sections can generate large stresses acting through the thickness of the column flange.

DRAFT

1.4 *Weldability*

The ability of a steel to be welded without causing significant problems is a function not only of the steel itself but other factors such as the welding procedure, the welding consumables, and so forth. Thus it is not possible to establish "weldability" in any absolute sense or to determine whether steels supplied to a given specification would or would not give rise to welding problems. In fact, it is likely that many steels, if supplied to the top end of the chemistry requirements of existing specifications, would cause problems with normal fabrication practices. The approach taken, therefore, is comparative and uses existing specifications and experience as bench marks by which to develop opinions on the likelihood of significant welding problems with the Draft specification. The study focuses on the major welding problems which have traditionally caused problems in practice such as hydrogen cracking in the heat affected zone and weld metal, hot cracking in the weld metal, lamellar tearing, and the toughness of the heat affected zone and the weld metal. A few other potential problems are discussed in connection with the effect of specific elements. Health and safety issues such as the effect of specific elements in the steel on welding fume are beyond the scope of the study.

**FOR COMMITTEE USE ONLY
NOT FOR PUBLICATION**

The study is primarily concerned with the chemical composition requirements and does not address other requirements of the specification such as tensile properties. It should be noted, however, that yield strength of the base metal affects the susceptibility to

hydrogen cracking [Graville, 1992] and increasing the minimum yield strength from 36 ksi (for A36) to 50 ksi is expected to increase crack susceptibility even if the composition remains the same.

1.5 Draft Chemical Composition Requirements

Table 1 shows the composition requirements in the Draft for heat analysis and the product composition limits based on the tolerances of ASTM A6. For comparison, the requirements of A36 and A572 Grade 50 have also been included, and it is observed that a steel meeting A36 or A572 Grade 50 would not necessarily meet the Draft specification.

The proposed specification is designed to permit a wide range of compositions for steel meeting the specified mechanical properties in a wide range of thicknesses. At one end of the spectrum the specification permits simple carbon steels similar to A36 in which manganese is the only additional alloying element, and where carbon could rise to the top limit of the specification, particularly in heavy sections, in order to meet strength requirements. At the other end of the spectrum multiple alloying elements derived from scrap, such as copper and nickel, could permit strength levels to be achieved at much lower carbon levels. A further limit on composition is imposed by the carbon equivalent cap given by

$$CE = C + \frac{(Mn + Si)}{6} + \frac{(Cr + Mo + V + Cb)}{5} + \frac{(Ni + Cu)}{15}$$

DRAFT

2.0 Hydrogen Cracking

Date:

2.1 General

FOR COMMITTEE USE ONLY

The risk of hydrogen cracking in the heat affected zone depends on many factors including the type of microstructure formed in the heat affected zone, the cooling rate of the weld, the level of retained hydrogen, and the stresses applied on the heat affected zone.

There is no single compositional factor which adequately predicts the susceptibility to cracking in all cases because the type of microstructure formed depends not only on the composition but on the details of the welding procedure, such as heat input.

00584

The various carbon equivalent formulae that have been presented in the literature are usually base on only one aspect of crack susceptibility and are usually empirically derived from experiments on limited composition ranges. For example, the IIW carbon equivalent

$$CE(IIW) = C + \frac{Mn}{6} + \frac{(Cr + Mo + V)}{5} + \frac{(Ni + Cr)}{15}$$

has been found to relate quite well to the hardenability of the steel. On the other hand, the formula

$$P_{cm} = C + \frac{Si}{30} + \frac{(Mn + Cu + Cr)}{20} + \frac{Ni}{60} + \frac{Mo}{15} + \frac{V}{10} + 5B$$

is a widely used measure of crack susceptibility which was developed directly from the results of several hundred cracking tests on high strength low alloy steels. In particular, it has proven to be a useful guide to the susceptibility of heat affected zones formed under relatively fast cooling conditions, such as small fillet welds or the root pass in groove welds.

The AWS D1.1 guidelines on preheat attempt to address both the tendency to form hard crack-susceptible microstructures (hardenability) as well as the sensitivity to cracking of a given heat affected zone (susceptibility). These guidelines are based on fairly severe cracking tests, and as pointed out recently by Yurioka in a recent review [Yurioka et al., 1994] tend to predict preheats higher than is often found adequate in practice. However, the guidelines provide a useful basis for comparing the cracking susceptibility of various materials and in particular provide insight into potential cracking problems that may be associated with the proposed specification.

DRAFT

Date:

In the AWS guidelines, the general hardenability and susceptibility characteristics of the steel are first examined by plotting the composition on a diagram which is divided into three zones (Fig. 2). Steels in Zone 1 have low carbon content and, despite the presence of other alloying elements that may raise the carbon equivalent, they generally have relatively soft heat affected zones and good crack resistance. Steels in Zone 2 include simple carbon steels and those with only limited alloying where crack susceptibility depends strongly on the cooling rate of the weld. For small welds on thick material, hard heat affected zones are formed with a high susceptibility to cracking. However, good crack resistance can be obtained if adequate heat input is provided and the welds cool sufficiently slowly to form soft heat affected zones. Steels on the left side of Zone 2 have very low hardenability and can accommodate a wide range of heat inputs without forming hard heat affected zones. Mov-

FOR COMMITTEE USE ONLY
NOT FOR PUBLICATION

ing to the right in Zone 2 restricts the welding conditions in which soft heat affected zones can be formed. Zone 3 represents the steels which form hard heat affected zones under most normal welding conditions. These steels have the poorest crack resistance and generally require preheat, even in thin sections.

DRAFT

2.2 Hardenability

Date:

In the Zone diagram in Fig. 2 the carbon equivalent is used as a rough guide to hardenability, but plain carbon steels have a lower hardenability than indicated by the carbon equivalent formula, and multiple alloyed materials may have a hardenability somewhat higher. This is because the carbon equivalent formula is a linear model, and it is well established that there are strong interaction effects amongst the various alloying elements involved in hardenability. Thus steels with multiple alloying elements sitting in Zone 2 close to the boundary with Zone 3 may, in fact, have their hardenability underestimated and should be further to the right than predicted from the carbon equivalent formula. Similarly, plain carbon steels with no alloying elements and relatively low manganese should lie to the left of the location indicated by the carbon equivalent formula and thus permit even lower heat inputs without resulting in hard heat affected zones.

**FOR COMMITTEE USE ONLY
NOT FOR PUBLICATION**

In order to obtain a clearer indication of the hardenability behavior of the various compositions possible within the proposed specification, hardening curves were generated for various example steels. The hardening curve is a plot of the maximum heat affected hardness against cooling time and is useful for determining heat affected zone hardnesses under specific welding conditions or for determining welding conditions necessary to restrict the heat affected zone hardness. The hardening curves have been estimated using a hardness model which is a modification of the model proposed by Suzuki [Graville, 1990]. It is emphasized that this is one of many available hardness models and others may produce different shaped curves, but this was selected because it attempts to include interaction effects.

In Fig. 3 the hardening curves for A572/50 and the Draft specification steel at the maximum carbon content of 0.23% are shown. In A572/50 the maximum manganese is 1.35% which together with a typical vanadium gives a CE of 0.5. In the Draft the manganese limit is 1.5% but with 0.23% C the maximum CE of 0.5 is reached at Mn = 1.45%.

The curves show that the Draft steel is slightly more hardenable than A572/50 under these conditions.

In Fig. 4 a comparison is made between two steels both having 0.17% C and 1.0% Mn. In one case the steel contains vanadium and in the other residual elements are present as follows: 0.1% Cu, 0.1% Ni, 0.35% Cr, 0.15% Mo. Both steels meet the Draft specification and the first steel is fairly typical A572/50. The graphs show a major increase in hardenability when the residual elements are included.

For the purposes of further exploring the hardenability behavior, three compositions, each meeting the maximum carbon equivalent requirement of the Draft, have been selected. These are listed in Table 2. In Steel 1, the carbon, vanadium, copper and nickel are at the maximum allowed. Manganese is limited by the carbon equivalent cap. Silicon is present at an average level for a killed steel. In Steel 2, the carbon is lower, chromium and molybdenum are at the maximum and no vanadium is present. In Steel 3, copper, nickel, chromium and molybdenum are present at the maximum levels permitted but the carbon level is low. The manganese level is limited by the carbon equivalent cap. The table also gives the calculated value of P_{cm} . The P_{cm} formula is dominated by the carbon level and thus the P_{cm} value is highest for Steel 1 and lowest for Steel 3, suggesting substantial difference in the crack susceptibility of these three materials.

The three trial compositions are plotted on the Zone diagram and shown in Fig. 2. Two of the compositions lie close to the boundary between Zone 2 and Zone 3 and are thus expected to have relatively low crack resistance and a limited range of welding conditions where crack-free welds would be produced. Steel 3 is well into Zone 1 and would be expected to have excellent crack resistance. For comparative purposes A36 at its maximum carbon content with an average manganese (in light of the low yield strength) and A572 Grade 50 with maximum carbon and manganese content are also plotted in the diagram.

The predicted hardening curves for the three steels are shown in Fig. 5 and show widely varying behavior despite the same carbon equivalent in all cases. The Steel 1 hardening behavior is likely to be similar to A36 or A572/50 with high carbon. Steel 1 has the highest hardness at short cooling times but Steel 2 produces high hardness over the widest

FOR COMMENT USE ONLY NOT FOR REPLICATION

DRAFT

range of cooling times. The high hardenability of Steel 2 results from the presence of residual elements and moderately high carbon and manganese levels. Steel 3 has a low carbon level and exhibits a flatter hardening curve with a significantly lower maximum hardness even at the shortest cooling times.

DRAFT

The guidelines in AWS D1.1 permit minimum heat affected zone hardnesses to be estimated from the carbon equivalent based on avoiding heat affected zones with hardnesses exceeding some critical value. This is very similar to the approach taken in the UK for calculating welding conditions to avoid hydrogen cracking. However, in view of the difference in hardenability characteristics, the estimated hardening curves are used directly in the present analysis. The critical cooling time to produce a maximum hardness of 400 Hv in Steel 1 is 3.5 seconds. This corresponds approximately to a 1/4 inch fillet weld on 1 1/2 inch thick material or 3/16 inch fillet weld on 1/2 inch material. For Steel 2 the critical time is 6 seconds which is roughly equivalent to a 5/16 inch fillet weld on 1 1/2 inch material or 1/4 inch fillet on 1/2 inch material. In each case it is assumed there is no preheat. It is therefore concluded that there would be a significantly higher risk of cracking in Steel 2 than in Steel 1 requiring significant changes in welding procedures to prevent cracking. On the other hand Steel 3, residing in Zone 1 and having a substantially lower P_{cm} value, is expected to have very good crack resistance.

It is thus concluded that the carbon equivalent cap proposed in the specification is not adequate to effectively control the resistance to hydrogen cracking, and steels meeting the maximum carbon equivalent could have widely varying susceptibility to cracking. The main difficulty is that the single carbon equivalent proposed does not adequately describe susceptibility for steels covering Zones 1 and 2 of the Zone diagram. For example, in order for Steel 2 to have a hardenability comparable to a higher carbon, A36 or A572 a carbon equivalent limit of about 0.45 would need to be applied. However, such a limit may be overly restrictive on the alloying elements if applied to a steel in Zone 1 with carbon less than 0.1%. Attempts to find carbon equivalent formulas that apply to a wide range of carbon and alloy levels have been made, and one formula proposed by Yurioka of Nippon [Suzuki, 1982] has been quite widely used. The formula is similar to the P_{cm} except it has an "accommodation factor" to provide a different weighting for alloys as carbon level changes. The Nippon formula is given by:

$$CEN = C + [0.75 + 0.25 \tanh\{20(C - 0.12)\}] \left[\frac{Si}{24} + \frac{Mn}{6} + \frac{Cu}{15} + \frac{Ni}{20} + \frac{(Cr + Mo + V + Cb)}{5} + 5B \right]$$

. Mills supplying line pipe to the Canadian market routinely supply to a maximum CEN. In Table 2 the CEN values have been determined for Steels 1, 2 and 3. It is evident that being based on a linear carbon equivalent CEN does not distinguish the hardenability characteristic of Steel 1 and 2.

DRAFT

The disadvantage of using CEN is that a single formula does not indicate the fundamental changes in the hardenability characteristics of the steel as it moves from Zone 1 to Zone 2 or 3. In particular, CEN does not indicate the maximum heat input that might be necessary to achieve crack-free welds. For example, a plain carbon steel with a relatively high CEN might be very weldable, providing crack-free welds under most welding conditions and only cause problems on very thick sections or very low heat input welds. There does not appear to be any advantage in using CEN and as a simple means of limiting composition the proposed carbon equivalent is probably as good as any. A simple approach would be to separate the compositions into two groups corresponding to Zones 1 and 2 and specify different maximum CE's. For example, setting CE to a maximum of 0.45 for steels with carbon greater than 0.1 (Zone 2) would provide hardenability roughly comparable to high carbon A36 or A572 Grade 50. Setting CE to a maximum of 0.5 for carbon level less than 0.1 would provide sufficient flexibility for composition in the low carbon steels.

It is interesting to note [Inagaki et al., 1986] that some Japanese specifications for weldable steel have been based on a maximum P_{cm} . For example, WES 3001-1983 has a requirements for general use HW36 (equivalent to grade 50) up to 50 mm thick of $P_{cm} = 0.32\%$ maximum. The only elements individually specified are $C = 0.2\%$ max., $P = 0.03\%$ max., and $S = 0.025\%$ max. All other elements are controlled by the P_{cm} cap. Steels at maximum carbon and maximum P_{cm} could have a CE exceeding the 0.5% specified in the Draft. However, for special crack resistant steels for welding without preheat (WES 3009-1983), the maximum P_{cm} is 0.20%.

It should be pointed out that achieving a carbon content less than 0.1% may not, by itself, be adequate to obtain good crack resistance. Lundin [Lundin et al., 1989] for example, has shown quite poor crack resistance in some low carbon steels and an inability of

carbon equivalent formulae to correctly predict behavior. It is also to be noted that some elements not appearing in weldability formulae may have significant effects on crack susceptibility. For example, it has been suggested that nitrogen could have a detrimental effect [Glover, 1984] although contrary evidence exists [Graville, 1992].

Columbium, although not appearing in the P_{cm} formula, has been shown [Inagaki et al., 1986] to have an effect when above 0.04%. It also enhances the effect of vanadium equivalent to an apparent increase in P_{cm} :

$$P_{cm}' = P_{cm} + \frac{V}{3} + \frac{Cb}{2} \quad (Cb > 0.04\%)$$

In lowering the carbon equivalent for steels with greater than 0.1% C, consideration could be given to thickness range. The proposed Draft has only one composition requirement for the complete range of thickness. In practice, however, it is normal practice to weld without preheat for sections up to 1 1/2 inch thick. Above 1 1/2 inch (covering most of the Groups 1, 2 and 3 shapes) the lowest carbon equivalent maximum should be aimed for, consistent with ability to meet strength levels. Above 1 1/2 inch (or Group 4 and 5 shapes) a higher carbon equivalent could be set allowing strength requirements to be met in thicker sections with the knowledge that welding procedures would include preheat.

DRAFT

3.0 Lamellar Tearing

Date:

3.1 Relation to Through-Thickness Ductility

FOR COMMITTEE USE ONLY
NOT FOR PUBLICATION

Lamellar tearing is a type of cracking that occurs in the heat affected zone of base metal when residual strains from welding act in the through-thickness direction, i.e., normal to the plane of rolling or working. The cracks have characteristic step-like appearance and have most often been associated with large T or corner joints in thick sections. Many factors influence the occurrence of lamellar tearing including joint type, restraint, and the presence of hydrogen, but the most significant is the through-thickness ductility of the material. Low through-thickness ductility results from the presence of inclusions flattened out during the rolling or forming process. These create planes of weakness which open up when welding stresses act normal to the surface, i.e., in the through-thickness direction.

The problem of lamellar tearing received considerable attention during the '70s and resulted in various guidelines for determining adequate through-thickness ductility to prevent lamellar tearing as well as the metallurgical means for improving steel quality. Fabricators developed methods for minimizing the occurrence of lamellar tearing including use of special welding techniques, buttering the material, and welding sequences that minimized restraint. However, in critical applications the purchase of material with guaranteed through-thickness ductility has been the preferred approach. Guidelines link the required through-thickness ductility as measured by the percentage reduction of area of a small through-thickness tensile specimen, to the application, i.e., type of joint and restraint.

As an example, the Japan Welding Engineering Society published WES 3008-1981 [Inagaki, 1982] which gave recommended values of the required through-thickness ductility ϕ_z to avoid lamellar tearing. These range from 15% reduction in area for fillet-welded cross (cruciform) joints to 25% for complete penetration single bevel T joints. For material less than 15 mm there is no requirement as lamellar tearing is considered unlikely in these thinner sections.

3.2 Relation to Sulfur Content

The through-thickness properties are a function of the density of non-metallic inclusions and the degree to which they have been flattened out during the rolling or working process. Inclusions result from the presence of impurities such as sulfur and also from the deoxidization processes in the steel. It has been found that the most dominant effect on through-thickness ductility comes from the sulfur content (Fig. 6). When low sulfur is achieved further improvements may be obtained by controlling the shape of the remaining sulfides, for example, by rare earth treatment, round sulfides having a less detrimental effect than elongated or flattened sulfides. The relationship between total sulfur content and reduction area indicates that steel with an assured level of through-thickness ductility could be obtained by simply specifying maximum sulfur levels without the need for through-thickness tensile testing. However, it is apparent from Fig. 6 that to obtain a reasonable assurance of say 15% reduction in area a maximum sulfur level of 0.01% must be achieved.

DRAFT

Date: : : : : :
Date: : : : : :

FOR COMMITTEE USE ONLY
NOT FOR PUBLICATION

This figure has been widely used as a maximum sulfur level in high quality steels, although for some applications lower values have been used. It is apparent that reducing the maximum sulfur level from say .045 to .025% would not provide any assurance of improved resistance to lamellar tearing and would not, therefore, offer any advantage to the purchaser. Thus, for general applications where lamellar tearing is not a consideration, there does not appear to be a basis for reducing the maximum specified sulfur level to a value lower than the proposed 0.045%. However, it is recognized that such a specification, along with other current specifications for structural steels, does not provide any assurance of resistance to lamellar tearing. In critical cases, such as the special moment resisting connection shown in Fig. 1 where an assured resistance to lamellar tearing may be desirable, this would have to be achieved by a supplementary requirement which could include a maximum sulfur level of .01%.

DRAFT

Date:

3.3 Other Effects of Sulfur

The presence of non-metallic inclusions influences the ductile fracture behavior of a material which is manifested by the Charpy V-notch upper shelf energy value. Fig. 1 shows a typical relation between upper shelf energy and sulfur content [Pickering, F.B. 1975]. Improvements in Charpy properties can therefore be achieved by lowering the sulfur level and this has been one of the main driving forces for lower sulfur levels over the past few decades. The role of sulfur will also be reflected in the HAZ Charpy properties. However, although lower sulfur may be a means of achieving improved toughness, specifying low sulfur levels may be redundant when the Charpy requirements themselves are specified.

**FOR COMMITTEE USE ONLY
NOT FOR PUBLICATION**

The achievement of very low sulfur, while having beneficial effects for lamellar tearing and ductile fracture resistance, may result in other effects both during steelmaking and welding. For example, during continuous steelmaking the rate of nitrogen pickup is influenced by sulfur level (Fig. 8, Irving, W.R., 1993) and the higher nitrogen level may have negative consequences if steps are not taken to control it. Low sulfur level has also been linked to increased sensitivity to hydrogen cracking in the heat affected zone. Two explanations have been proposed for this. First, the presence of sulfide inclusions act as nuclei for ferrite as the heat affected zone transforms from austenite on cooling. Facilitating ferrite formation lowers the hardenability, and therefore reducing the number of nuclei by having very low sulfur levels effectively increases the hardenability of the material and the

00588

risk of heat affected zone cracking [Hart, 1978]. In addition, it is believed that sulfide inclusions act as traps for hydrogen thus lowering the sensitivity to hydrogen embrittlement. Removing these traps by lowering the sulfur level apparently increases the risk of hydrogen cracking in the heat affected zone.

These possible negative side effects of very low sulfur are generally regarded as modest, particularly compared with the benefits of low sulfur on ductile fracture behavior and resistance to lamellar tearing. As far as welding is concerned, resulfurizing steel or specifying a *minimum* sulfur level has never been deemed appropriate, although such practice has been applied for preventing hydrogen flakes in [forging] [Smith et al. 1968]

DRAFT

Date:

4.0 Hot Cracking

FOR COMMITTEE USE ONLY

4.1 Heat Affected Zone Hot Cracking

NOT FOR PUBLICATION

Hot cracking may occur in the weld metal or heat affected zone (HAZ) although the latter is less common in modern structural steels. HAZ hot cracking is sometimes termed liquation cracking or hot tearing. It occurs when impurities form low melting point eutectics in the high temperature part of the HAZ close to the fusion boundary. On cooling, the liquid films between the austenite grains cannot support the shrinkage strains, and small cracks result. Such cracks may not be easily detected by non-destructive means, but they may initiate larger cracks or show up as poor ductility during qualification tests. Even without the occurrence of cracks, the partial formation of liquid films may lower HAZ toughness, especially in high heat input welds such as electroslog.

HAZ hot cracking is primarily a function of the base metal composition. Research during the '60s (discussed in reference [Bailey, 1994]) found that sulfur and carbon had detrimental effects while manganese was beneficial. Fig. 9 shows that cracking risk is high in a 0.2% carbon steel when the sulfur level exceeds 0.05% or when the manganese/sulfur ratio is less than 15~20.

It is important to note that no minimum manganese level is required in the Draft specification and that it would be theoretically possible to supply steel with very low manganese to sulfur ratios and high carbon. The minimum manganese and maximum carbon

and sulfur levels in several specifications for structural steels are given in Table 3. Except for shapes less than 426 lb/ft in A36, all weldable grades listed have minimum manganese levels specified. In addition, A572 requires the manganese/carbon ratio to be not less than two, although this appears to be redundant for grade 50 in light of the maximum carbon level specified. The omission of a minimum specified manganese level in the Draft thus appears to be a departure from established practice.

DRAFT

4.2 *Weld Metal Hot Cracking*

Date:

Hot cracking in the weld metal—usually termed solidification cracking—arises when liquid becomes trapped between solidifying grains and cracks open up as the metal shrinks. It may occur anywhere in the weld metal but is most often found along the weld centerline. Hot cracking is influenced by the welding procedure—most importantly the welding speed and the depth-to-width ratio of the bead—and the composition.

**FOR COMMITTEE USE ONLY
NOT FOR PUBLICATION**

The composition of the weld metal is determined both by the welding consumables and by the base metal through dilution. Some elements, such as copper and nickel that do not participate in chemical reactions in the weld pool, transfer from the base metal to the weld metal without loss. Under these conditions the weld metal composition for these elements may be determined from the dilution factor. Other elements such as manganese are chemically active in the weld pool and the final weld metal composition cannot be predicted with ease. For the present purpose reference weld metal compositions were conservatively estimated by assuming a very high dilution factor of 80% and 100% transfer factors, together with typical levels of alloying elements from the welding consumables. The resulting weld metal compositions were used as references for determining the potential for weld metal weldability problems. The weld metal reference compositions are shown in Table 4. Three base metals are chosen representing a carbon steel with maximum sulfur and phosphorus but no other alloys, a low carbon steel with maximum nickel, copper, chromium and maximum sulfur and phosphorus, and the same low carbon steel with more typical sulfur and phosphorus levels.

The effects of composition was investigated by Jones [Jones, 1959] who found a detrimental effect of carbon and sulfur and a beneficial effect of manganese (Fig. 10). The crack severity increased sharply with carbon levels over 0.13% requiring a far higher manganese/sulfur ratio to prevent cracks. He recommended a minimum manganese/sulfur ratio

of 35 for a carbon level of 0.15% maximum but later authors (e.g., Borland [Borland, 1961]) considered lower values acceptable.

Ostrovskaya [Ostrovskaya, 1964] developed the following carbon equivalent formulas for sensitivity to hot cracking:

For C = 0.09 - 0.14%

$$C_{eq} = C + 2S + \frac{P}{3} + \frac{Si - 0.4}{10} + \frac{Mn - 0.8}{12} + \frac{Ni}{12} + \frac{Cu}{15} + \frac{Cr - 0.8}{15}$$

and for C = 0.14 - 0.25%

$$C_{eq} = C + 2S + \frac{P}{3} + \frac{Si - 0.4}{7} + \frac{Mn - 0.8}{8} + \frac{Ni}{8} + \frac{Cu}{10} + \frac{Cr - 0.8}{10}$$

These formulae show a dominant effect of carbon, sulfur and phosphorus with other elements having a relatively mild effect. As carbon increases, the effect of these other elements also increases.

Bailey and Jones [Bailey et al., 1978] studied solidification cracking in submerged arc welds and proposed the following formula as a measure of crack susceptibility:

Units of crack susceptibility (UCS)

$$= 230 C + 190 S + 75 P + 45 Cb - 12.3 Si - 5.4 Mn - 1$$

(for carbon levels less than 0.08, C is taken as 0.08).

The range of validity was 0.08 - 0.23% C; 0.01 - 0.05% S; 0.01 - 0.045% P; 0.15 - 0.65% Si; 0.45 - 1.6% Mn; 0 - 0.07% Cb. There was no significant effect of elements up to the following amounts: 1% Ni, 0.5% Cr, 0.4% Mo, 0.07% V, 0.3% Cu, 0.02% Ti, 0.03% Al, 0.002% B, 0.01% Pb, 0.03% Co. Although the critical value of UCS depends on the welding procedure, the author concluded that values above 30 presented a high risk of cracking while in some typical trials threshold values were above 20.

In Table 4 the UCS values have been calculated for the three example weld metals and it is clear that the effect of carbon dominates. Example 1, the plain carbon steel, has a high risk of solidification cracking with a UCS value of 49. This is reduced to 20 when the

carbon is lowered to 0.07% in the base metal even with the presence of maximum columbium, sulfur and phosphorus. Reduction of the sulfur and phosphorus to more typical levels further lowers the UCS to 13 indicating very low risk of cracking.

The elements nickel, copper, chromium do not appear in the UCS formula and therefore, even at their maximum values do not contribute to the UCS. It should be noted, however, that the levels chosen in examples 2 and 3 are beyond the range of validity of the UCS formula. In the following section the effects of copper are discussed in greater detail.

DRAFT

4.3 *Effects of Copper*

The well-known effect of copper on hot shortness in steel has resulted in a very cautious approach to using copper as a deliberate alloying element. Similarly, the well-known copper contamination of welds that occurs when a copper contact tip touches the weld metal has also generated concern over detrimental effects of copper in weld metal. There are, however, several phenomena which must be discussed in the context of setting maximum copper levels in steel specifications. For reference, the maximum copper level in several specifications is shown in Table 5.

4.3.1 *Fundamentals of Copper Phase Diagram.*

The iron-copper phase diagram [Le May et al., 1982] is shown in Fig. 11. Copper is completely miscible in the liquid state with the melting temperature ranging from 1538°C at the 100% iron end of the diagram down to 1085°C for 100% copper. Copper has a face centered cubic structure and forms a substitutional solid solution in γ -iron (up to about 10~12% Cu) and also in α -iron (up to 2.1% at 850°C). Below 850°C the solid solution of copper in α -iron is in equilibrium with ϵ -phase which is almost pure copper with a small amount of iron in solution. Above 850°C the equilibrium phases are γ -iron - copper solution and ϵ -phase. At ~1090°C the ϵ -phase melts.

The limited solubility of copper in ferrite at lower temperatures provides the potential for copper being used as a precipitation hardening element, and this approach has been

used in a number of steels in recent years. Generally, copper levels exceeding 1% are required in practice, although copper levels less than this value can cause precipitation hardening after heating. This raises the possibility of detrimental effects on heat affected zone toughness both in the as-welded condition and particularly after the post-weld heat treatment.

DRAFT

4.3.2 *Surface Hot Shortness*

Date:

Liquid copper (or ϵ -phase) in contact with austenite wets the grain boundaries and leads to grain boundary penetration and cracking, or hot shortness. The risk of copper contamination from a welding contact nozzle is well known, and arises when copper comes into contact with the weld when it is above 1085°C. Copper contamination has been observed [Savage et al., 1978a; Savage et al., 1978b; Nippes et al., 1982] in austenitic materials that have been contaminated by copper tooling. In the case of conventional surface hot shortness during steel rolling and forming, the liquid copper is produced by the preferential oxidation of iron at the surface of the steel when it is heated for rolling or forming. Since the reheating temperature is higher than the melting point of copper, oxidation of the iron causes a concentration of copper in the liquid state at the surface. This penetrates the austenite grain boundaries which then open up as surface cracks during subsequent hot working. This mechanism may operate in other situations where preferential oxidation can occur, for example, during flame cutting, and this is discussed more fully in a later section.

**FOR COMMITTEE USE ONLY
NOT FOR PUBLICATION**

The ability of the copper-rich phase to penetrate an austenite grain boundary is influenced by the presence of other elements which affect the wetting action (as measured by the dihedral angle between the austenite grains) and the solubility of copper in austenite (Fig. 12). Thus tin, antimony, and arsenic are known to have a deleterious effect on hot shortness while nickel is beneficial. Manganese has little effect [Hebraken et al., 1982]. It is found that a nickel-to-copper ratio in the range 0.5 ~ 1.0 is effective in controlling surface hot shortness. High copper steels such as A710 with copper 1.00 - 1.30% have nickel 0.70 - 1.00%.

It should be noted that the mill scale on a high copper steel may be enriched in copper and there is the potential for this to cause problems in welding if not removed [Okada et al., 1982]. When copper in the steel is derived from scrap, it is usually accompanied by tin.

Table 5 shows a typical statistical analysis of copper and tin contents in an electric furnace steel. Typically tin is about one tenth the copper level while nickel and chromium are one half. Thus with a copper maximum of 0.6% a tin content up to 0.06% is expected.

DRAFT

4.3.3 Effect of Copper on Hot Cracking

Date:

A different set of concerns exist when a copper-containing steel is welded. Rather than concentration of copper by preferential oxidation of iron at the surface followed by grain boundary penetration of the austenite, the principal concern is the effect of copper diluted directly into the weld metal. The principal concern has been the potential effect on solidification cracking and numerous studies have been undertaken to investigate this.

FOR COMMITTEE USE ONLY
NOT FOR PUBLICATION

The work of Bailey and Jones [Bailey et al., 1978] discussed earlier showed that copper up to 0.3 had no effect on solidification cracking in submerged arc weld metal and the Ostrovskaya formulae show a relatively small effect, especially at low carbon. Blake [Blake, 1978] reported on the effects of copper in mild and low alloy steels and concluded that CO₂ welds were immune to hot cracking with copper levels up to 0.45%. Miyoshi [Miyoshi et al., 1976] examined the effect of copper on weldability of line pipe including a study of hot cracking using the Varestraint test. Results are shown for two steels in Fig. 13. At 0.11% carbon and 1.1% manganese, copper levels up to 1% could be tolerated without hot cracking. However, in the steel with 0.16% carbon and 1.45% manganese, hot cracks were observed when the copper content exceeded 0.5%. They concluded that at least 0.5% Cu in high grade line pipe does not show any detrimental effect on weldability.

Okada, in a comprehensive review of copper-containing steels [Okada et al., 1982], cites the systematic study of hot cracking by Matsuda using the Varestraint test in which specific elements were added to a base composition. Copper was the worst element with severe cracking occurring at levels of copper exceeding 0.3% (see Fig. 14). The carbon level (0.18%) of the base steel in Matsuda's work should be noted together with the manganese level (0.95). The levels of sulfur and phosphorus in the base steel are not known.

The general conclusion from these studies is that copper appears to have a detrimental effect on hot cracking tendency in weld metals, but that this is a function of the car-

bon level. The studies showing marked detrimental effects of copper used steels with carbon exceeding around 0.14% and most studies show the major elements influencing hot cracking are carbon, phosphorus and sulfur. Thus it appears the tolerable level of copper can be linked to the carbon level and also possibly to the level of sulfur and phosphorus. The modern generation of copper precipitation hardening steels (such as A710) with copper over 1% have low carbon levels (less than 0.07%), low sulfur and phosphorus (less than 0.025%), and these steels are apparently being welded without major problems [Lundin, et al., 1990]. The data suggests that with carbon levels in excess of 0.15% a weld metal content of over 0.3% copper could increase the risk of hot cracking.

In most studies on the effect of copper, the metal was added as a pure element. There does appear to be any work on the combined effects of copper and other impurities, such as tin, that would normally be present when copper is derived from scrap. Borland [Borland, 1961] found an effect of arsenic when present at 0.2% but concluded that since this level was far higher than anticipated in steel, no significant effect is expected under normal conditions.

DRAFT

5.0 Toughness

Date:

5.1 General

FOR COMMITTEE USE ONLY

NOT FOR PUBLICATION

For most applications structural steel shapes are supplied without Charpy V notch impact test requirements. In some cases, particularly heavy section tension members, impact tests are specified and these tests would also be required for the HAZ and weld metal in groove weld procedure qualifications. The Draft provides for impact testing as a standardized supplementary requirement (S5 from ASTM A6 /A6M) and as an added supplementary requirement for Group 4 and 5 structural shapes. A typical requirement would be 20 ft-lb (27J) at 70°F (20°C) in base metal, HAZ and weld metal.

Even in cases where impact testing of the steel is not a requirement, very low toughness in the HAZ or weld metal could lead to fracture initiation during fabrication, erection, or service. Thus it is important to identify the effects of base metal composition on HAZ and weld metal toughness. This can only be done in a general way as the situation is highly complex and required levels of toughness depend on the application. HAZ and weld metal toughness is also a strong function of the welding procedure. Increasing heat

input normally lowers toughness while the complex thermal cycles experienced in multi-pass welds may either improve or lower toughness. Further changes in toughness may occur if the weld is stress relieved, although this is not likely in most building applications. In the following sections, the effect of composition on toughness in the HAZ and weld metal is reviewed to determine if there is a basis for restricting the levels of elements specified in the Draft.

DRAFT

5.2 Heat Affected Zone Toughness

Date:

A considerable amount of work on the effects of composition on HAZ toughness has been undertaken. Much of this has been spurred by the offshore structures industry from a concern over "local brittle zones" (LBZs). However, it should be noted that this has largely been a problem during CTOD (crack tip opening displacement) testing and there is a continuing dialogue on the true significance of LBZs [de Konig et al., 1988]. In the context of buildings, therefore, the relevance of conclusions drawn from CTOD tests must be approached with caution. But there are also some studies using the Charpy test which will also be included in the discussion.

**FOR COMMITTEE USE ONLY
NOT FOR PUBLICATION**

Ito [Ito et al., 1973] studied the effect of a number of elements on the heat affected zone bond brittleness. They developed formulae for the compositional effects for two different cooling times. One inch (25 mm) thick plate was used with one pass made by SAW from each side, the CVN specimen notch being in the HAZ of the second side. The natural cooling time 800-500°C was 50 seconds and a faster cooling time of 11 seconds was achieved by water cooling. The results for the faster cooled weld may not have been the same if a lower heat input had been used to achieve a rate of 11 seconds.

Their results are summarized in Figs. 15 and 16 and the composition effects are given by the formulae:

$$\text{For 11 s} \quad P_{BA} = C - \frac{Cu}{6} - \frac{Ni}{5} - \frac{Mo}{11} + 4S \quad (\%)$$

$$\text{For 50 s} \quad P_{BB} = C + \frac{Mn}{10} + \frac{Cu}{6} + \frac{Cr}{12} + \frac{Mo}{13} - \frac{Ni}{50} \quad (\%)$$

Carbon has the most significant detrimental effect but the role of other elements depends on the type of microstructure formed. Nickel is always beneficial. The similarity between the P_{BB} formula and conventional carbon equivalents underlines the relation between toughness and hardenability in this work. The dominant role of carbon is further demonstrated by CTOD tests in Fig. 17 from Miyoshi [Miyoshi et al., 1974].

Haze [Haze et al., 1988] studied the effects of composition on HAZ toughness using the CTOD test. Results are summarized in Fig. 18 where the height of the bars is a measure of the detrimental effect on HAZ toughness. Elements could be grouped according to the magnitude of their influence:

B, N >> C, Cr, Mo, Cb (Nb), V > Si, Cu, Ni, Mn.

Improvements in HAZ toughness were achieved by minimizing impurities (e.g., nitrogen) and reducing carbide-forming elements, such as columbium, together with low carbon. Where precipitation hardening was required to achieve strength, copper provided a useful alternative to columbium and vanadium because of its limited effect on HAZ toughness.

DRAFT

Many studies have been directed towards the effect of columbium (niobium) on HAZ toughness. Some show a detrimental effect with increasing columbium levels [Hannerz, N.E. 1976] especially at high heat inputs (Fig. 19) but the effects depend on several other factors, most notably the carbon. For example, Fig. 20 [Heisterkamp, F., et al. 1990] shows a relation between carbon and columbium level for achieving good CTOD properties in the HAZ. The greatest tolerance to carbon is achieved at about 0.02 ~ 0.03% Cb while at 0.07% C up to 0.04% Cb could be tolerated. The latter value is confirmed by the data in Fig. 21 [Nakano et al., 1988].

Nitrogen can be present in steel either combined as nitrides or other complex particles, or as free nitrogen, i.e., in interstitial solution. It is well established [Gladman et al., 1975] that free nitrogen has a detrimental effect on toughness (see Fig. 22) and can cause strain aging embrittlement. Nitride formers such as aluminum, vanadium and titanium are added to steel both for the purpose of removing free nitrogen and for the precipitation hardening and grain refinement roles of the nitrides.

In the HAZ nitrides may dissolve leaving free nitrogen [WRC, 1988] which has an adverse effect on the toughness (Fig. 23). The extent to which nitrides dissolve depends on the element involved and the thermal cycle. In the high temperature part of the HAZ of high heat input single pass weld all nitrides, except titanium nitride, dissolve with a corresponding loss of toughness. In multipass welds and in HAZs where the specimen notch samples various zones, the measured toughness is dependent on the relative level of nitride formers and total nitrogen. Fig. 24 shows some results for aluminum and Fig. 25 shows there is an optimum ratio of titanium to nitrogen to produce favorable HAZ toughness. Boron may also be used [Ohnishi et al., 1988] to advantage with carefully balanced levels of titanium and nitrogen. However, without such balancing boron has a marked detrimental effect on HAZ toughness.

DRAFT

In a general purpose steel specification it is probably impractical to attempt the control of HAZ toughness through balancing nitrogen level with the level of nitride formers, although the Draft does include a minimum ratio for vanadium to nitrogen. It may also be impractical to specify minimum levels of aluminum or titanium, but setting a maximum to a nitrogen content would be beneficial. The Draft specifies a maximum nitrogen of 0.015% only when added as a supplement to vanadium, but no maximum is specified in other cases. This requirement appears to derive from earlier specifications for ingot cast BOF and open hearth steels where, unless added as a supplement, the nitrogen level was assumed to be adequately low. However, in the context of the present Draft there is the possibility of significant variation in nitrogen content of the steel, and a maximum level should be specified for all cases. In setting a maximum nitrogen level for heat analysis it should be noted that the product analysis may exceed the heat analysis by 0.005 according to A6.

The effect of copper on HAZ toughness has been reviewed by Okada [Okada et al. 1982]. He cited a study by Masumoto in which the data from 300 steels were analyzed in which it was found that copper levels up to 1.6% improve heat affected zone toughness of submerged arc welds with heat inputs of 4 and 10 kJ/mm as long as no aging treatment is applied. Also cited was Tanaka et al.'s paper which included SMAW at 4.5 kJ/mm and electrode gas welds at 20 kJ/mm heat input. The results are shown in Fig. 26 and indicate no significant effects of copper on the heat affected zone toughness up to 1% copper. Hannerz [Hannerz, 1983] investigated the effects of copper content in two steels welded at two heat inputs. Results are given in Fig. 27 showing that copper has no significant effect up to 1% in the as-welded condition. The potential for precipitation hardening during

stress relief suggests a possible deterioration in toughness but Harnetz found no major effect.

DRAFT

Date:

**FOR COMMITTEE USE ONLY
NOT FOR PUBLICATION**

Christoffel [Christoffel et al., 1989] showed that copper in the weld metal from 0.5% copper added to a conventional carbon steel (A516) resulted in weld metal embrittlement after long term exposure to elevated temperatures in the range 329-371°C. Morariu [Morariu et al., 1992] studied the effects of copper on heat affected zone toughness after post-weld heat treatment. The 2.2% copper steel resulted in copper precipitation hardening and a detrimental effect on toughness. In other work on copper-strengthened A710 tests showed a deterioration in toughness in the HAZ after post-weld heat treatment at 1050°F (565°C), [G-83-4].

No data on the effect of tin on HAZ toughness could be found, but as a solid solution hardener even small quantities of tin in steel (0.01%) can reduce ductility [Hubbard, 1977]. It is also reported that 0.048% Sn imparts severe temper embrittlement. There is, therefore, a real possibility of significant effects of tin on HAZ toughness, especially in multipass welds or after stress relief. Research on this will be required.

5.3 *Weld Metal Toughness*

Many of the effects of elements in the HAZ are also evident in the weld metal. The weld metal composition, however, is only partly determined by the base metal composition and other factors may dominate. For example, nitrogen has a detrimental effect on weld metal toughness, but the nitrogen level is largely determined by the effectiveness of shielding. Thus, at normal levels the base metal nitrogen level is not a primary factor. Some elements, however, transfer efficiently to the weld metal, and base metal content becomes a primary factor in determining weld metal properties. The effect of a specific element may be different in the weld metal than the HAZ because of a different microstructural environment.

Columbium under some conditions may improve weld metal toughness, but most workers have found detrimental effects at high levels [Dolby, 1981]. Typically, weld metals show a tolerance for columbium up to 0.03 ~ 0.04% in the as-welded condition but significant deterioration of toughness with increasing columbium in the stress relieved state [Jesseman, 1975].

A similarly complex situation is also observed with vanadium [Dolby 1982], where for weld metals typically used in structural applications vanadium up to 0.05% may be moderately beneficial on toughness. For high vanadium levels good toughness in the weld metal can be achieved with special alloying.

DRAFT

The influence of copper on weld metal toughness has been derived by Hannerz [Hannerz, 1987] whose own results are shown in Fig. 29. He concludes that copper up to 0.45% or possibly up to 0.85% is not detrimental to toughness and may be beneficial, particularly in the stress relieved condition.

**FOR COMMITTEE USE ONLY
NOT FOR PUBLICATION**

6.0 Other Weldability Issues

6.1 Stress Relief Cracking

Although structural shapes are not subject to thermal stress relief in the majority of cases, the material should be tolerant to such a treatment should it be applied. Cracking may occur in the HAZ of some materials during stress relief, and composition is a major factor. Okada [Okada et al., 1982] cite the study of Ito and Nakanishi which resulted in the following formula:

$$P_{SR} = Cr + Cu + 2Mo + 10V + 7Cb + 5Ti - 2$$

Stress relief cracking may occur if P_{SR} is positive. The effect of copper is shown in Fig. 30, and it has also been shown [Balaguer, J.P., et al., 1989] that a Cu-containing HSLA100 steel base on A710 is susceptible to stress relief cracking.

If the elements in the formula are set at the maximum values permitted by the Draft, the value of P_{SR} is 0.75 suggesting a slight susceptibility to cracking. At more typical vanadium levels P_{SR} is negative. However, as pointed out by Lundin [Lundin et al., 1990] the formula can only be regarded as a very rough guide.

Other work points to the role of trace elements like Sn, P, Sb in stress relief cracking as indicated by the following formulae:

00594

$$\text{Severity} = 0.2\text{Cu} + 0.44\text{S} + \text{P} + 1.8\text{As} + 1.9\text{Sn} + 2.7\text{Sb}$$

$$\text{X (embrittling factor)} = \frac{(10\text{P} + 5\text{Sb} + \text{Sn} + \text{Al})}{100}$$

These formulae were not effective when applied to Cu-containing HSLA steels [Lundin et al., 1990]. The role of trace elements, however, may be particularly important for electric furnace steels where tin in particular is usually present with the copper. Although the composition requirements of the Draft specification do not suggest a major problem from stress relief cracking, the potential for it exists if certain elements, particularly vanadium, are at the high end of their range.

DRAFT

6.2 Thermal Cutting

Date:

Steel members having flame cut edges are frequently incorporated in structures with as-cut edges, i.e., without any further grinding to reduce surface roughness or to remove the heat affected zone. It is known for some time now [Goldberg, 1973; Goldberg, 1974; Plecki et al., 1977; Ho et al., 1981] that the fatigue crack initiation behavior of the as-cut surface depends on the cut edge quality as indicated by surface roughness and presence of resolidified metal. These characteristics of the cut edge quality, however, depend primarily on the cutting parameters and not on the steel composition.

FOR COMMITTEE USE ONLY
NOT FOR PUBLICATION

More recently, however, Wilson [Wilson, 1987] has confirmed the presence of microcracks at the cut edge surface in HSLA bridge steels that varied in thickness from 1 to 4 inches. Microcracks were observed in both oxy-fuel and plasma cut surfaces. This study had been undertaken after the failure of steel members that had been deployed with as-cut surfaces in two bridges; subsequent investigation revealed the presence of cracks at the cut surfaces, although it is not clear if these microcracks were considered to be initiation sites of the failure.

In this study, thermal cut surfaces were produced in twenty one bridge steels (A572, A588 and A36) using a variety of cutting variables. The steels represented a carbon equivalent range of about 0.38 to 0.58. Carbon content varied from 0.11 to 0.21 wt. % and Cu content from 0.02 to 0.43 wt. %. The CVN toughness of the steel varied from 4 to 135 ft-lb at 40°F.

The objective of this study was to examine the relationship of the as-cut surface condition to the steel chemistry and cutting variables. The cracks, however, could not be observed visually and scanning electron microscopy had to be employed to observe the 1 to 2 grain diameter deep, intergranular microfissures. The intergranular nature of these microfissures suggests a mechanism for their formation that is similar to the one causing hot shortness in steels during hot rolling described earlier.

DRAFT

Since thermal cutting involves oxidation of the surface, substantial concentration of Cu, Sn, etc., could occur and result in penetration of these elements at the surface. If the mechanism is similar to hot shortness, it suggests that Se, Sb, As could play a major role and that Ni could reduce the incidence of microcracks. At present, however, no research has been published to confirm this. Unfortunately, the Wilson study does not report the presence of these elements in the steels investigated except for Cu, nor did it include any microprobe or local microanalysis at the microfissures in the SEM to verify this speculation. Copper alone does not seem to be sufficient at least not when present in amount up to 0.43 wt. %, since the microfissures in Wilson's study were apparent in all the steels irrespective of their chemical composition.

Date: _____
FOR COMMITTEE USE ONLY
NOT FOR PUBLICATION

The significance of these microcracks in the study was indirectly examined by means of a bend test (3/8 in. thick) that subjected the whole width of the cut edge to a large strain (mandrel diameter equal to 4 times bend specimen thickness). The bend failures/cracks were found to initiate from the grain boundary fissures and superior bend ratings (0 to 2, in steps of 0.1 depending on the extent of cracking at the tension surface: none or hairline (0), short cracks with visible opening (0.1 to 1), large crack across specimen width or complete failure (1.1 to 2)) were related to (a) lower cut edge hardness, (b) higher steel CVN toughness and (c) lower steel carbon content.

While the exact mechanism for the formation of or the structural significance of the grain boundary fissures present at the cut surfaces are not known, it is inferred that the potential for brittle fracture initiation from as-cut surfaces would be higher for steels that contain carbon at the high end of the range examined by Wilson and for steels that have relatively poor CVN toughness. Any role for elements such as Cu, Sn, As and Sb in this context is not established and requires further work.

DRAFT

7.0 Conclusions and Suggestions

Date:

The Draft specification aims to cover a wide range of chemistry options in the full range of thicknesses. It permits traditional carbon and carbon-manganese steels as well as low carbon types with significant levels of alloy elements. By attempting to cover several types of chemistry options within a single requirement, the possibility exists for significant alloy levels to be combined with high carbon. These combinations have the potential for causing weldability problems such as weld metal hot cracking and heat affected zone hydrogen cracking.

The Draft controls the combination of elements by imposing a maximum carbon equivalent. The level (0.5%) is presumably selected to allow strength requirements to be met over the full thickness range and chemistry options. This level, however, could permit chemistry combinations (high carbon, significant alloys) with the potential for weldability problems.

The review found a lack of data on the effects of several elements and combinations, most notably tin. It is also noted that many existing compositional formulae (such as P_{em}) were not developed for electric furnace steel and their suitability for such materials has not been established. It is clear that research is needed to examine more closely the effects of these elements on several aspects of weldability including hardenability, susceptibility to hydrogen cracking, hot cracking, and toughness.

Based on the opinions developed from the review and analysis, the following suggestions are made which it is believed will reduce weldability problems associated with the Draft specification:

- 1 Lower the carbon equivalent maximum for steels with greater than about 0.1% carbon, particularly for shapes of Groups 1, 2, and 3.
- 2 Set a minimum manganese level.
3. Set a maximum total nitrogen level.
4. Include an additional supplementary requirement with 0.01% maximum sulfur for applications where lamellar tearing is a concern.

5. Report or monitor tin levels.
6. Conduct studies to examine the weldability behavior, including hardenability and susceptibility to hydrogen cracking, of a range of compositions within the specification.

DRAFT

Date:

References

FOR COMMITTEE USE ONLY

NOT FOR PUBLICATION

Bailey, N. 1994. "Weldability of Ferritic Steels," Abington Publishing, Cambridge, UK [G-1994-7]

Bailey, N., and Jones, S.B. 1978. "The Solidification Cracking of Ferritic Steel During Submerged Arc Welding," *Welding Journal*, 57(8), Aug., Res. Suppl. pp. 217-s to 231s. [G-1978-5]

Balaguer, J.P., Wang, Z., and Nippes, E.F. 1989. "Stress-Relief Cracking of a Copper-Containing HSLA Steel," *Welding Journal*, 68(4), April, Res. Suppl., pp. 121-s to 131-s. [G-1989-2]

Blake, P.D. 1978. "Effects of Copper in Welding Mild and Low Alloy Steels," *Metal Construction*, 10(11), Nov., pp. 545-547. [G-1978-4]

Borland, J.C. 1961. "Suggested Explanation of Hot Cracking in Mild and Low Alloy Steel Welds," *British Welding Journal*, Vol. 8, Nov., pp. 526-540. [G-1961-1]

Christoffel, R.J., and Silvia, A.J. 1989. "Embrittlement of a Copper Containing Weld Metal, Residual and Unspecified Elements in Steel." ASTM STP 1042. A.S. Melilli and E.G. Nisbett, Eds., American Society for Testing and Materials, Philadelphia, pp. 232-242. [G-1989-6]

de Konig, A.C., Harston, J.D., Naylor, K.D., Ohm, R.K. 1988. "Feeling Free Despite LBZ," 7th Int. Conf. Offshore Mech. & Arctic Eng., Houston, Texas, Feb. 7-12. Publ. ASME. [F-1988-1]

00596

Dolby, R.E. 1981. "The Influence of Niobium on the Microstructure and Toughness of Ferritic Weld Metal—a Review," *Metal Construction*, 13(11), Nov., pp. 699-703. [G-81-3]

DRAFT

Dolby, R.E. 1982. "The Influence of Vanadium on the Microstructure and Toughness of Ferritic Weld Metal—a Review," *Metal Construction*, 14(3), Mar., pp. 148-153. [G-1982-8]

FOR COMMITTEE USE ONLY

NOT FOR PUBLICATION

Gladman, T., Dulieu, D., McIvor, I.D. 1975. "Structure-Property Relationships in High-Strength Microalloyed Steels," Proc. of Microalloying '75 Conf., Oct. 1-3, Wash, DC (Union Carbide 1977) pp. 32-55. [G-1975-1]

Goldberg, F. 1973. "Influence of Thermal Cutting and its Quality on the Fatigue Strength of Steel," *Welding Journal Research Supplement*, Sept., pp. 392s-404s.

Goldberg, F. 1974. "The Effect of Residual Stress and Quality of Thermal Cutting Edges on the Fatigue and Static Strength of Steel," *Australian Welding Journal*, Sept./Oct., pp. 127-134.

Glover, A.G. 1984. "Effect of Base Plate Nitrogen Content on the Cracking of the Girth Weld Root Pass," *Welding Institute of Canada Report RC159/1/84*. [H-1984-24]

Graville, B.A. 1990. "Hydrogen Cracking Sensitivity of HSLA Steels," *The Metallurgy, Welding, and Qualification of Microalloyed (HSLA) Steel Weldments*. Int. Conf., Houston, Nov. 6-8, pp. 127. [H-1990-11]

Graville, B.A. 1992. "Hydrogen Cracking in the Reheated Heat Affected Zone of Pipeline Girth Welds," *Int. Conf. Pipeline Reliability*, Calgary, June 2-5. Paper VI-4. Publ. Gulf Publ. [H-1992-4]

Habraken, L., and Lecomte-Beckers, J. 1982. "Hot Shortness and Scaling of Copper-Containing Steels," *Copper in Iron and Steel*. I. Le May and L. McD. Schetky, Eds., pp. 45-81. John Wiley & Sons, New York. [G-1982-2]

Hannerz, N.E. 1976. "Weld metal and HAZ toughness and hydrogen cracking susceptibility of HSLA steels as influenced by Nb, Al, V, Ti, and N." Int. Conf. Welding of HSLA (microalloyed) structural steels, Rome, Nov. 9-12, 1976. Pub. ASM. pp. 365-401.

Hannerz, N.E. 1983. "Weld Metal and Heat Affected Zone Toughness as Influenced by Copper," Copper in Steel. Proc. Part II, Luxembourg, May 25-27, pp. 5.1 to 5.22. [G-1983-2]

DRAFT

Hannerz, N.E. 1987. "Review on the Influence of Copper Content on Weld Metal Properties," *IIW Doc.* IX-1487-87. [G-1987-1]

Date:

FOR COMMITTEE USE ONLY

Hart, P.H.M. 1978. "Low Sulphur Levels in C-Mn Steels and Their Effect on HAZ Hardenability and Hydrogen Cracking," Int. Conf. Trends in Steel and Consumables for Welding, London, Nov., The Welding Institute. [H-1978-11]

NOT FOR PUBLICATION

Haze, T., Ohno, Y., Kawashima, Y., Chijiwa, R., Aihara, S., Uchino, K., Tomita, Y., Mimura, H. 1988. "Steel Plates With Superior HAZ Toughness for Offshore Structures," Nippon Steel Technical Report No. 36, Jan., pp. 39-48. [F-88-14]

Heisterkamp, F., Hulka, K., Batte, A.D., 1990. "Heat Affected Zone Properties of Thick Section Microalloyed Steels - a Perspective," The Metallurgy, Welding, and Qualification of Microalloyed (HSLA) Steel Weldments. Int. Conf., Houston, Nov. 6-8, pp. 659-681.

Ho, N-J., et al. 1981. "The Fatigue Resistance of Plasma and Oxygen Cut Steel", Welding Journal Research Supplement, Nov., pp. 231s-236s.

Hubbard, M.W., and Southall, D. 1977. "The Effect of Residual Elements on Properties," SCRATA Proc. of the 22nd Annual Conference on Steel Castings Production, Paper 3, pp. 1-7. [G-1977-2]

Inagaki, M. 1982. "Newly Published Specifications for Lamellar Tearing in Japan," *IIW Doc.* IX-1255-82. [G-1982-6]

Inagaki, M., Ito, Y., and Komizo, Y. 1986. "Standard for Weldable High Strength Steel Plates and Weld Cracking Material Parameter P_{cm} ," *IIW Doc.* IX-1412-86. [G-1986-3]

00597

Irving, W.R., 1993, "Liquid Steel Supply," Continuous Casting of Steel, Ed. Irving, W.R., Publ. The Institute of Materials, 1993, pp. 22-36. [G-1993-2]

Ito, Y.; Ikeda, M., Nakanishi, M., and Kohyama, A. 1973. "The Effects of Alloying Elements on Charpy Impact Properties of Welded Bond," *IIW Doc. IX-842-73*. [G-1973-1]

DRAFT

Jesseman, R.J. 1975. "Columbium Pickup in High-Dilution, Submerged Arc Weld Deposits," Proc. of Micro Alloying '75 Conf., Oct. 1-3, Wash, DC (Union Carbide 1977) pp. 578-591. [G-1975-2]

Date:.....

FOR COMMITTEE USE ONLY

Jesseman, R.J., and Schmid, G.C. 1983. "Submerged Arc Welding a Low-Carbon Copper-Strengthened Alloy Steel," *Welding Journal*, 62(11), Nov., Res. Suppl. pp. 321-s to 330-s. [G-1983-4]

NOT FOR PUBLICATION

Jones, P.W. 1959. "An Investigation of Hot Cracking in Low-Alloy Steel Welds," *British Welding Journal*, June, pp. 282-290. [G-1959-1]

Kitada, T., Tagawa, H., Matsumoto, K., Taira, T., Sugiyama, T. 1986. "Steel Plates for Off-shore Structures and Ice Breaking Vessels," 1986 Offshore Mechanics & Arctic Engineering (Tokyo) Vol. 2 ASME. [F-86-32]

Le May, I., and Krishnadev, M.R. 1982. "Fundamental Metallurgical Considerations," Copper in Iron and Steel. I. Le May and L. McD. Schetky, Eds., pp. 5-41. John Wiley & Sons, New York. [G-1982-1]

Lundin, C.D., Gill, T.P.S., Qiao, C.Y.P., Wang, Y., Khan, K.K. 1989. "Carbon Equivalence and Weldability of Microalloyed Steels," Ship Structure Committee Report SSC-357. [G-1989-9]

Lundin, C.D., Khan, K.K., Gill, T.P.S. 1990. "PWHT/Reheat/Stress Rupture Cracking and Heat Affected Zone Toughness in Cu-Precipitation Hardenable Steel-ASTM A710," Proc. Int. Conf. "The Metallurgy, Welding, and Qualification of Microalloyed (HSLA) Steel Weldments," Nov. 6-8, Houston, TX, Pub. AWS., pp. 250-275. [G-1990-2]

Morariu, S., Doru Pascu, R., Farbas, N., and Moisa, T. 1982. "Investigations Concerning the Influence of Weld and Post-Weld Thermal Cycles on the Copper Alloyed Steels," *IIW Doc. IX-1225-82*. [G-1982-7]

DRAFT

Miyoshi, E., Hasebe, S., Benyo, K., Yamaguchi, Y. 1974. *IIW Doc. IX-878-74*. [G-1974-1]

Date:

**FOR COMMITTEE USE ONLY
NOT FOR PUBLICATION**

Miyoshi, E., Hasebe, S., and Bessyo, K. 1976. "Effect of Copper on the Weldability of Line Pipe", *IIW Doc. IX-968-76*. [G-1976-1]

Nakano, Y., et. al 1988. "Preheat and PWHT-Free, 150 mm Thick API 2W Grade 60 Steel Plate for Offshore Structures," OMAE, Houston, pp. 89-94. [G-1988-3]

Nippes, E.F., and Ball, D.J. 1982. "Copper-Contamination Cracking: Cracking Mechanism and Crack Inhibitors," *Welding Journal*, 61(3), Mar. Res. Suppl. pp. 75-s to 81-s. [G-1982-5]

Ohnishi, K., Suzuki, S., Inami, A., Someya, R., Sugisawa, S., Furusawa, J. 1988. "Advanced TMCP Steel Plates for Offshore Structures," Microalloyed HSLA Steels-Proc. Conf. Chicago, Sept. 24-30. ASM, pp. 215-224. [H-88-10]

Okada, H., Sekino, S., Hosoi, Y., and Murata, T. 1982. "Copper-Containing Structural Steels," *Copper in Iron and Steel*. I. Le May and L. McD. Schetky, Eds., pp. 83-111. John Wiley & Sons, New York. [G-1982-3]

Ostrovskaya, S.A., and Paton, E.O. 1964. "Assessing the Resistance of Steel to Hot Cracking in the Weld Metal," *Avt. Svarka*, No. 1. pp. 7-12. [G-1964-1]

Pickering, F.B. 1975. "High-strength, low-alloy steels—a decade of progress," *Proc. of Microalloying '75 Conf.*, Oct. 1-3, Wash, DC (Union Carbide 1977) pp. 9-30.

Plecki, R., et al. 1977. "Fatigue Resistance of Oxygen Cut Steel," *Welding Journal Research Supplement*, Aug., pp. 225s-230s.

Savage, W.F., Nippes, E.P., and Mushala, M.C. 1978a. "Copper-Contamination Cracking in the Weld Heat-Affected Zone," *Welding Journal*, 57(5), May. Res. Suppl. pp. 145-s to 152-s. [G-1978-1]

Savage, W.F., Nippes, E.P., and Mushala, M.C. 1978b. "Liquid-Metal Embrittlement of the Heat-Affected Zone by Copper Contamination," *Welding Journal*, 57(8), Aug. Res. Suppl. pp. 237-s to 245-s. [G-1978-2]

Shiga, C., 1990. "Effects of steelmaking, alloying and rolling variables on the HAZ structure and properties in microalloyed plate and linepipe," *The Metallurgy, Welding, and Qualification of Microalloyed (HSLA) Steel Weldments*. Int. Conf., Houston, Nov. 6-8, pp. 327-350.

Smith, N., and Bagnall, B.I. 1968. *Brit. Weld. J.*, V.15, pp. 63-69. [H-1968-4]

Suzuki, H. 1982. "Carbon equivalent for Steel Weldability," *IIW Doc. IX-1230-82*. [H-1982-2]

Wilson, A.D. 1987. "Thermal Cutting of HSLA Bridge Steels," Report prepared for AISI, August.

WRC. 1988. Japan Pressure Vessel Research Council, "Review of Properties of TMCP Steel-Pressure Vessel Steels for Low Temperature Service," *WRC Bulletin # 334*, June. [F-1988-11]

Yurioka, N., and Kasuya, T. 1994. "A Chart Method to Determine Necessary Preheat in Steel Welding," *IIW Doc. IX-1740-94*. [G-1994-4]

DRAFT

Date:

**FCC COMMITTEE USE ONLY
NOT FOR PUBLICATION**

DRAFT

Date:

Table 1. Chemical requirements.

FOR COMMITTEE USE ONLY**Heat Analysis (max.) FOR PUBLICATION**

	A36	A572/50	Draft (6)	Draft
Carbon	0.26	0.23	0.23	0.27
Manganese	(1)	1.35 (4)	1.5	1.62
Phosphorus	0.04	0.04	0.035	0.045
Sulfur	0.05	0.05	0.045	0.055
Silicon	(2)	0.40 (2)	0.40	0.45
Nickel			0.45	0.48
Chromium			0.35	0.39
Molybdenum			0.15	0.16
Copper	(3)	(3)	0.60	0.63
Vanadium		0.15 (5)	0.15 (5)	0.17
Columbium (niobium)		0.05 (5)	0.05 (5)	0.06

- (1) Manganese 0.85 - 1.35% for shapes over 426 lb/ft.
 (2) Silicon 0.15 - 0.40% for shapes over 426 lb/ft.
 (3) Minimum 0.2 copper when specified.
 (4) Manganese minimum 0.5%.
 (5) Columbium plus vanadium 0.15% maximum. Nitrogen (0.015% max.) when added as supplement to vanadium shall be reported and minimum ratio vanadium to nitrogen shall be 4 to 1.
 (6) Maximum carbon equivalent (heat analysis) is 0.5% where

$$CE = C + \frac{(Mn + Si)}{6} + \frac{(Cr + Mo + V + Cb)}{5} + \frac{(Ni + Cu)}{15}$$

00599

DRAFT

Date:

FOR COMMITTEE USE ONLY**NOT FOR PUBLICATION**

Table 2. Example compositions based on maximum carbon equivalent

	Steel 1	Steel 2	Steel 3
C	0.23	0.17	0.07
Mn	0.8	1.1	1.25
P	0.035	0.035	0.035
S	0.045	0.045	0.045
Si	0.2	0.2	0.2
Ni	0.45	0.1	0.45
Cr		0.35	0.35
Mo		0.15	0.15
Cu	0.6	0.1	0.6
V	0.15		0.08
Cb			
CE	0.497	0.5	0.498
P _{cm}	0.329	0.266	0.212
CEN	0.463	0.455	0.291

DRAFT

Table 3. Minimum manganese levels in various specifications for shapes
(Heat Analysis) Date:

**FOR COMMITTEE USE ONLY
NOT FOR PUBLICATION**

Specification	C % max.	S % max.	Mn % min.	Comments
A36	0.26	0.05	None	Shapes < 426 lb/ft
			0.85	Shapes > 426 lb/ft
A572/50	0.23	0.05	0.5	
A588	0.17	0.05	0.5	Grade K
CSA G40.21/350	0.28 (0.32 for >20 mm)	0.05	None	General grade
	0.23	0.05	0.5	Weldable grade
	0.22	0.04	0.8	Toughness grade
Draft	0.23	0.045	None	

00900

DRAFT

Date:

FOR COMMITTEE USE ONLY

Table 4. Reference weld metal compositions.

	Steel Example			Weld Metal Example		
	1	2	3	1	2	3
C	0.23	0.07	0.07	0.208	0.08	0.08
Mn	0.6	1	1	0.78	1.1	1.1
Si	0.2	0.2	0.2	0.26	0.26	0.26
Cb		0.05	0.05		0.04	0.04
Cu		0.6	0.6		0.5	0.5
Ni		0.45	0.45		0.36	0.36
Cr		0.35	0.35		0.28	0.28
Mo		0.15	0.15		0.12	0.12
P	0.035	0.035	0.01	0.03	0.03	0.01
S	0.045	0.45	0.02	0.04	0.04	0.02
	UCS			49	20	13

DRAFT

Table 5. Maximum copper levels in structural steels. Date:

FOR COMMITTEE USE ONLY
NOT FOR PUBLICATION

Specification	C % maximum	Cu % maximum
A36	0.26	0.2 min, when specified No maximum
A572	0.23	0.2 min, when specified No maximum
A710	0.07	1.3
A588 (K)	0.17	0.5
A871	0.2	1.0
G40.21/350A	0.2	0.6

Table 6. Statistical data on copper and tin levels from typical sample of electric furnace steel.

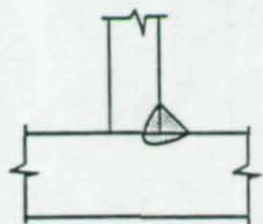
	Tin %	Copper %
Mean	0.0215	0.3556
Coefficient of variation	0.2353	0.1553
Minimum value	0.012	0.210
Maximum value	0.045	0.490

(Sample size = 117)

DRAFT

Date:

FOR COMMITTEE USE ONLY
NOT FOR PUBLICATION



1. Single pass fillet weld



2. Single pass electroslag weld



3. Multipass groove weld



4. Multipass groove weld in moment resisting connection

Figure 1. Examples of weld joints encountered in welding structural shapes.

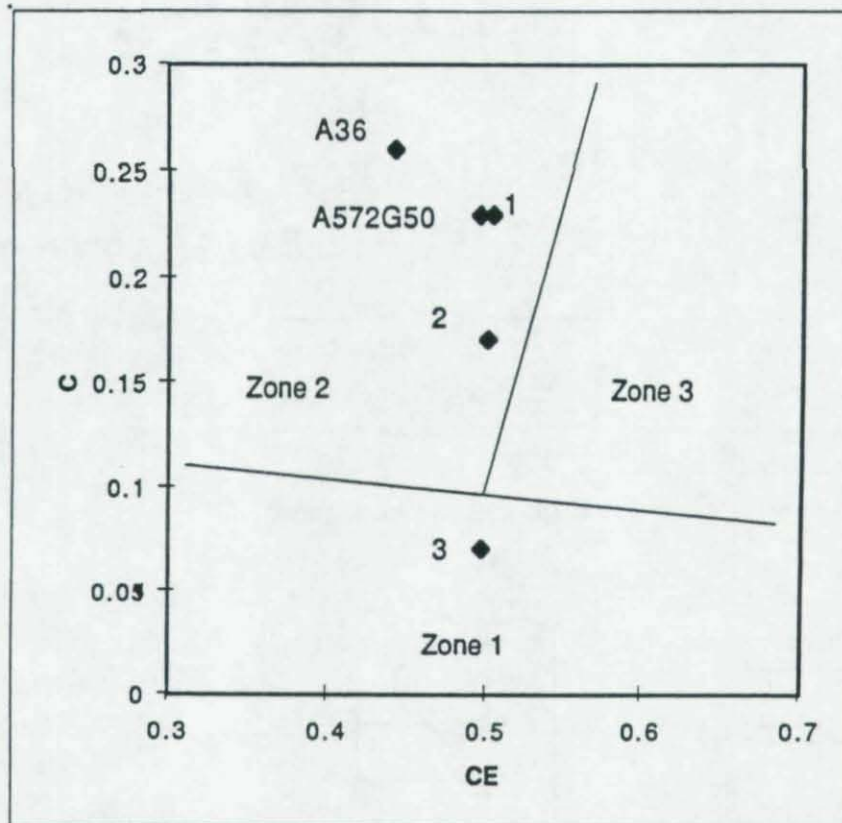


Figure 2. Zone diagram for estimating weldability behavior showing location of example steels.

DRAFT

Date:

FOR COMMITTEE USE ONLY
NOT FOR PUBLICATION

00602

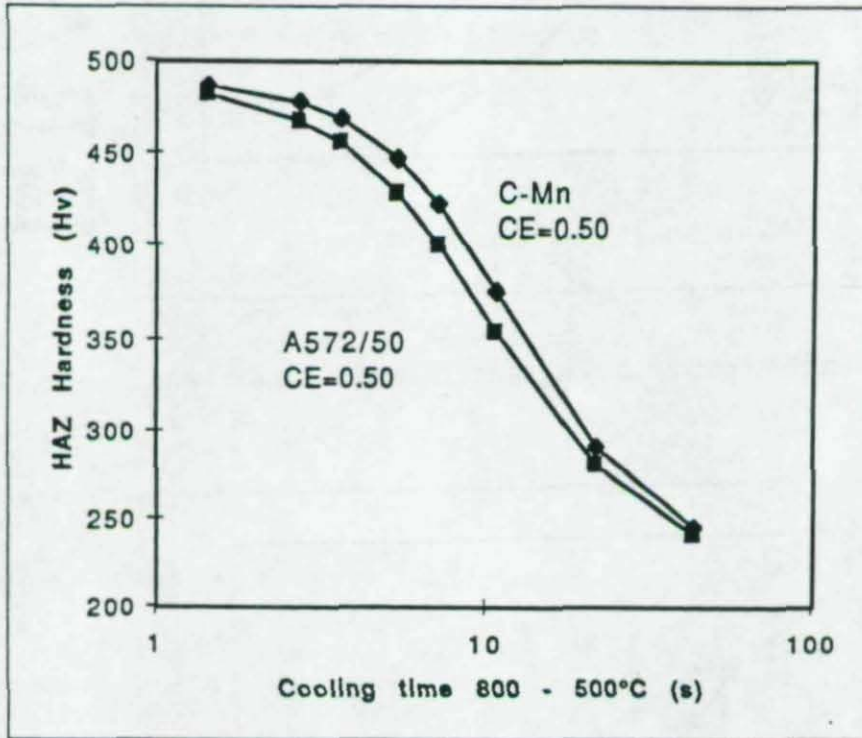


Figure 3. Estimated hardening curves for A572/50 and C-Mn steel with equal carbon equivalent.

DRAFT

Date:

**FOR COMMITTEE USE ONLY
NOT FOR PUBLICATION**

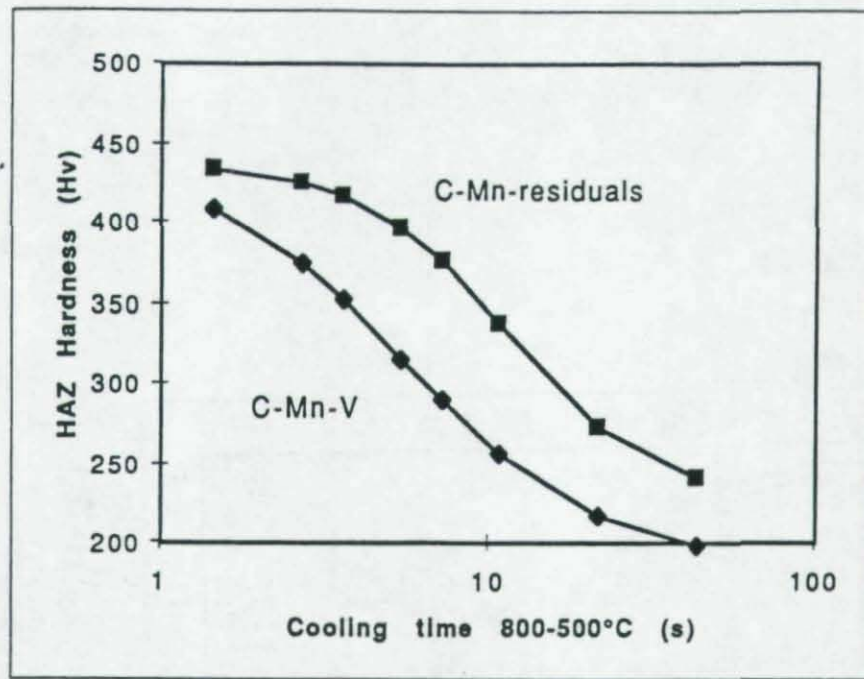


Figure 4. Hardening curves showing effect of residuals at the same carbon level.

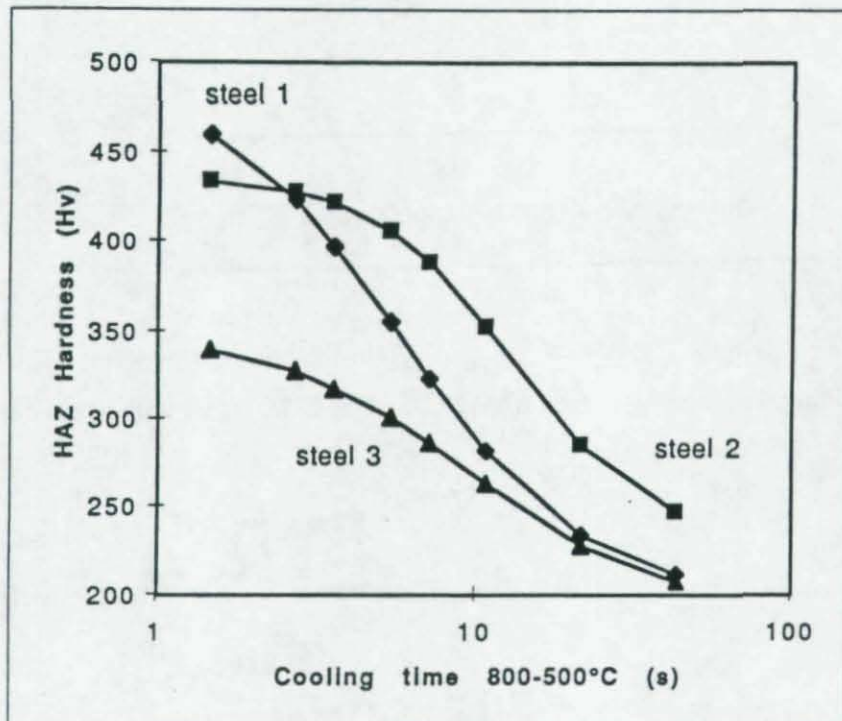


Figure 5. Hardening curves for three example steels with the same carbon equivalent.

DRAFT

Date:

**FOR COMMITTEE USE ONLY
NOT FOR PUBLICATION**

00603

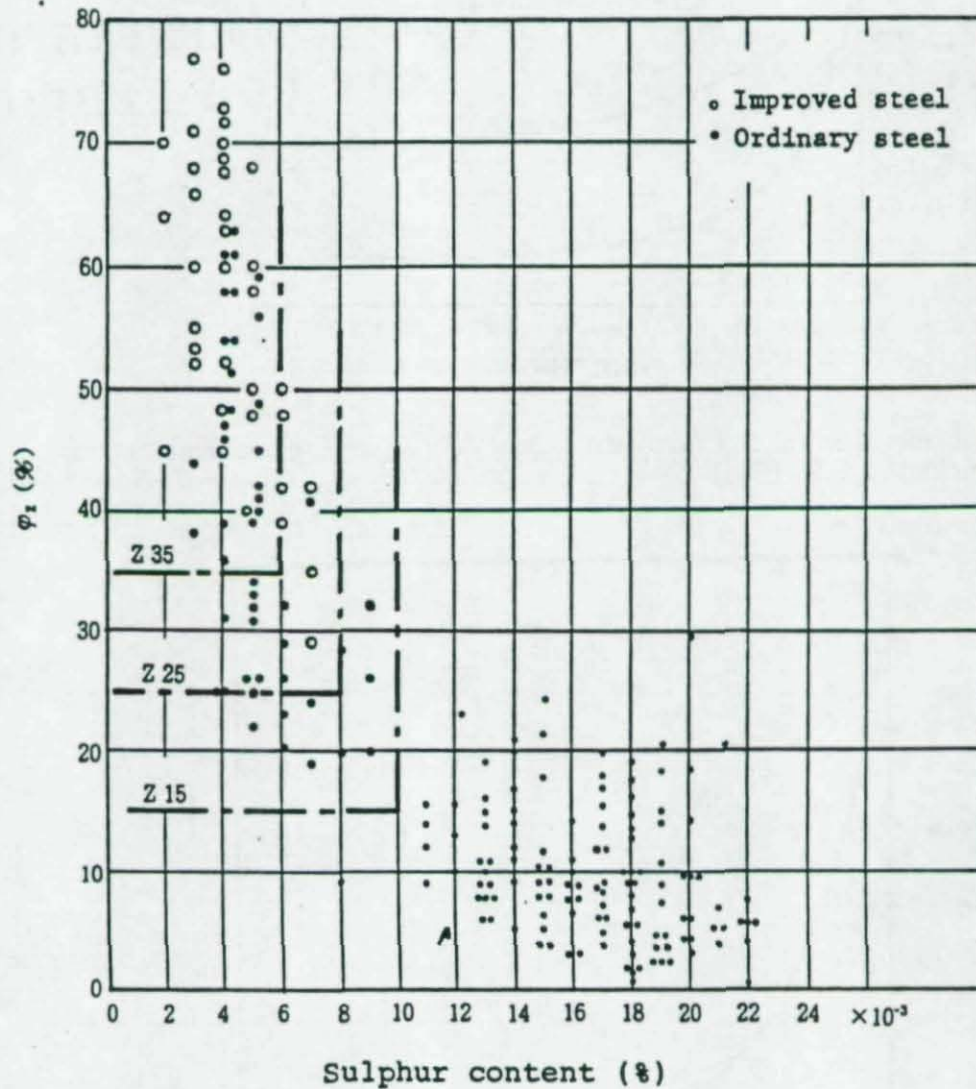


Figure 6. Relationship between sulfur content and reduction of area in through-thickness direction, ϕ_2 . [Inagaki, M. 1982]

DRAFT

Date:

FOR COMMITTEE USE ONLY
NOT FOR PUBLICATION

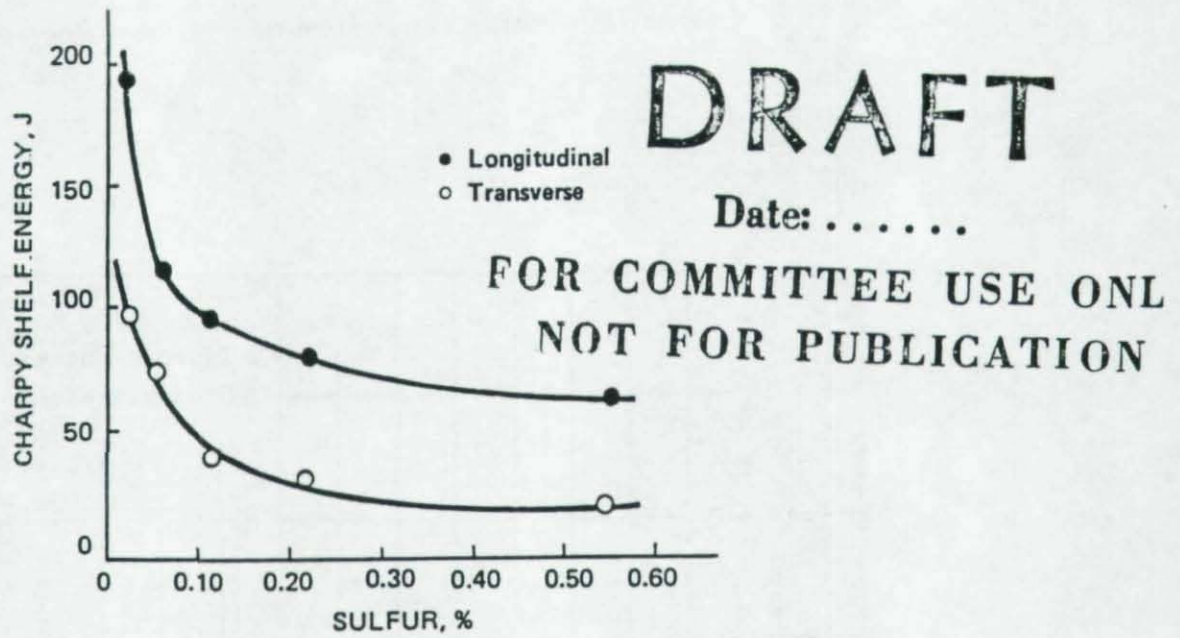


Figure 7. Effect of sulfur on Charpy shelf energy during longitudinal and transverse testing. [Pickering, F.B. 1975]

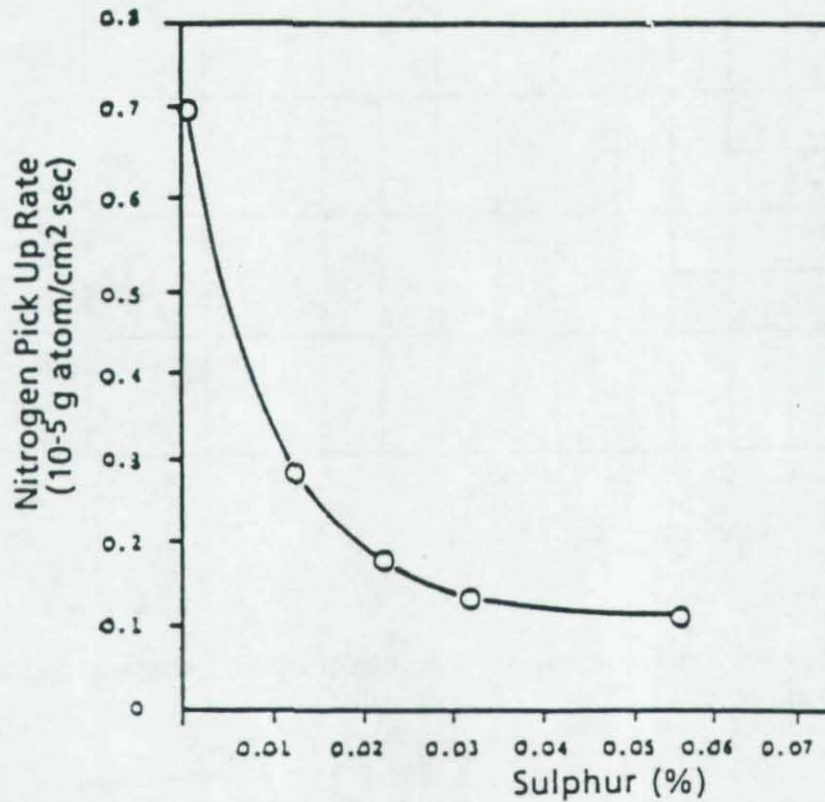


Figure 8. Effect of sulfur on the rate of nitrogen pickup. [Irving, W.R., 1993]

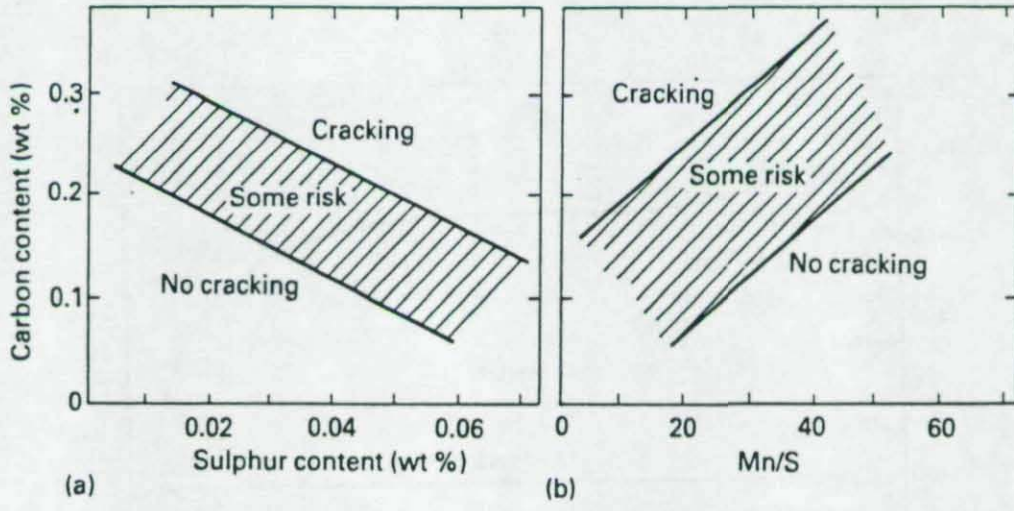


Figure 9. Relationship between steel composition and occurrence of HAZ hot cracking (liquation cracking) in welds with heat inputs of 50 kJ/in. (2 kJ/cm) [Bailey, 1974 after Widgery]

DRAFT

Date:

FOR COMMITTEE USE ONLY

NOT FOR PUBLICATION

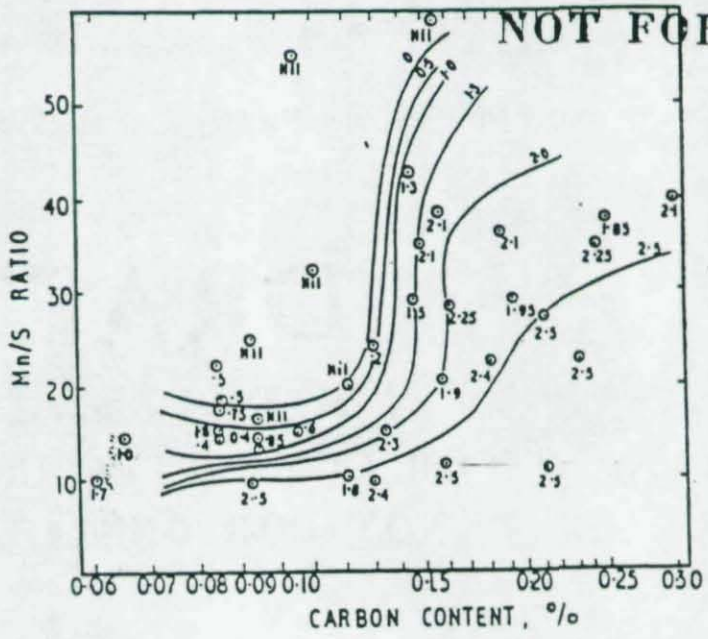


Figure 10. Effect of carbon and Mn/S ratio on severity of cracking in hot cracking test. The lines represent contours of equal severity. [Jones, 1959]

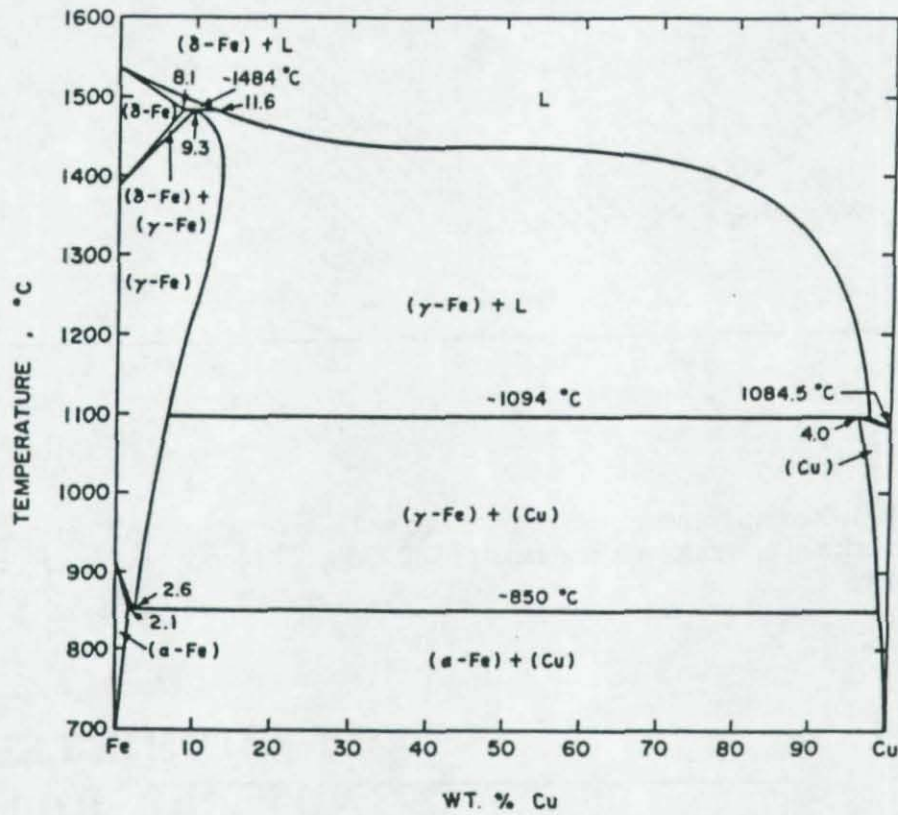
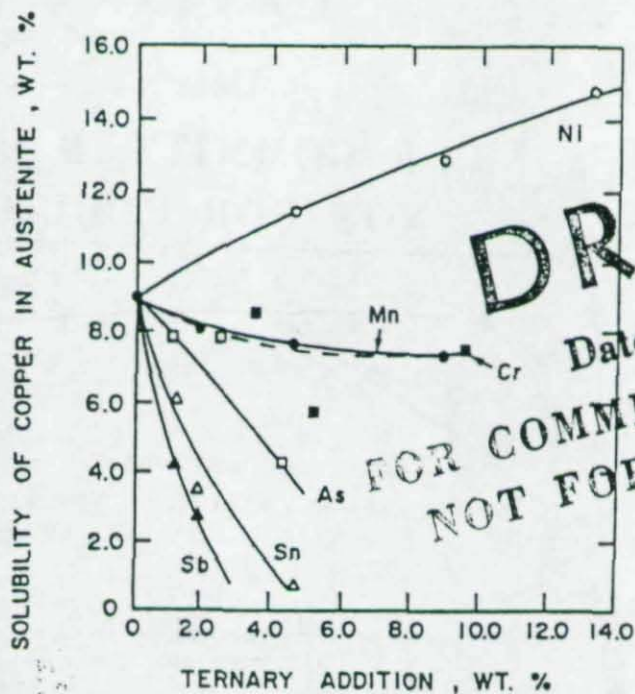


Figure 11. The iron-copper phase diagram. [Le May, I., et. al. 1982].

DRAFT

Date:

**FOR COMMITTEE USE ONLY
NOT FOR PUBLICATION**



DRAFT
 Date:
 FOR COMMITTEE USE ONLY
 NOT FOR PUBLICATION

Figure 12. Effect of ternary additions on solubility of copper in austenite at 1250°C. [Habraken, L., et. al. 1982]

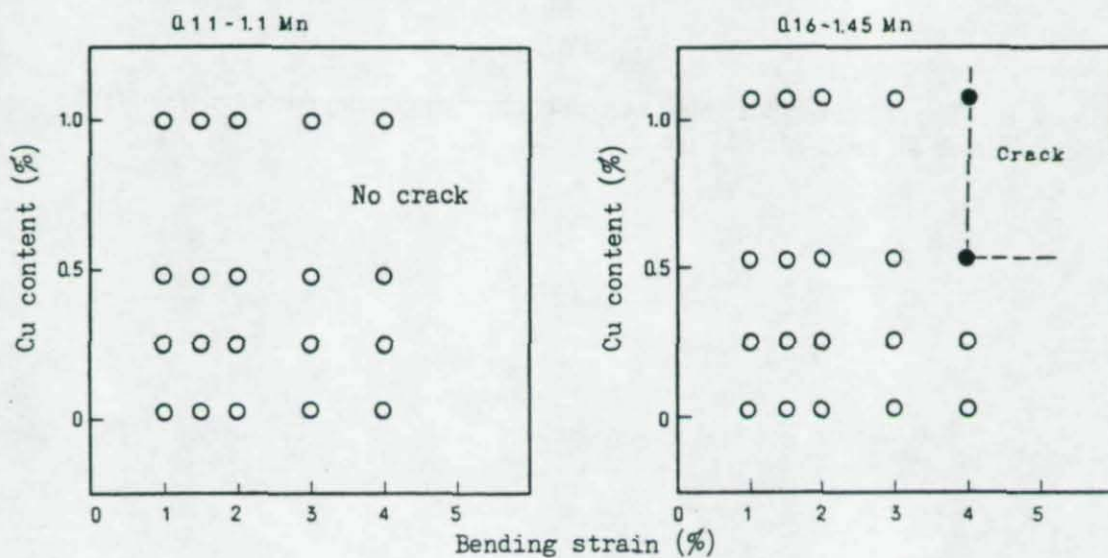


Figure 13. Effect of copper content on cracking in V-restraint test. [Miyoshi, E., et. al. 1976]

DRAFT

Date:

FOR COMMITTEE USE ONLY
NOT FOR PUBLICATION

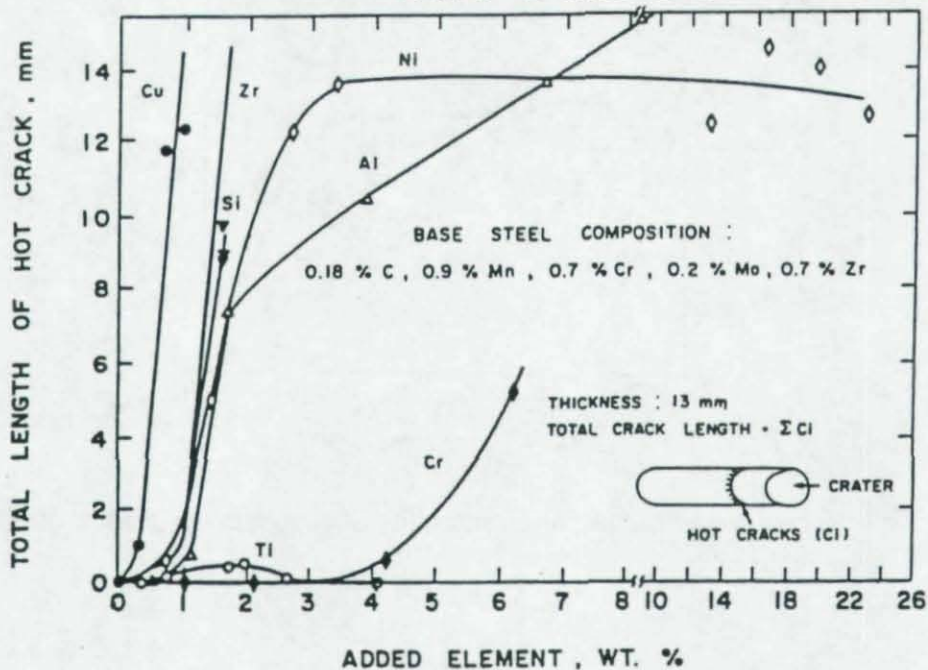


Figure 14. The effect of added elements on hot cracking using the Varestraint test. [Okada, H., et. al. 1982, after Matsuda]

DRAFT

Date:

FOR COMMITTEE USE ONLY

NOT FOR PUBLICATION

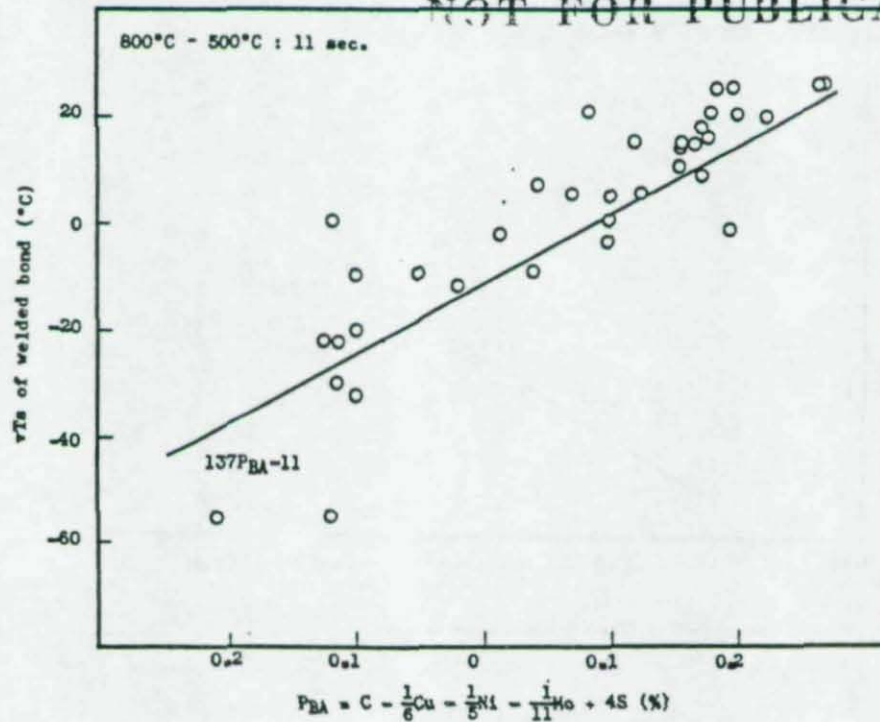


Figure 15. Relationship between formula of susceptibility in steel for bond brittleness (P_{BA}) and measured Charpy vT s of welded bond when quenched microstructure of martensites and lower were formed in the cooling time on the critical range of about 11 sec. [Ito, Y., et. al. 1973]

DRAFT

Date:

FOR COMMITTEE USE ONLY
NOT FOR PUBLICATION

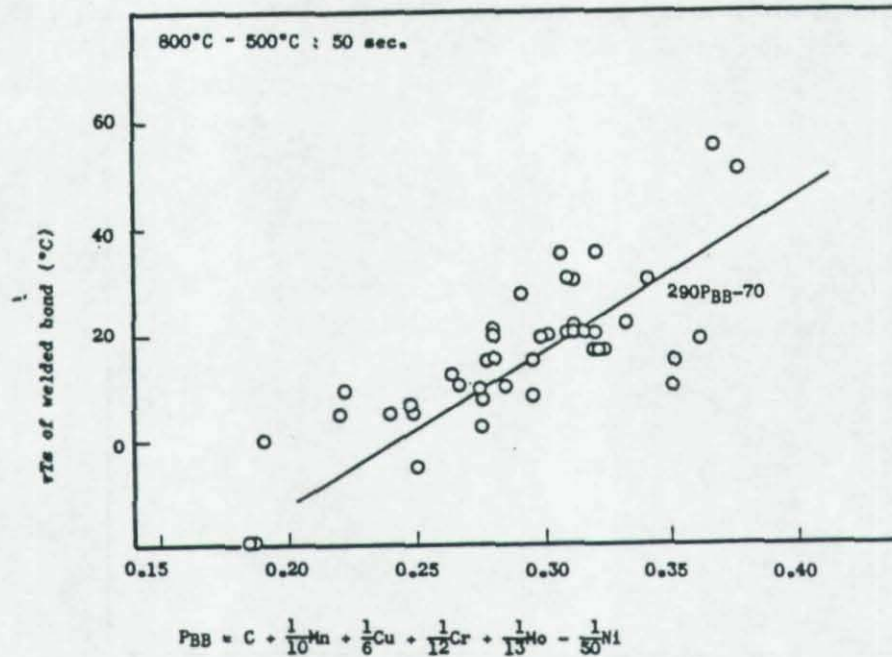


Figure 16. Relationship between formula of susceptibility in steel for bond brittleness (P_{BB}) and measured Charpy vT_s of welded bond when the intermediate microstructure of upper bainites and ferrites were formed in the cooling time on the critical range of about 50 sec. [Ito, Y., et. al. 1973]

DRAFT

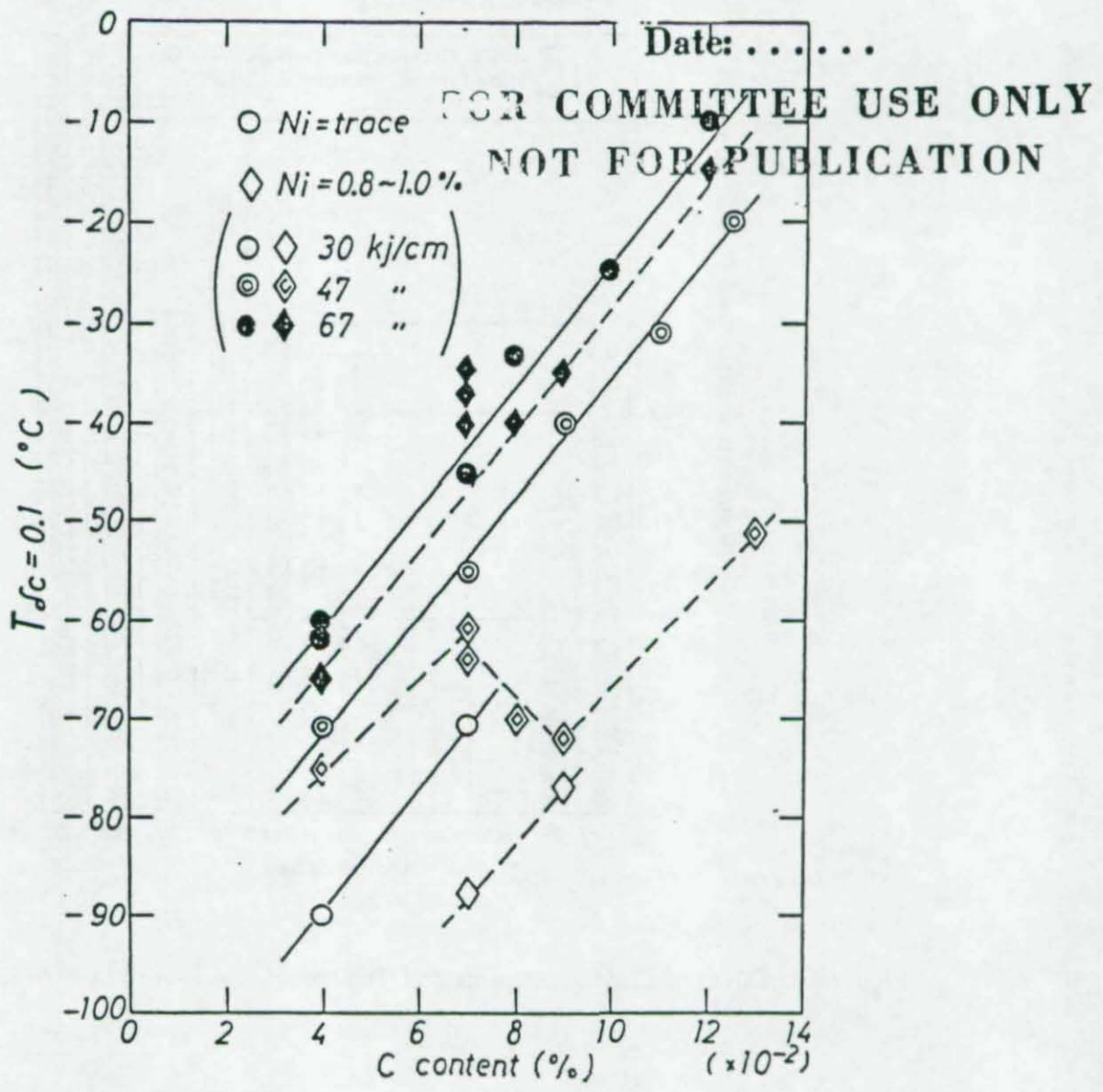


Figure 17. The relation between CTOD transition temperature and carbon content. [Miyoshi, E., et al., 1974]

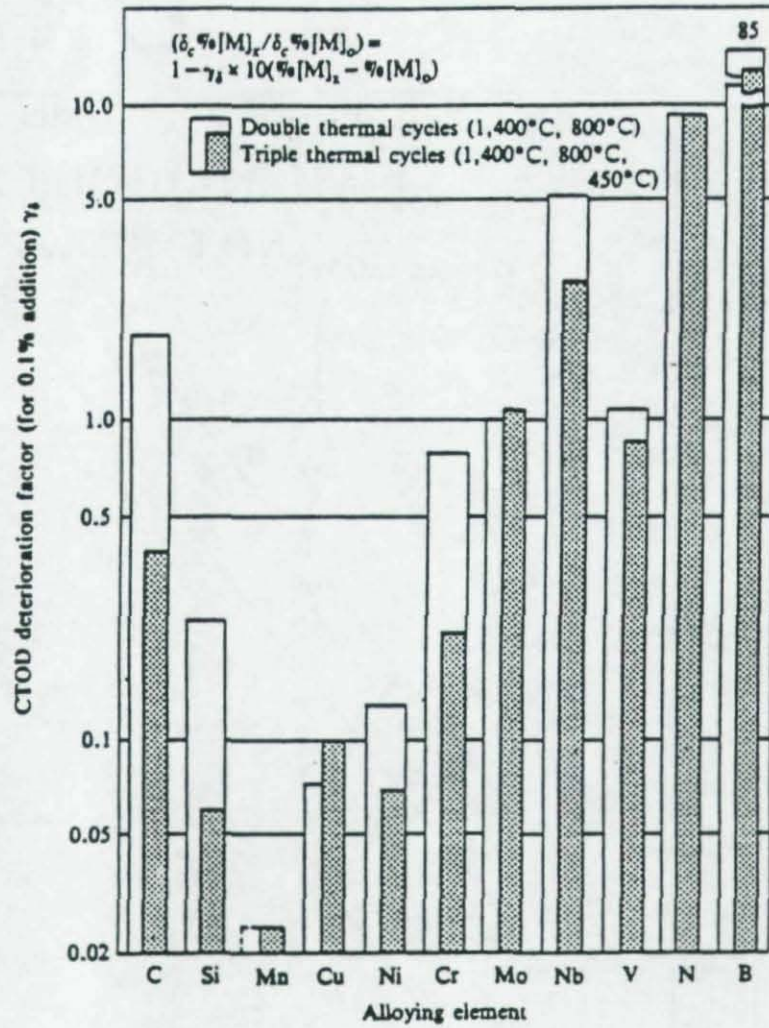


Figure 18. Effect of alloying elements on CTOD toughness in the HAZ. [Haze, T., et. al. 1988].

DRAFT

Date:

**FOR COMMITTEE USE ONLY
NOT FOR PUBLICATION**

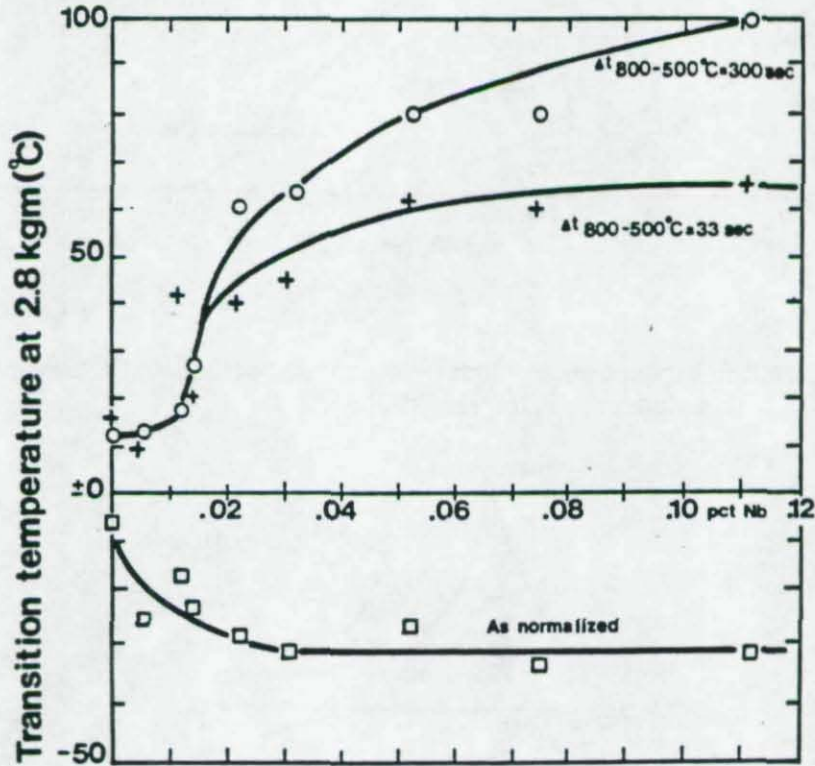


Figure 19. The influence of HAZ simulation on the transition temperature of treated steels. C = 0.19, Mn = 1.33 pct, T_{max} = 1350°C . [Hannerz, N.E. 1976]

DRAFT

Date:

FOR COMMITTEE USE ONLY
NOT FOR PUBLICATION

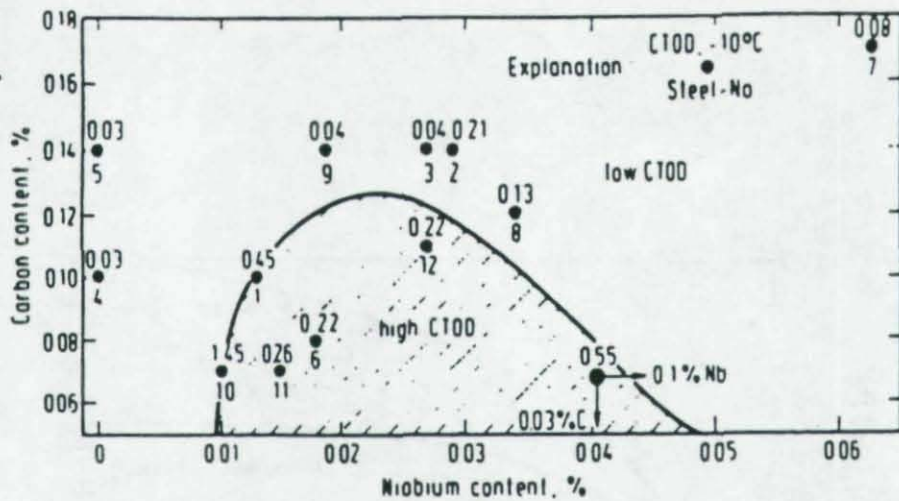


Figure 20. Relation between columbium (niobium) and carbon and achievable CTOD values at -10°C . [Heisterkamp, F., et. al. 1990]

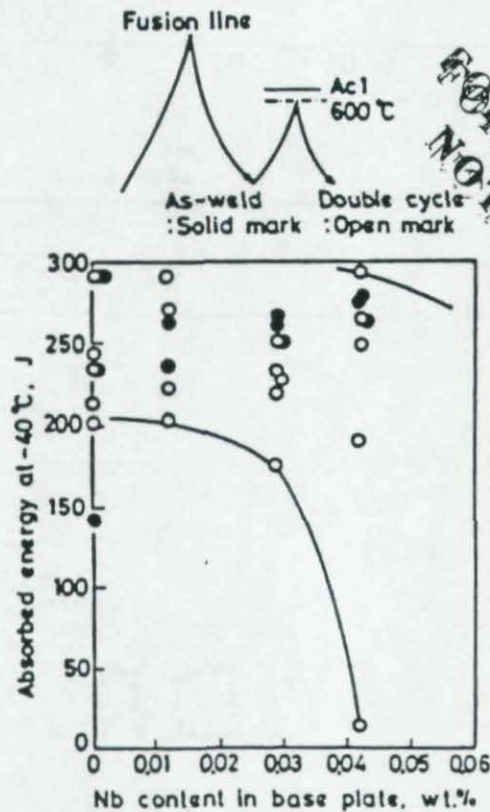


Figure 21. Effect of columbium (niobium) content on toughness of subcritically reheated grain coarsened HAZ. [Nakano, Y., et. al 1988]

DRAFT
 Date:
 FOR COMMITTEE USE ONLY
 NOT FOR PUBLICATION

60900

DRAFT

Date:

FOR COMMITTEE USE ONLY
NOT FOR PUBLICATION

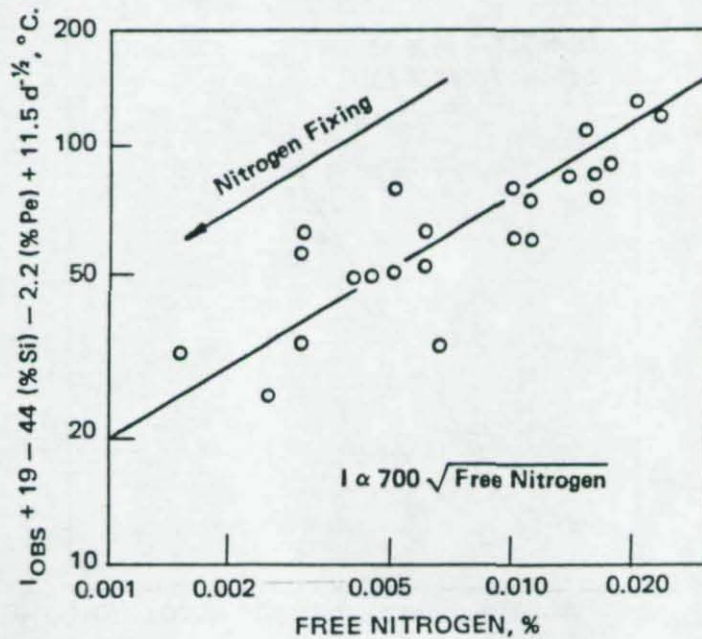


Figure 22. The effect of free nitrogen on the impact-transition temperature of normalized carbon-manganese steels (silicon-killed). The impact-transition temperature (I) has been corrected for differences in silicon content, pearlite percentage and ferrite-grain size. [Gladman, T., et. al. 1975]

DRAFT

Date:

FOR COMMITTEE USE ONLY

NOT FOR PUBLICATION

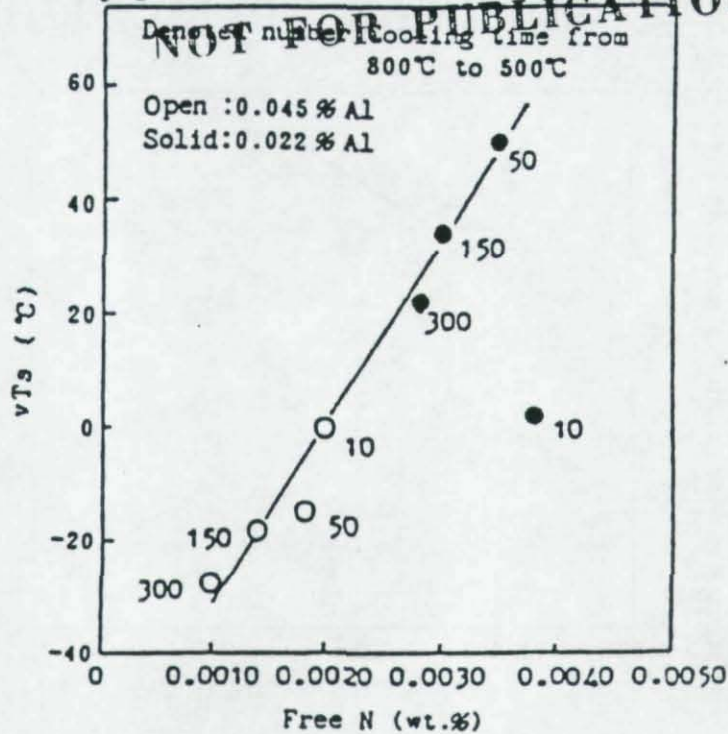


Figure 23. Effect of free-N on simulated HAZ toughness. [WRC. 1988]

DRAFT

Date:

FOR COMMITTEE USE ONLY
NOT FOR PUBLICATION

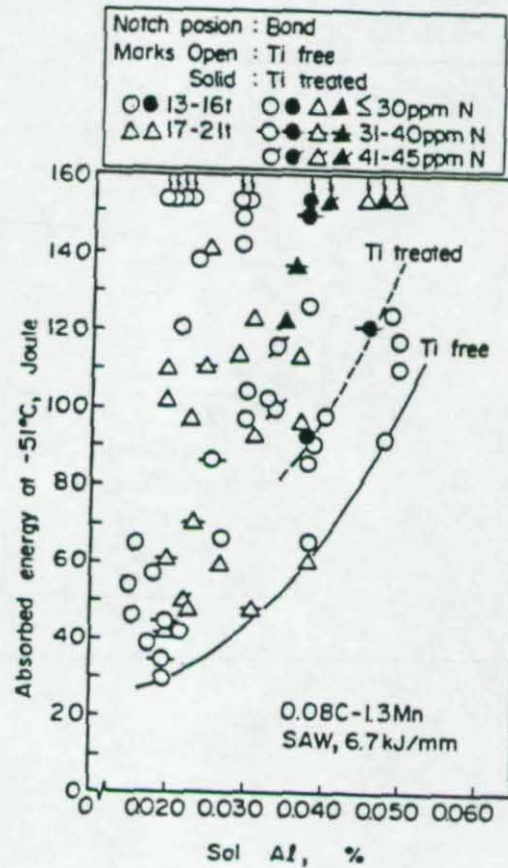


Figure 24. Effects of Al, N and Ti on HAZ toughness of 0.08% C - 1.3% Mn steels. [Kitada, T., et al. 1986]

DRAFT

Date:

FOR COMMITTEE USE ONLY
NOT FOR PUBLICATION

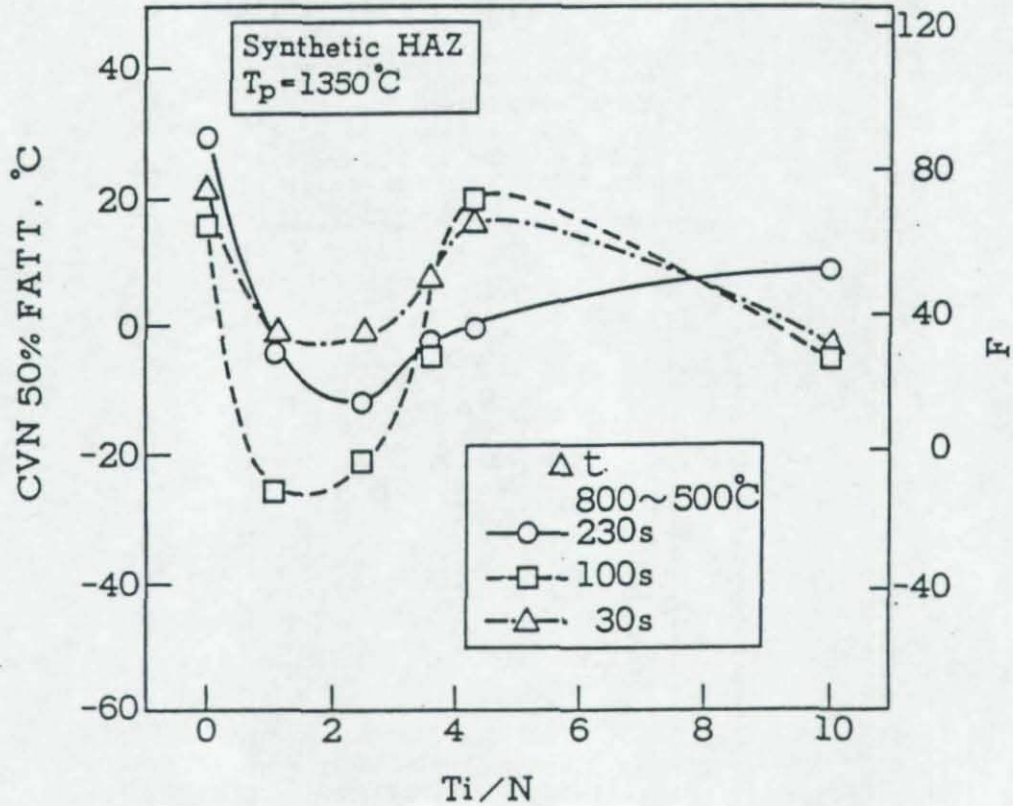


Figure 25. Effect of titanium to nitrogen ratio, Ti/N, on synthetic HAZ toughness, CVN 50% FATT. [Shiga, C. 1990]

DRAFT

Date:

FOR COMMITTEE USE ONLY
NOT FOR PUBLICATION

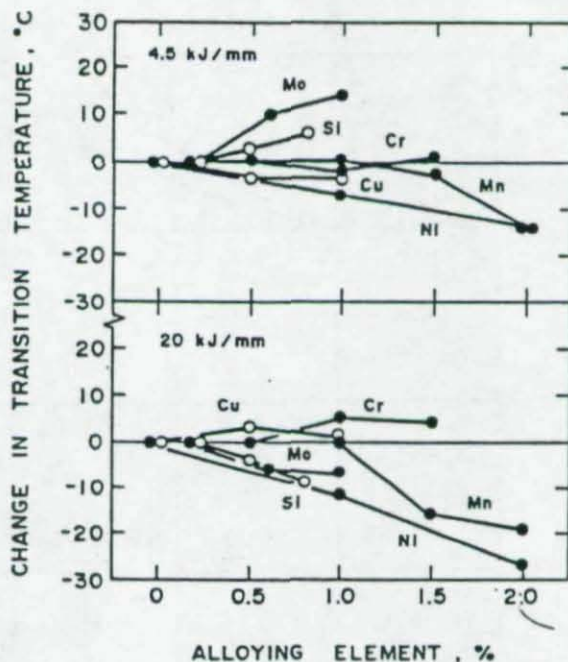


Figure 26. The effect of alloying elements on the shift of the Charpy impact transition temperature at the fusion line after two different welding procedures. [Okada, H. et. al. 1983 after Tanaka, et. al.]

DRAFT

Date:

FOR COMMITTEE USE ONLY
NOT FOR PUBLICATION

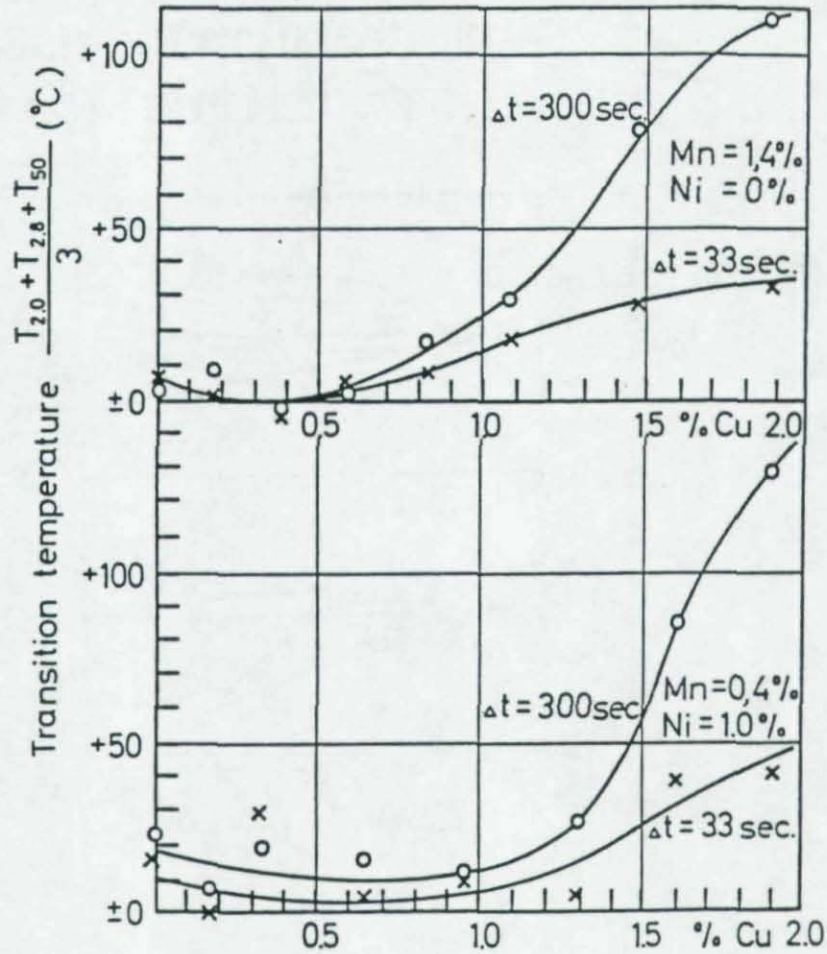


Figure 27. The influence of copper and heat input on HAZ Charpy transition temperature of CMn and CMnNi steel. [Hannerz, N.E. 1983]

DRAFT

Date:

FOR COMMITTEE USE ONLY
NOT FOR PUBLICATION

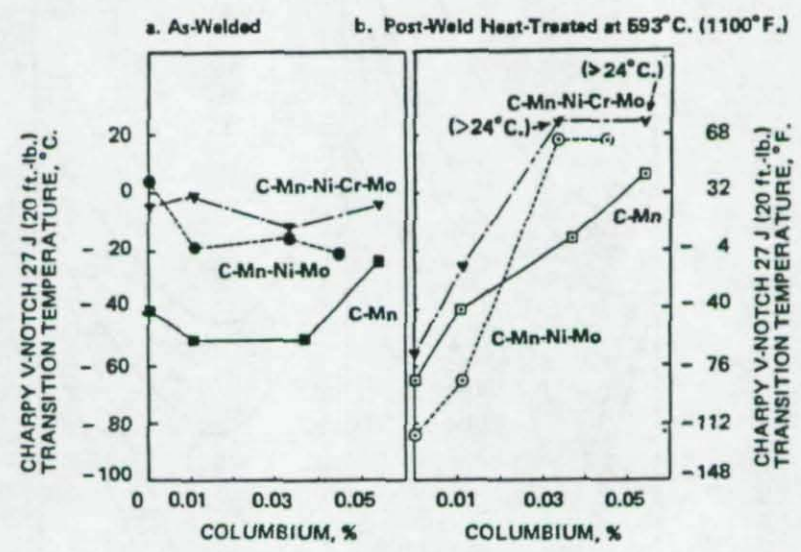


Figure 28. Effect of columbium content in two-pass submerged-arc weld deposits on Charpy V-notch 27 J (20 ft-lb) transition temperature. [Jesseman, R.J. 1975]

DRAFT

Date:

FOR COMMITTEE USE ONLY

NOT FOR PUBLICATION

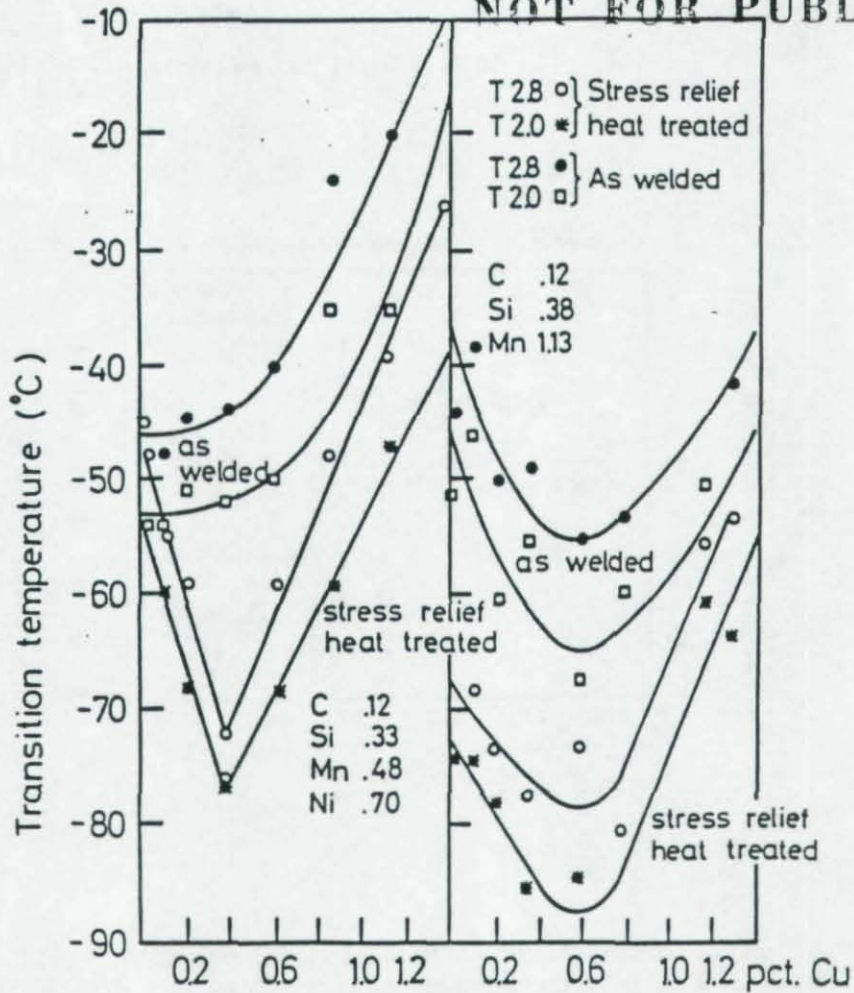


Figure 29. The influence of copper on Mn and CMnNi high heat input weld metal in the as-welded and in their stress relieved condition. (Hannerz) T2.8 is Charpy-V transition temperature at 2.8 kgm, etc. [Hannerz, N.E. 1987]

DRAFT

Date:

FOR COMMITTEE USE ONLY
NOT FOR PUBLICATION

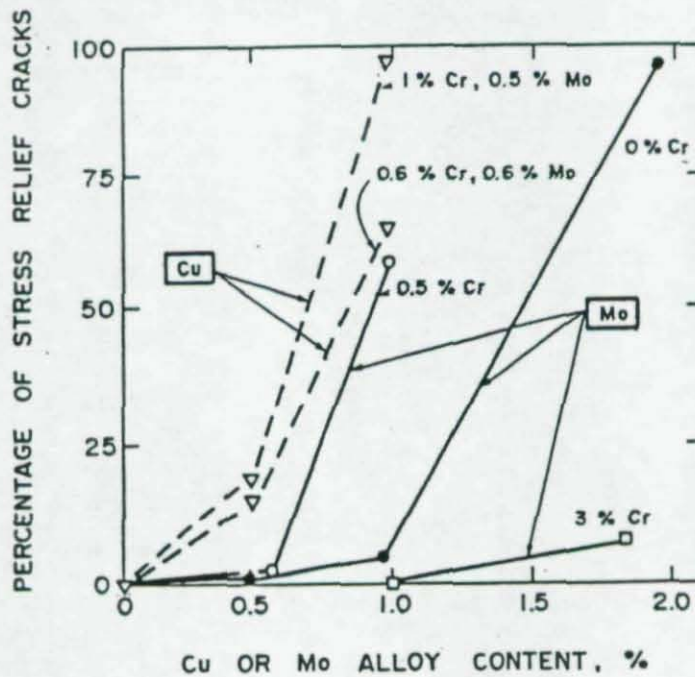


Figure 30. The effect of copper and molybdenum on stress relief cracking in low alloy steels. [Okada et al., 1982 after Ito and Nakanishi]

AISC E&R Library



8506

RR3046
v. 2

8506

Contents

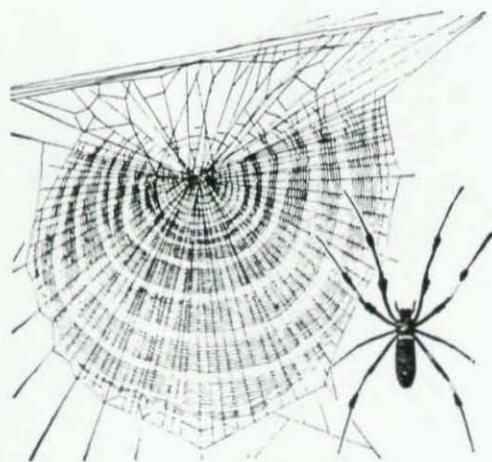
	Page
Foreword.....	1
Introduction to Cable Structures.....	2
Steel Cable Creates Novel Structural Space Systems.....	14
Some Outstanding Buildings.....	22
Design Examples.....	34
Wire Rope and Strand for Structures.....	40
Connections and Hardware.....	49
Socketing.....	72
How We Make Bethlehem Wire Rope and Strand.....	74
Glossary.....	77

Introduction to Cable Structures

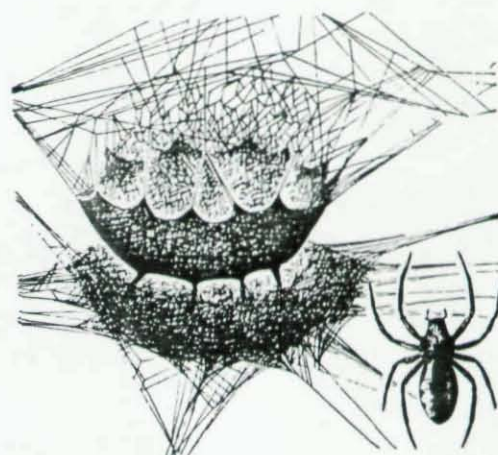
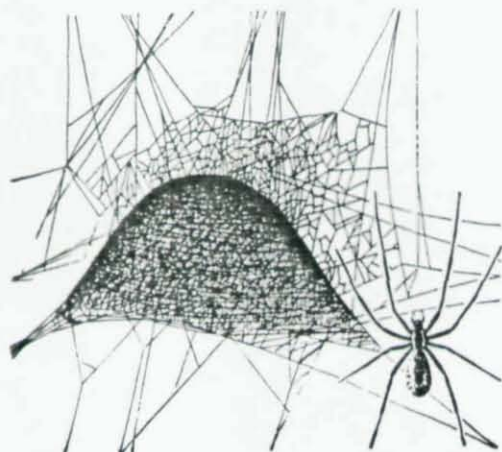
by Richard M. Gensert

The Spider Web

The most obvious cable structure in nature is the spider's web. As a single-plane structure, the web normally takes on the form of a radial pattern for the primary members, and a nearly concentric form, or spiral for the secondary members.



A dome-shaped web consists of concentric or hoop members acting as primary elements; the inter-connecting members are in a random pattern.



The bowl-shaped web consists entirely of random members that make up this doubly curved surface. Hoop forces cannot exist due to the bowl shape and the tie-downs.

Since forms in nature are influenced by environment, growth rate of the species, age and time, specific tension of organic materials, heredity, and other factors, it is difficult to separate each influencing or motivating cause. Nevertheless, we can be certain of one determinant, and that is the minimal effect—every line, every angle, every curvature defines an equilibrium between forces that are acting and the forces they resist.

Likewise, in building structures we should be looking for the same efficiency; that is the optimum effect. In spite of man's frailties, he has made a concerted effort to match, and at times to surpass, nature's highly sophisticated approach to design.

Early Suspension Structures

It is difficult to determine when the first man-made suspension structures were built. Most likely they were bridges rather than buildings. The state of the art in Java, Burma, and surrounding countries leads one to think that this type of structure originated in the Far East where bamboo and hemp were used for cables and suspenders. In China, rope and iron chains were used for

Richard M. Gensert is Principal, R. M. Gensert Associates, Consulting Engineers, Cleveland and Pittsburgh.

The Catenary Curve

During the 18th Century, science was merely a means or medium for serving theology. The interest in a deity often took on the form of mathematical and physical investigation into minimum or maximum conditions of natural phenomena. The curvature of a projectile path, the flow of magnetic forces, the motion of light, all were studied as a means of realizing the metaphysical and theological principle of achieving the greatest effect with the least effort.

The catenary curve was also part of this great effort in the study of the minimal effect. A chain, suspended from two fixed points, will assume that form at which the center of gravity is in the lowest possible position. With this principle in mind, Jakob Bernoulli in 1690 determined the equation of the catenary. The Scottish mathematician, D. Gregory, in 1697, published a treatise on the properties of the catenary, wherein he determined its form as a graphical representation of equal forces positioned at equal distances along a cable and in equilibrium with each other and their reactions.

The Italian mathematician and engineer, Poleni, in 1748, established other forms of a free cable supporting different magnitudes of loads at various positions along its length. The parabola was formed by positioning equal forces at equal distances along a horizontal between the two supports of the cable.

Modern Suspension Bridges

Thus, during the 18th Century, equations for the shape of cables under various loading conditions and their static analysis were developed. That century also produced the first modern suspension bridge, built in North America in 1796, by J. Finley.

The 19th Century produced many suspension bridges, particularly in the United States. The first suspension systems used either iron chains or flat iron bars. In 1816, the first wire cable suspension bridge was built, and in 1870, Roebling built the Brooklyn Bridge with its secondary cable system that counteracts the aerodynamic effect ordinarily referred to as "flutter."

Structural Concept

To better understand the cable as a flexible spanning element, we might first compare it with the rigid spanning element commonly known as the "truss."

Trusses are rigid, horizontal spanning elements that support loads by means of internal bending resistance. The bending resistance is accomplished by compression and tension forces working simultaneously within the framework as shown on page 5. Trusses can be shaped to fit their moment diagrams and their shear diagrams.

If a cable is flexible and cannot withstand compression and shear, we could draw an analogy with the truss by removing those portions that withstand compression and shear.

We find it necessary to replace the internal horizontal compression force of the truss with external tension forces for the cable to keep it in equilibrium. The depth of the truss withstanding bending now becomes the sag of the cable, and the bottom chord defines the cable profile.

Structural Geometry and Stress

If we keep the sag, span, and the total load on the cable at a constant value, the slope (θ) of the cable at its support will vary with the shape of the cable, which in turn is directly affected by the distribution of the load. As the slope varies, so does the tension within the cable. Thus the total cable load concentrated at the center will produce a stress in the cable at its support that is larger than that stress produced when the load is uniformly distributed.

Sag/span ratios have been plotted against maximum cable tension, horizontal reaction at support, and weight of cable for both uniform loads and their equivalent concentrated load at center span. The optimum values are evident from the abrupt change in curvature of the graphs. From these graphs, one can see that cable economy is dependent upon cable shape. (See page 6.)

Structural Feasibility

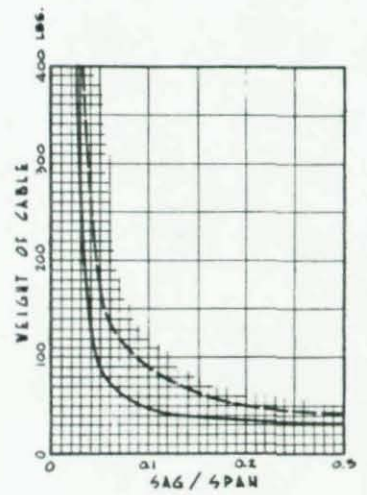
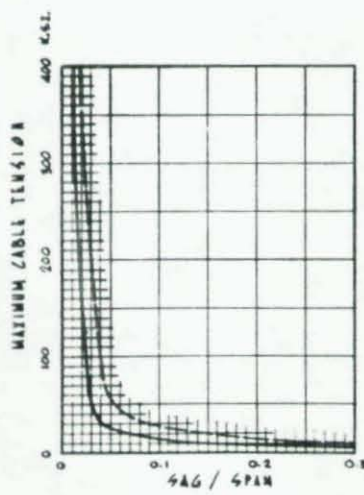
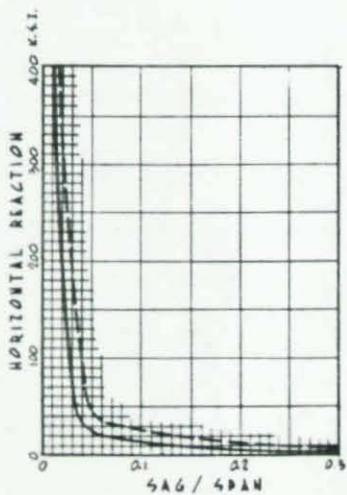
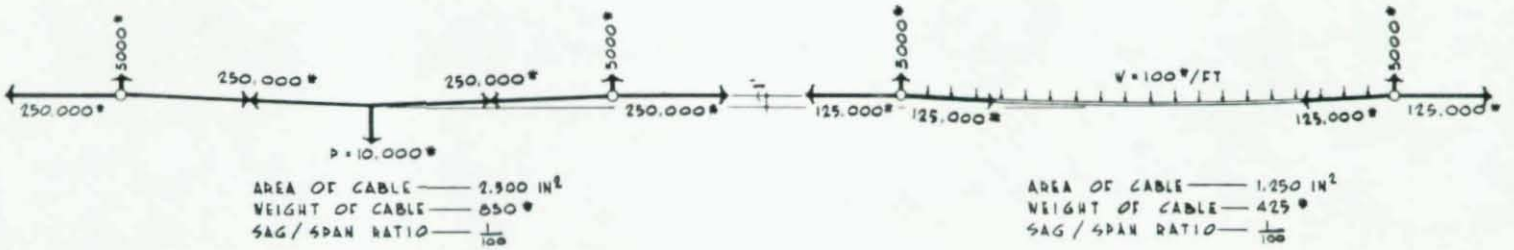
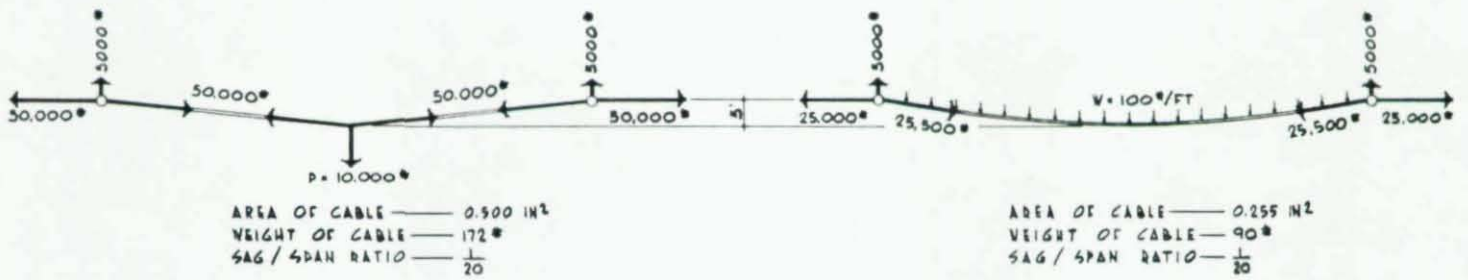
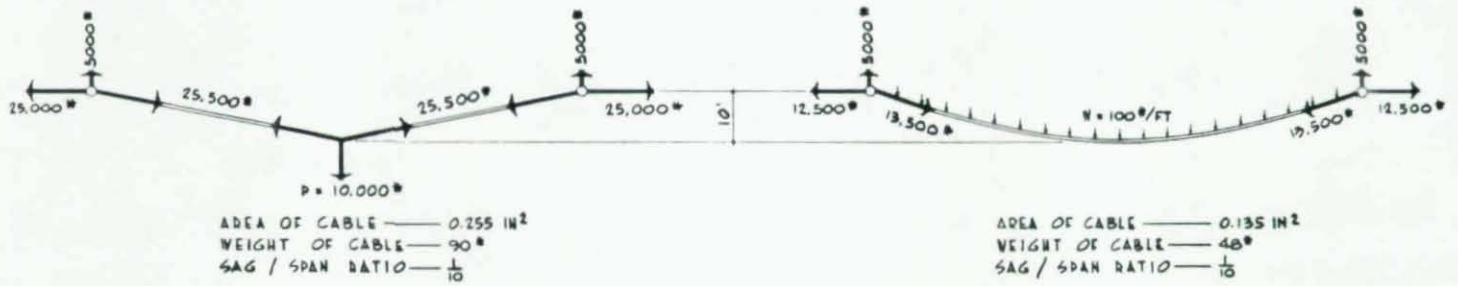
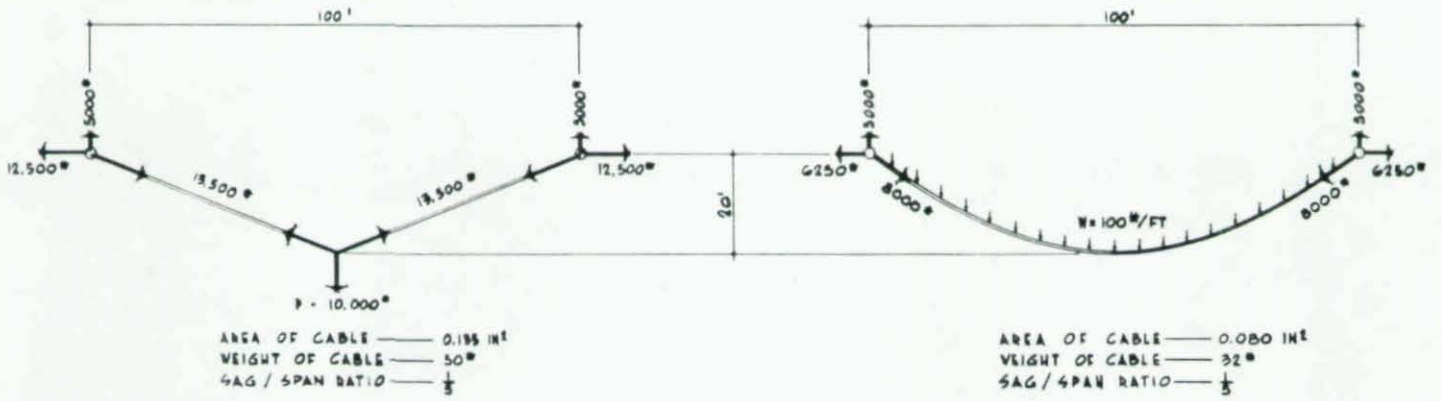
The justification of a cable structure over the plate-girder, truss, or arch can best be shown in the accompanying sketches. (See page 7.) Note that an increase in span causes structural economic problems with the plate-girder as both shear buckling and bending instability are concerned. The truss suffers from connection costs and depth of construction. The arch suffers from compression buckling, leaving the cable limitations as a function of dead weight and anchorages.

Lev Zetlin developed an ingenious approach to this problem in the United States Pavilion at Brussels, by incorporating a double set of cables with a compression ring that not only produced a self-anchoring system, but also produced a vibration-resistant system. A set of convex and concave cables springing from the same point produces a reaction on the boundary compression ring as much as twice the value of that produced by a single cable. The roof is a double-plane system.

Structural Proportions

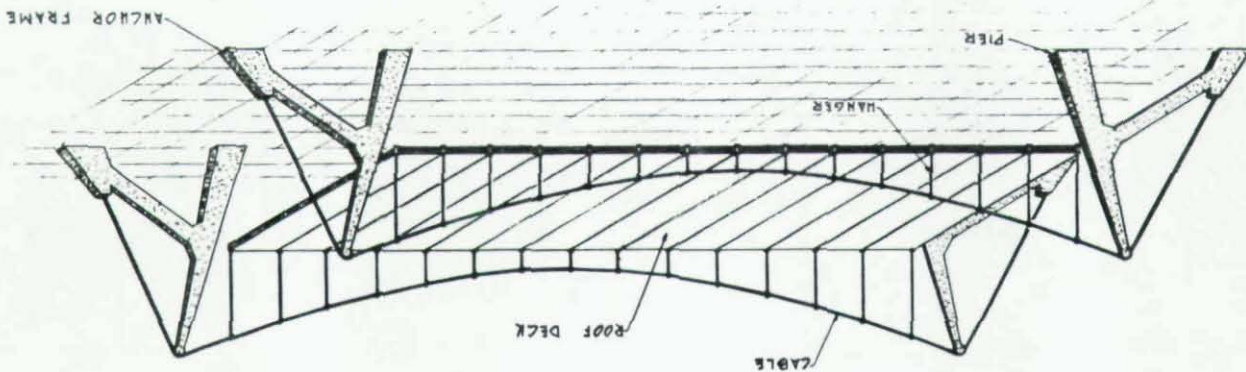
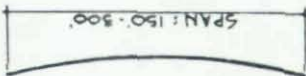
Let's consider some possible span limitations and proportions of cable systems as they may pertain to the three types of roof curvature, i.e. single curvature, double curvature (+), and double curvature (-). (Pages 8-12.)

The few possibilities in cable-supported roof structures presented in this introduction to the subject are limited by regular forms of single or double curvature. If we consider non-regular and asymmetrical forms, the possibilities are unlimited.

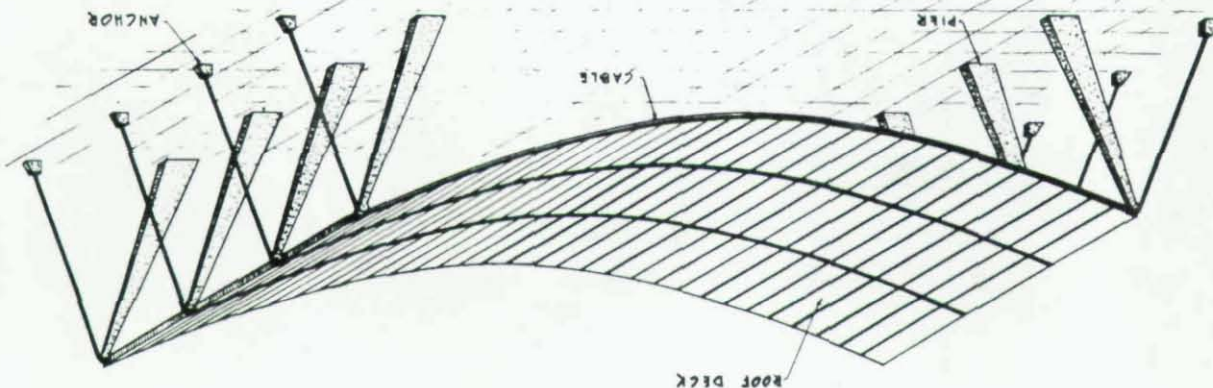
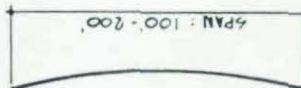


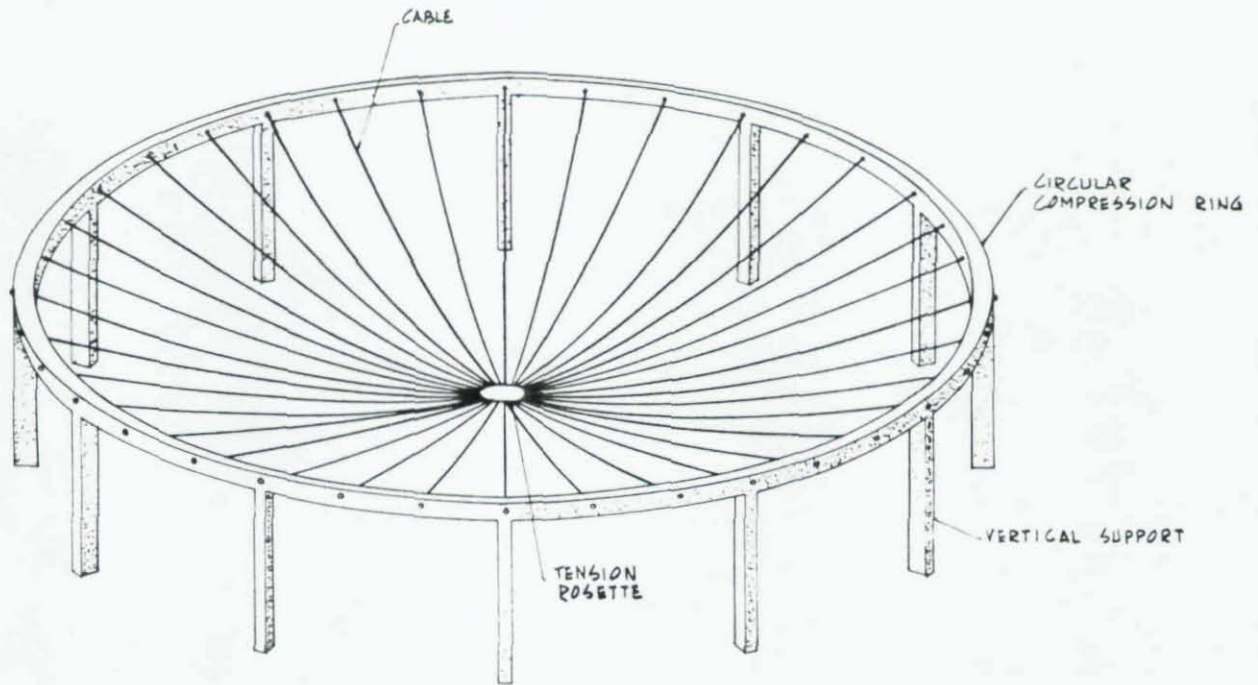
ROOFS WITH A SINGLE SET OF CABLES
SINGLE CURVATURE

ROOT DECK IS HUNG FROM CABLES.
CABLES ARE SPACED 10 TO 25 FT. O.C.
THE NUMBER OF NATURAL FREQUENCIES IS REDUCED BY THE
COMBINATION OF HEAVY ROOT DECK AND HANGERS.
TYPICAL SAG / SPAN RATIO: $\frac{1}{8}$ TO $\frac{1}{10}$

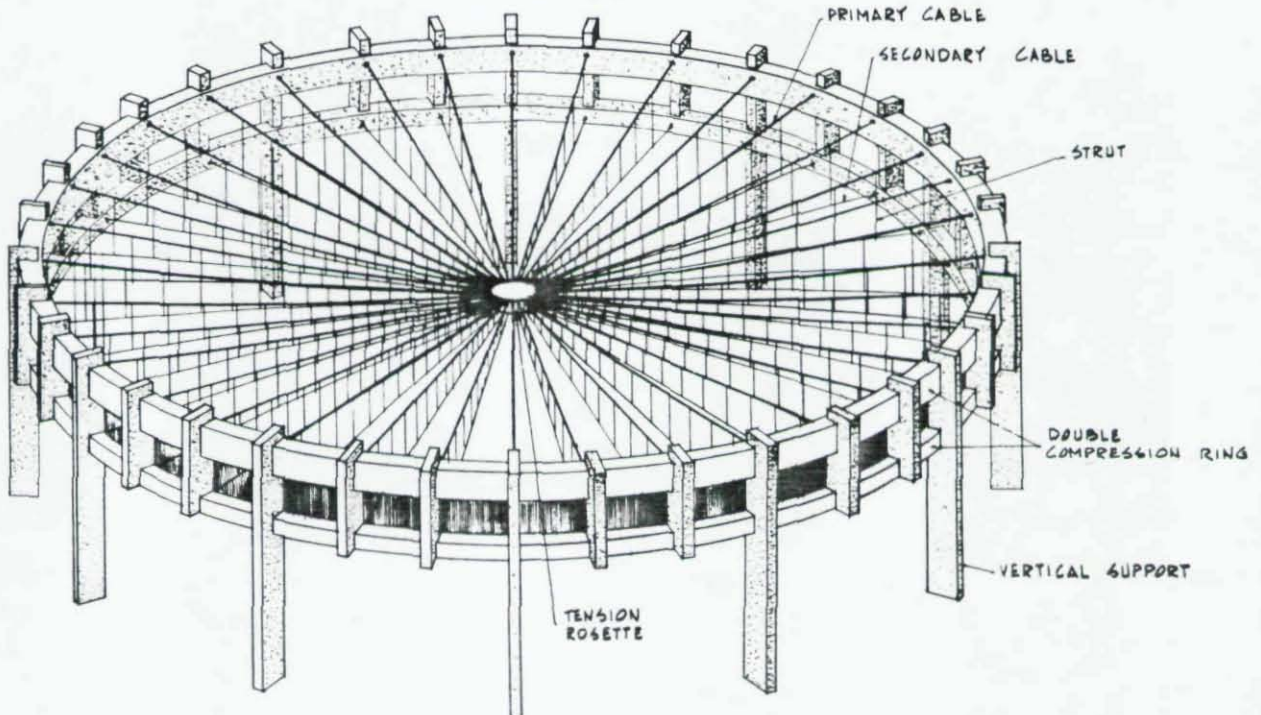
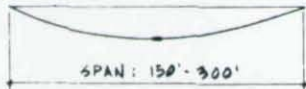


ROOT DECK IS SUPPORTED ON CABLES.
CABLES ARE USUALLY SPACED 4 TO 12 FT. O.C.
THESE CABLES HAVE A LARGE NUMBER OF NATURAL FREQUENCIES
AND FLUTTER WILL OCCUR WHEN THE FREQUENCY OF THE APPLIED
WIND LOAD MATCHES THAT OF THE CABLES. TO DECREASE THE
EFFECTS OF RESONANCE IT IS NECESSARY TO INCREASE
THE WEIGHT OF THE ROOT DECK.
TYPICAL SAG / SPAN RATIO: $\frac{1}{8}$ TO $\frac{1}{9}$

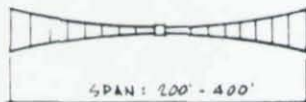




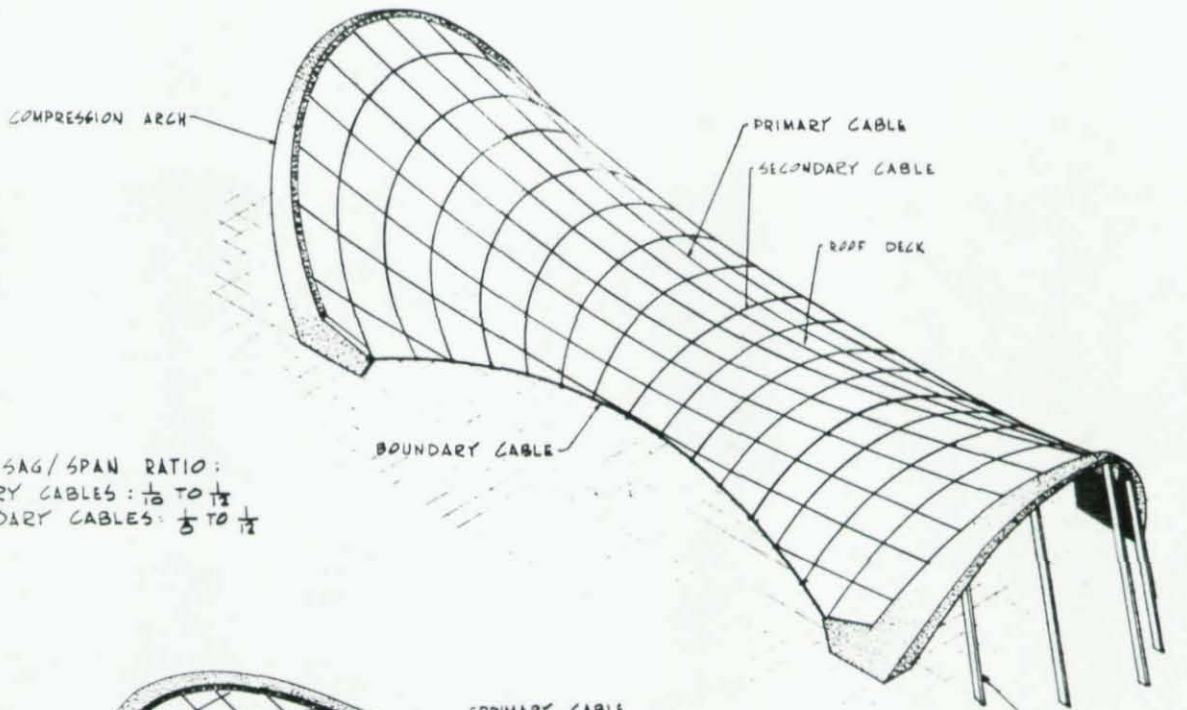
ROOF DECK IS SUPPORTED ON CABLES.
 THE ROOF DECK IS SUSCEPTIBLE TO FLUTTER FROM WIND.
 THIS RESONANCE MAY BE REDUCED BY PRESTRESSING
 THE CABLES AGAINST A CONCRETE ROOF DECK.
 TYPICAL SAG / SPAN RATIO : $\frac{1}{4}$ TO $\frac{1}{10}$



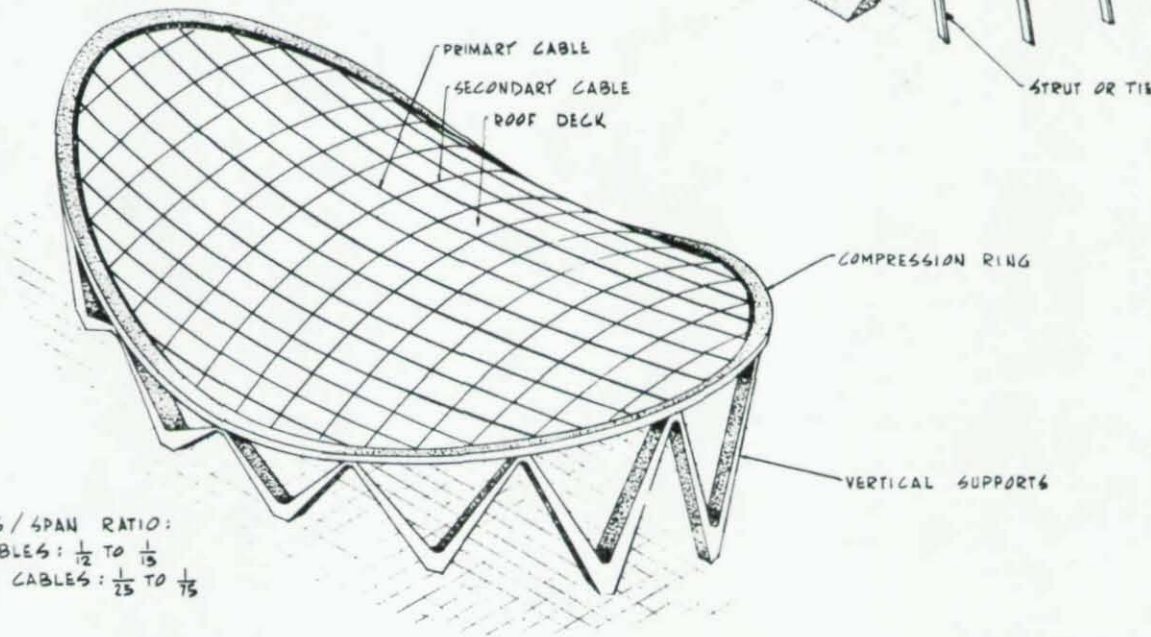
ROOF DECK IS SUPPORTED ON CABLES.
 SECONDARY CABLES HAVE DIFFERENT TENSION FORCE
 THAN PRIMARY CABLES. THIS DAMPENING EFFECT
 ELIMINATES FLUTTER.
 TYPICAL SAG / SPAN RATIO : $\frac{1}{12}$ TO $\frac{1}{15}$



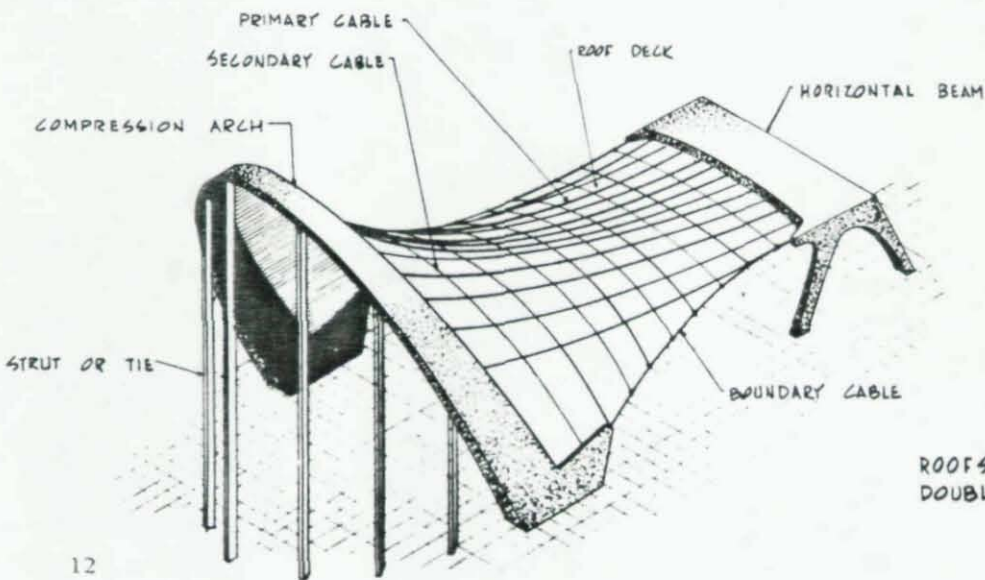
ROOFS WITH SINGLE OR DOUBLE SET OF CABLES
 DOUBLE CURVATURE (+)



TYPICAL SAG / SPAN RATIO:
 PRIMARY CABLES: $\frac{1}{10}$ TO $\frac{1}{12}$
 SECONDARY CABLES: $\frac{1}{5}$ TO $\frac{1}{12}$



TYPICAL SAG / SPAN RATIO:
 PRIMARY CABLES: $\frac{1}{12}$ TO $\frac{1}{15}$
 SECONDARY CABLES: $\frac{1}{25}$ TO $\frac{1}{15}$



ROOFS WITH A DOUBLE SET OF CABLES
 DOUBLE CURVATURE (-)

Steel Cable Creates Novel Structural Space Systems

LEV ZETLIN

Reprinted from "Engineering Journal" of The American Institute of Steel Construction, with permission.

STRUCTURAL ENGINEERING is inherently a creative profession. Nevertheless, as often practiced, structural engineers are involved mainly in the design of a few well known structural systems, while research and development are usually directed towards greater economy of material and labor in those systems.

However, creativeness in structural engineering should be measured by the evolving of structural systems which offer more flexibility for architectural planning and which could be constructed more economically than structural systems of yesterday. Flexibility could be measured by greater span lengths and aesthetics of the structural systems. Such structural systems could be left exposed and thus save in exterior finishes.

The theoretical principles which would govern such structural systems have to be based on the following considerations:

1. Avoid flexural members as far as practicable.
2. Attempt to utilize the material either in direct tension or direct compression.
3. Utilize geometry of the structure in resisting the loads.
4. Design the entire structure as a whole to resist the load; i.e., the characteristics of the entire structure as a whole entity should be considered in the structural analysis, rather than that of individual members (leaving to chance the interaction between the members).

Structural systems that could be evolved on the basis of these principles are bound to result in significant savings of construction cost. They would offer tremendous flexibility in architectural layouts and would contribute to the aesthetics of a structure. These principles would offer an infinite number of shapes, new forms and would open new horizons in the construction planning. Such an approach to engineering would indeed contribute to the progress of construction.

Application of the above mentioned principles would

Lev Zetlin is Principal, Lev Zetlin & Associates, Consulting Engineers, New York, N. Y.

generally result in space structural systems; namely, systems which carry the superimposed load in three dimensions, as opposed to plane structural members which carry the load in two dimensions only.

One of the most beneficial methods of achieving exciting structural systems, particularly in the United States with its advanced construction techniques and high ratio of labor to material costs, is the high strength cable, particularly the bridge strand.

One of the high dividends of using strands is that one can create a structure where the roof, rather than being supported by the structure below, actually holds the entire structure together, resulting in significant economy in the superstructure, the supporting elements and the foundations. It will be noted that space structures with strands would be subjected essentially to tensile stresses. The big difference between a conventional space structure, and a "tension" space structure, is that the stresses in the component members of a "tension" space structure could be predetermined by the designer. A simplified summary is that a tension space structure is equivalent to a structure prestressed in its entirety.

This article deals with the theoretical aspects of suspension cables and elimination of their elastic instability. Some of the applications of dampened suspension systems are also discussed.

STRUCTURAL BEHAVIOR OF A SUSPENDED CABLE; DYNAMIC INSTABILITY

Modern high strength cables and strands offer a material which is four to six times stronger than, and at a cost that is only twice as much as, ordinary structural steel. Furthermore since a cable is subjected to tension only, the possibility of buckling is precluded and, hence, its entire cross sectional area may be utilized at the maximum permissible stress. The resulting structure is not only light but also effects further economy in the foundations.

Because of these advantages, the use of cables as the principal structural members for suspension roofs for intermediate and large spans stands to reason. Indeed, many attempts have been made by the engineers of many countries in this direction. One obvious structural solu-

Use a 2-in. diameter galvanized bridge strand with cross sectional area of 2.43 sq in., weighing 8.48 lbs per linear foot. Factors of safety and allowable design stresses in strands are beyond the scope of this presentation.

Angle α (see Fig. 2) of the cable at the anchorage point is given by

$$\tan \alpha = 4f/l = 4/15 = 0.267 \quad (3)$$

$$\alpha = 0.2618 \text{ radians } (15^\circ) \quad (4)$$

Vertical reaction V is

$$V = T \sin \alpha = 116 \times 0.2588 = 30 \text{ kips} \quad (5)$$

Horizontal reaction H is

$$H = T \cos \alpha = 116 \times 0.9659 = 112 \text{ kips} \quad (6)$$

It will be noted that the horizontal component of H at the anchorage point also represents the tension at midspan of the cable.

The actual tension along the cable varies from maximum value $T_1 = 116$ kips at the anchorage point to the minimum value $H = 112$ kips at center of span. For small ratios of sag-to-span, it may be assumed that the cable is subjected to a uniform tension $T_1 = 116$ kips.

For small sag-to-span ratio, the approximate initial length of the cable (before the application of q) is given by

$$L = l [1 + (8/3)(f/l)^2] = 303.5 \text{ ft} \quad (7)$$

Elastic elongation of the cable is

$$\Delta L = T_1 L / EA \quad (7a)$$

where E = modulus of elasticity (approximately 24,000 ksi) and A = cross sectional area of cable (2.43 sq in. for 2 in. diameter strand).

Therefore, from (2) and (7)

$$\Delta L = 0.605 \text{ ft} = 7.25 \text{ in.} \quad (8)$$

Increase in sag, Δf , due to the cable elongation of ΔL is

$$\Delta f = \frac{\Delta L}{(16/15)(f/l)[5 - 24(f/l)^2]} = 1.75 \text{ ft} \quad (9)$$

Discussion of results:

Total deflection due to combined dead and live loads is not of particular interest. Of interest is the live load deflection. Since in static design the behavior of cables is directly proportional to the superimposed load, live load deflection for our problem is $1.75 \times (30/50) = 1.05$ ft. This gives a ratio of deflection to span of $1.05/300 = 1/286$.

The tension in the cable depends solely on the magnitude of q and the geometry of the cable, i.e., its shape

(in our case parabola), span and sag. In accordance with (8), the total sag of the cable under q is $20 + 1.75 = 21.75$ ft.

In accordance with (1), as the sag increases, the tension decreases; for a sag of 21.75 ft the tension drops approximately from 116 kips to $116(20/21.75) = 107$ kips. Actually, under a tension of 107, the sag will be slightly less than 21.75 ft; at equilibrium, the tension in the cable will be somewhere between 116 and 107 kips (closer to 107 kips) and the total sag will be between 20 ft and 21.75 ft (closer to 21.75 ft).

This example of the decrease of the tension in the cable illustrates an important characteristic of suspension roofs; destructive internal forces and reactions on abutments are reduced when deflections are increased. This characteristic should be utilized in investigating the actual factor of safety of suspension roofs. In general, at incipient collapse, the forces which tend to destroy a suspension roof are being gradually reduced, and this stabilizes the structure.

Dynamic Behavior—A description of the phenomenon of flutter and of self-exciting vibrations in a suspension roof would entail a lengthy mathematical treatise. However, elimination of flutter could be explained through consideration of natural frequencies of the individual cables. For this reason, natural frequencies of the cable in the above example will be computed, and a few observations made.

Natural frequency of a suspended cable depends on the load attached to it, and the tension in the cable. The natural frequencies of a tight cable are given by

$$W_n = n(\pi/l)\sqrt{T/(q/g)} \quad (10)$$

where g = acceleration due to gravity; n = any integer; other terms as defined previously.

The difference between l and L , as shown before, is small; hence, equation (10) could be used.

Since T is proportional to the applied load q , the natural frequencies do not depend on the magnitude of load applied to the cable. It should be noted, however, that this independence of natural frequencies from the load hold only if: (a) tension T is computed on the basis of the initial sag f (in our example, $f = 20$ ft) and (b) there is no other tension in the cable except that due to the uniformly distributed load only. Condition (a) is of minor significance and is accurate enough for practical purposes. Condition (b), on the other hand, is of major significance. If the tension T in the cable is due to a combination of uniformly distributed loads and a series of concentrated loads, the natural frequencies of the cable would depend on the locations and relative magnitudes of the concentrated loads. This latter fact should be borne in mind later in this presentation when dampening is discussed.

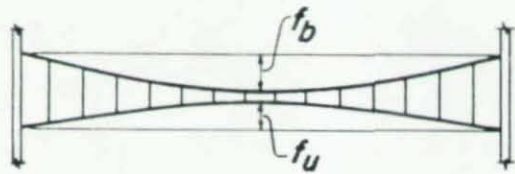


Figure 6

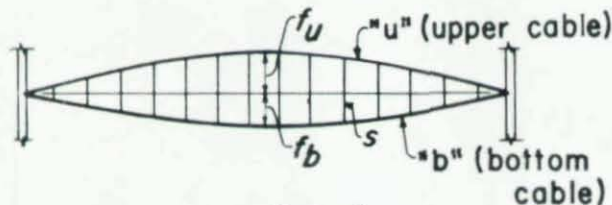


Figure 7

Examples are shown in Figs. 6 and 7, but the following discussion will be limited to Fig. 7. The suspension roof is composed of two layers of cables. Cables **b** in the lower layer are similar to the primary cables in the previously solved example; the upper layer of cables **u** contains one cable corresponding to each cable **b** in the lower layer. Each cable **b** in the lower layer is connected to the corresponding cable **u** in the upper layer by struts **s** in Fig. 7.

Cables **b** and **u** are erected with initial tension (prestress) T_b and T_u , respectively. The magnitude of these tensions depends on the spread ($f_u + f_b$) (Fig. 7), number and location of struts and the size and weight of cables **b** and **u**. When thus erected, the only vertical load that the cables carry are their own weight and the weight of the struts.

As dead load (e.g., roof deck) and live load are applied, the assembly of the two cables (with the struts) acts essentially as a beam with a span l . Consequently, the tension on the top cable **u** is decreased by amount ΔT_u , while the tension in the bottom cable **b** is increased by amount ΔT_b . Magnitudes of ΔT_u and ΔT_b depend on the magnitude and distribution of the applied dead and live loads and sizes of cables. If, under the most critical combination of dead and live loads, the value of ΔT_u is less than T_u , while $T_b + \Delta T_b$ is less than the design capacity of the lower cable **b**, both cables **b** and **u** will remain under tension without overstress. Also, the following should be noted:

- Values of ΔT_u and ΔT_b could vary within a wide range during the service life of the roof.
- The value of $T_u - \Delta T_u$, i.e., the residual tension in the upper cable at any time should not be too small to cause undesirable sag of the upper cable between struts (the upper cables may be supporting the roof deck).
- Residual tension $T_u - \Delta T_u$ and $T_b + \Delta T_b$ in the upper and lower cables respectively should be

such that the deflection of the assembly of Fig. 7 is not excessive.

Let us now consider the dynamic properties of the two individual cables **b** and **u** in Fig. 7, under any superimposed load which causes decrease ΔT_u in tension of the upper cable and increase ΔT_b in tension of the lower cable.

Referring to equation (10): Natural frequencies of the bottom cable are

$$W_b = n \frac{\pi}{l} \sqrt{\frac{T_b + \Delta T_b}{q_b/g}} \quad (11)$$

Natural frequencies of the upper cable are

$$W_u = n \frac{\pi}{l} \sqrt{\frac{T_u - \Delta T_u}{q_u/g}} \quad (12)$$

where in (11) and (12), q_b and q_u are the weights per linear foot of the bottom and upper cables, respectively.

It will be noted that $T_b + \Delta T_b$ increases with the load, while $T_u - \Delta T_u$ decreases with the load.

When the complete dead load has been applied, natural frequencies are:

for the lower cable:

$$W_b = n \frac{\pi}{l} \sqrt{\frac{T_b + \Delta T_{bd}}{q_b/g}} \quad (13)$$

for the upper cable:

$$W_u = n \frac{\pi}{l} \sqrt{\frac{T_u - \Delta T_{ud}}{q_u/g}} \quad (14)$$

Therefore, if under dead load, T_b is always made to be greater than T_u , it is seen from (13) and (14) that the natural frequencies of the lower cable, W_b , and the upper cable, W_u , corresponding to a particular value on the integer n will always have different values at any magnitude of the live load.

When a cable vibrates, its actual geometry is a superposition of several of its fundamental modes, as well as of the modes due to forced vibration (i.e., due to the frequency of the externally applied dynamic load). From the preceding discussion, therefore, it follows that under a given externally applied dynamic force, the geometry of vibration of the lower cable will always tend to be different from that of the upper cable, as shown in Fig. 8, which shows the two cables in an imaginary situation without the struts.

In the suspension roof shown in Fig. 7, the lower cable is connected to the upper cable by struts **s**. If one of the cables, say the lower one, tends to be excited by an externally applied dynamic load and, therefore, tends to assume a certain geometry at a particular instant, the upper cable, due to its different characteristic, would tend to assume a different geometric configuration.

$$q_w + q_i + (p - \Delta q_i) \quad (17)$$

while the upper cable has to be designed for a tension caused by a uniformly distributed load

$$q_i - \Delta q_i \quad (18)$$

- f. In practice, there must be enough residual tension left in the upper cable under the most critical superimposed load, to keep its sag between consecutive struts to permissible maximum, depending on the type of roof deck used.

Equation (16) together with (17) and (18) are very important to the designer in the initial stages of choosing size of cables and the amount of the initial tension T_{iu} . (In practice, a designer should use an equation similar to (16), except that q_i is given in terms of A_u and A_b , as well as f_u and f_b ; this will give him insight into the choice of desirable values for f_u and f_b .)

It will be noted from (16) that if $A_u = A_b$, the lower cable will carry a tension due to q_i plus $\frac{1}{2}p$; if A_u is considerably greater than A_b , the additional tension in the lower cable will be that due to but a fraction of p ; if A_b is considerably greater than A_u , the additional tension in the lower cable will be due to almost complete intensity of p .

It is hoped that this discussion will give the designer enough background and general understanding of the load resistance characteristics of a suspended roof consisting of two layers of prestressed cables to enable him to choose sizes of, and initial tensions in, the cables. This step will, therefore, be eliminated from this presentation and we shall proceed with the calculations of tensions and dynamic characteristics of our example, assuming that the assembly of Fig. 9 consists of the following:

Lower cable: $2\frac{1}{4}$ dia. strand, $A_b = 3.11$ sq in., weighing 10.83 lbs per lin ft

Top cable: $1\frac{7}{8}$ dia. strand, $A_u = 2.14$ sq in., weighing 7.42 lbs per lin ft

Initial tension in the upper cable, $T_{iu} = 90$ kips.
Therefore:

$$q_i = 200(90/116) = 155 \text{ lbs per lin ft}$$

$$q_i + q_w = 155 + 25 = 180 \text{ lbs per lin ft}$$

Initial tension in bottom cable:

$$T_{ib} = (180/155) \times 90 = 104.2 \text{ kips}$$

Natural frequencies:

$$W_u = 6.52, 13.04, 19.56$$

$$W_b = 5.83, 11.66, 17.49$$

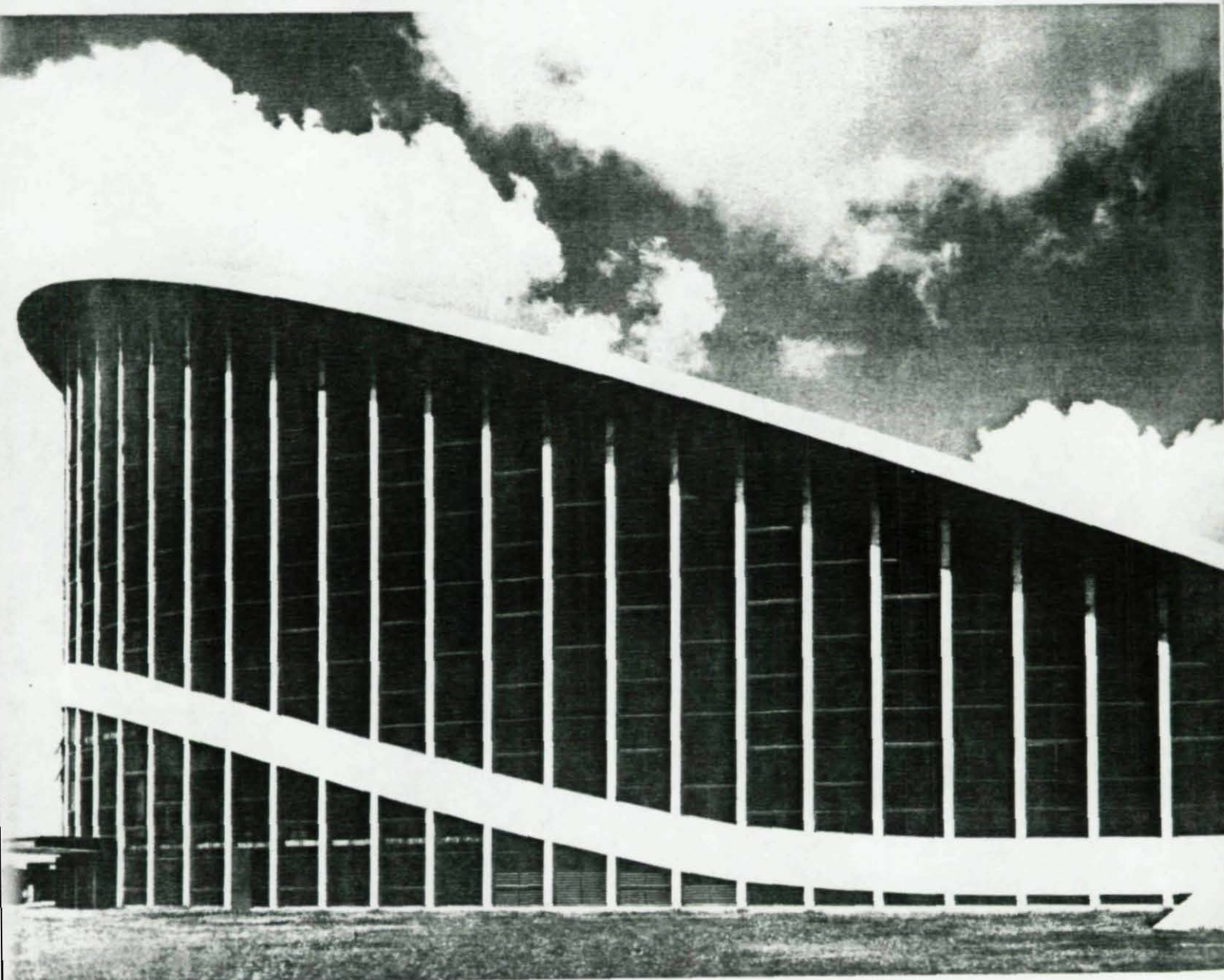
Also:

$$\Delta q_i = p \frac{2.14}{2.14 + 3.11} = p \times 0.408$$

In connection with the natural frequencies, the following reasoning was pursued:

- In a single suspended cable, as in Fig. 1, the tension is always proportional to the load. Hence, in accordance with equation (10), the natural frequency of a suspended cable under its own weight or in conjunction with a superimposed load stays the same.
- Natural frequency of either the bottom of the upper cable in Fig. 9, where they are separated by struts and where most of the load is exerted and transmitted through the struts, could be calculated only after a lengthy mathematical procedure.
- In the opinion of the writer, however, the actual natural frequency of each of the cables is not of practical importance. As long as the natural frequencies of each of the cables are computed using the same common condition, and as long as the frequencies thus computed are different from each other, there is sufficient assurance that the two cables would tend to vibrate in different modes (under one specific externally applied dynamic force), and thus flutter would be eliminated.
- To satisfy requirement (c) above, it is adequate to compute the natural frequencies by equation (10), using the total span of the cable, the actual existing tension, and only the weight of the cable itself. (Note the condition of the bottom cable between two consecutive struts, when the roof deck is applied to the upper cable.)
- Several rude test models with double layer of cables were subjected to various pulsating loads but, as expected, did not exhibit any flutter tendencies. A double layer suspension roof designed by the writer per above-mentioned principles was completed in 1959 in the northern part of the United States. During the years since its completion this roof has exhibited no tendency to flutter even though, in addition to heavy winds, mechanical and air conditioning equipment, billboards and other items were placed between the two layers of cables or hung from them. To the best knowledge of the writer, all other single layer suspension roofs without rigid membrane or guy-anchors, did exhibit flutter tendencies within such a time span.
- In choosing the initial tensions and geometrical configuration in Fig. 9, the designer should ascertain that at the application of the entire dead load the natural frequencies of the upper and lower cables are different and that as the load increases, the natural frequencies diverge further. This will assure that at no time and under no live load would the natural frequencies of the two cables coincide.

Some Outstanding Buildings



**North Carolina
State Fair Building,
Raleigh, N. C.**

The State Fair Arena at Raleigh, North Carolina, completed in 1953, was the first major cable-suspended roof structure built in the United States.

The Arena's structural theory, although radically different from conventional designs, is eminently logical. Picture two men grabbing each other by both hands in an attempt to pull each other off balance. Instinctively, they brace their feet and slant their bodies to create as stable a condition as possible. This is similar to the action of the two opposing arches in the Arena, with the cables acting as the arms, spanning and supporting the roof.

The grid of roof cables consist of 47 main cable assem-

Villita Assembly Hall

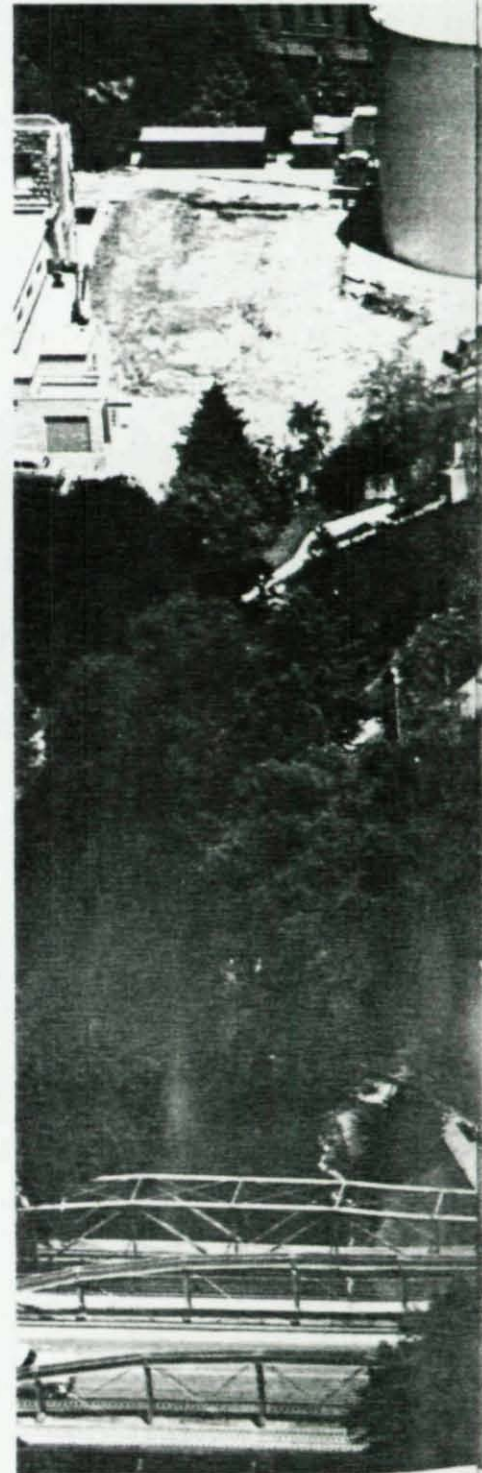
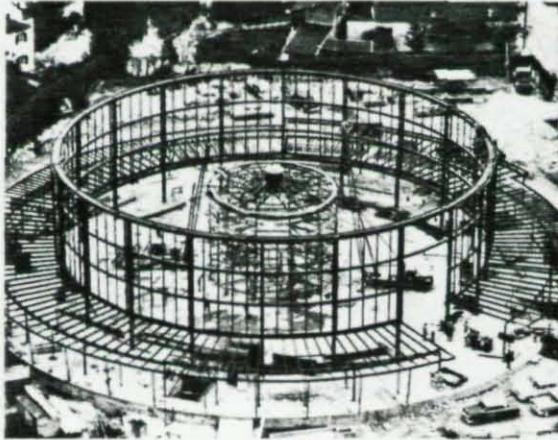
One of the simplest forms of cable-suspended roof structures is the circular roof. Cable assemblies are strung from a steel tension ring in mid-air to an exterior steel compression ring which rests on the outside wall columns. In plan, it resembles a bicycle wheel.

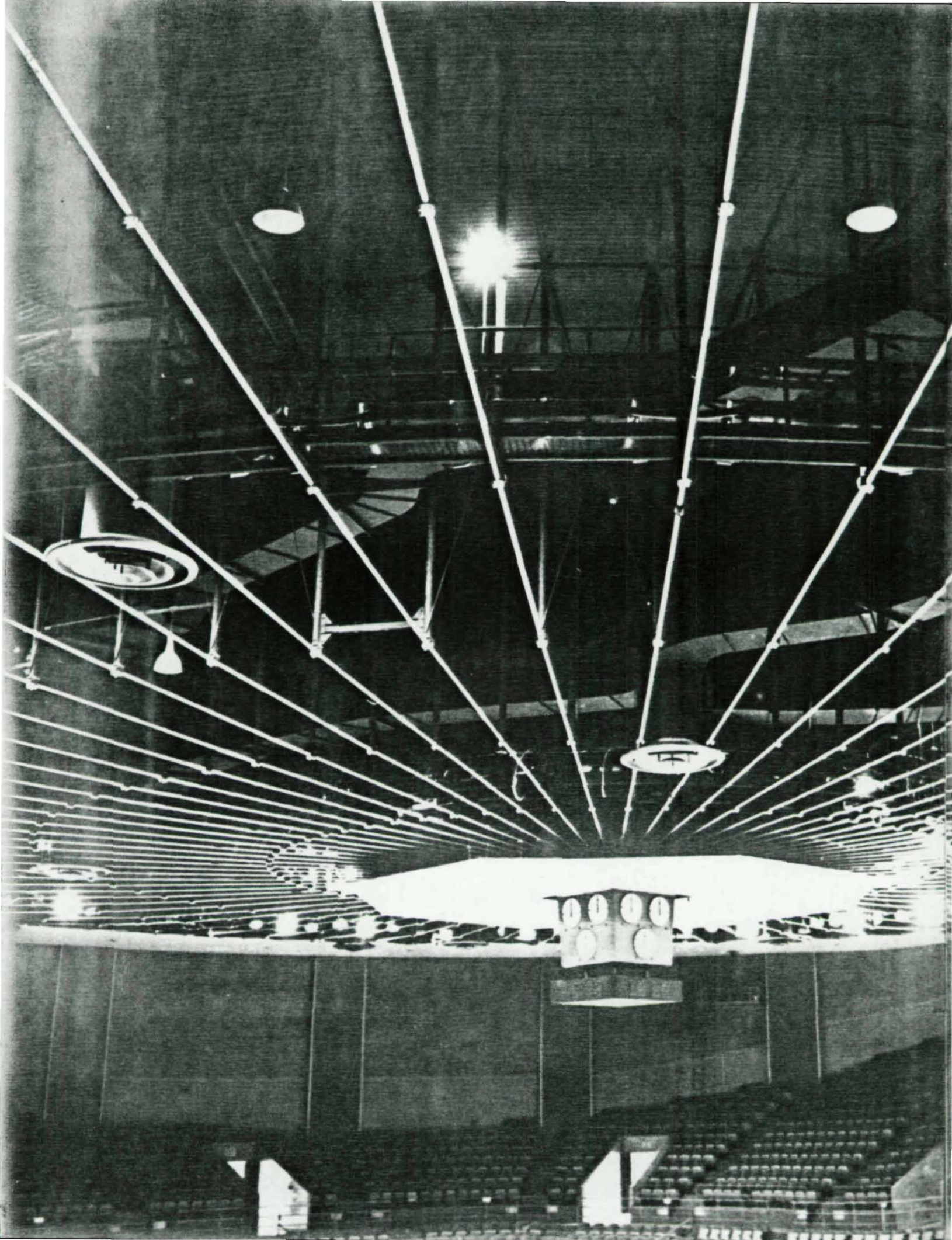
The Villita Assembly Hall saucer-shaped roof is supported by 200 assemblies approximately 47 feet long of $1\frac{1}{16}$ in. diameter zinc-coated prestretched strand. Each assembly has a swaged open clevis attached to one end, and a swaged eye terminal and turnbuckle attached to the other end.

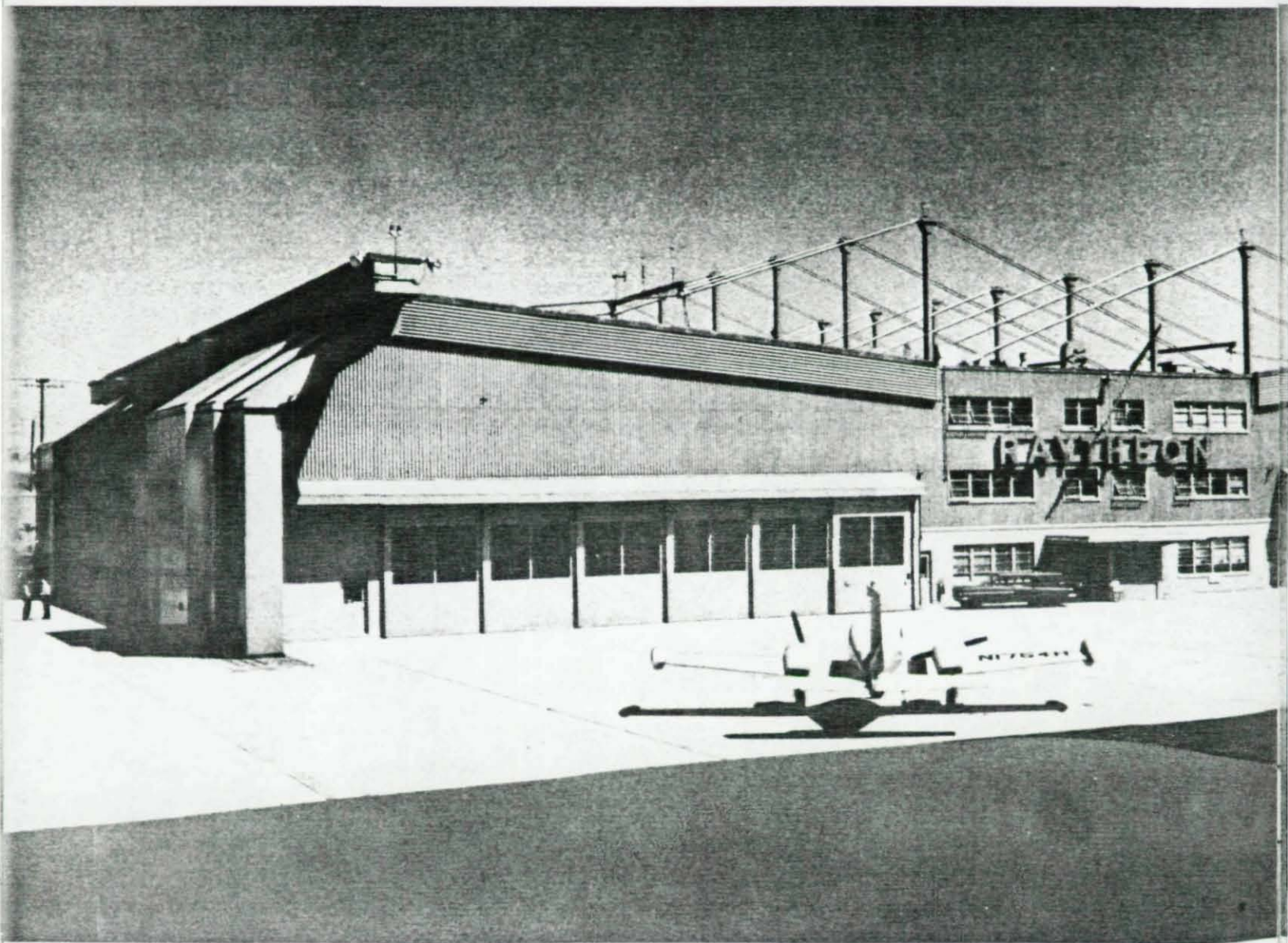
This roof structure covers a building approximately 132 feet in diameter with column-free interior area.

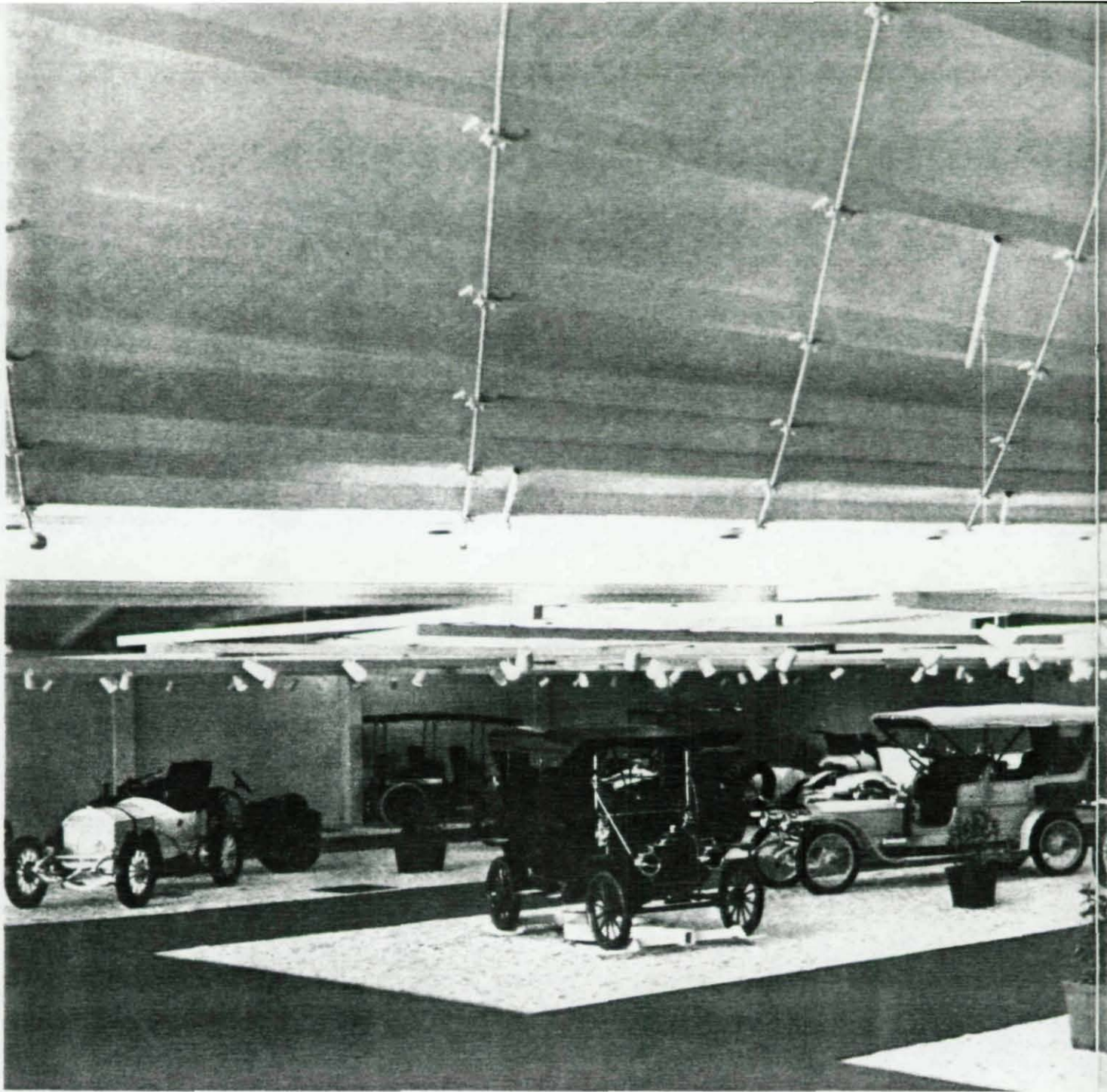
For a force diagram of this building, see Page 34.

The building is owned by the City Public Service Board of San Antonio, Texas. O'Neil, Ford and Associates of San Antonio were the architects, with W. E. Simpson Company, also of San Antonio, the structural consulting engineers. G. W. Mitchell of San Antonio was the general contractor. Alamo Iron Works, also of San Antonio, was the steel fabricator and erector. Steel cable assemblies were furnished by Bethlehem Steel Corporation, Williamsport Plant.









Autorama Building, Petit Jean Mountain, Arkansas

This building, located at Petit Jean Mountain, Arkansas, serves as an Antique Automobile Museum. The cable-suspended roof design employs a squared variation of the compression ring principle to provide a 22,500-square-foot, column-free exhibit area.

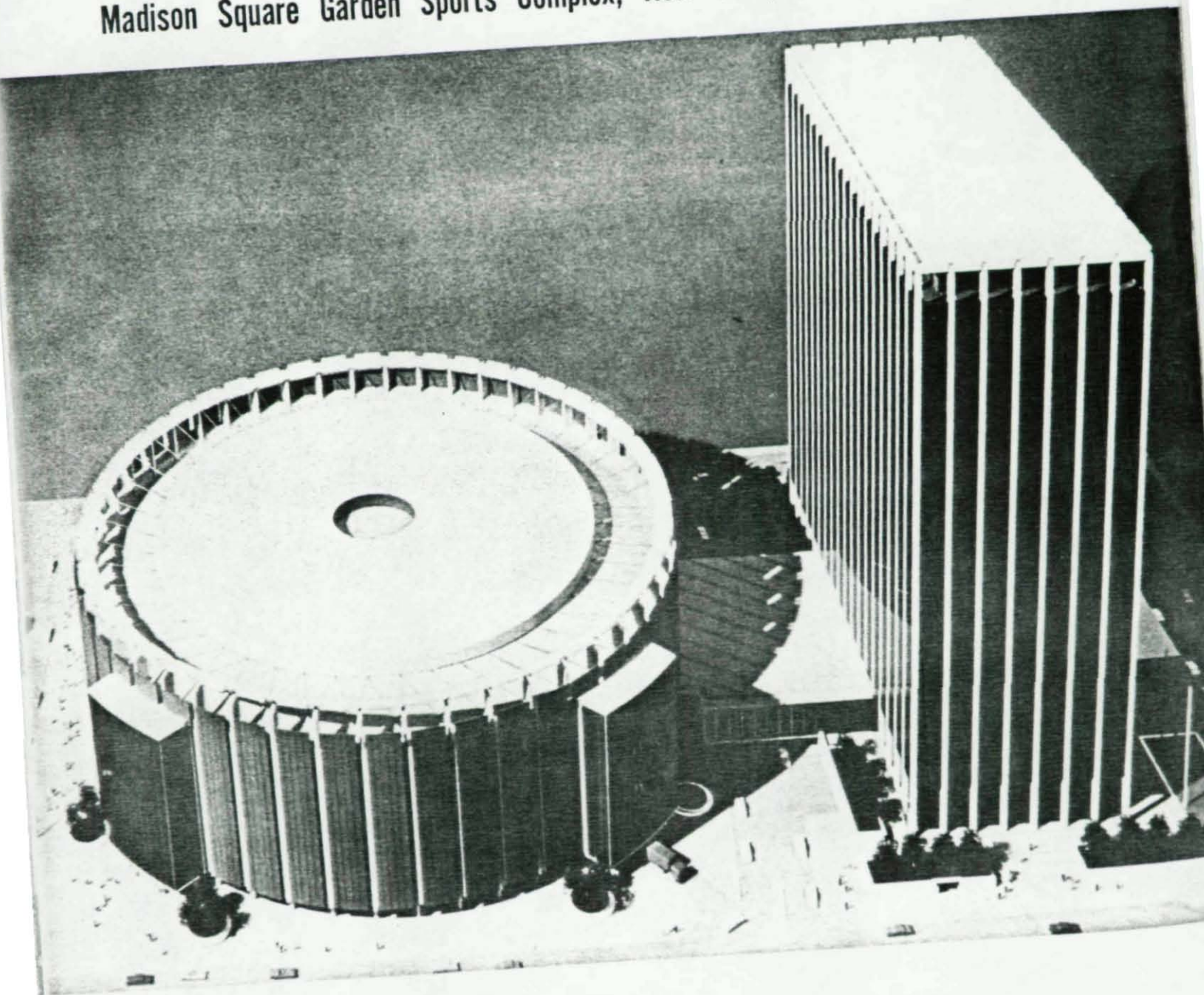
Radiating from the four corner posts, the steel cables pass through a cruciform steel strut which stabilizes the roof and divides it into four equal parts.

The roof cables utilized were 24 assemblies varying in length from 146 feet to 200 feet. The 1 1/4 in. diameter lengths of zinc-coated prestretched bridge strand have

Type 7 Anchor Sockets attached to each end.

Building owner is Winthrop Rockefeller of Winrock Farms, Arkansas. Ginocchio, Cromwell, Carter and Neyland of Little Rock, Arkansas, were the architects. Severud-Perrone-Fischer-Sturm-Conlin-Bandel of New York, N.Y., served as the structural engineers. General contractor was Pickens-Bond Construction Company and erector was Kelley-Nelson Construction Company, both of Little Rock, Arkansas. Steel fabricator was Arkansas Foundry Company of Little Rock, Arkansas. Steel cable assemblies were furnished by Bethlehem Steel Corporation, Williamsport Plant.

Madison Square Garden Sports Complex, New York, N. Y.



Design Examples

The Villita Assembly Hall (Figure 1), San Antonio, Texas, is a classic example of a radial-type cable-suspended system. The cables act as the main supporting system for the roof construction. The truss-work shown in the diagram is not a primary structural component of the roof system, but simply a series of ceiling frames hung from the cables.

The central portion of the roof structure is made up of radial trusses with a peripheral tension ring and an inner ring which also serves as the base for the ventilation frame. Radial trusses, like spokes in a bicycle wheel, reinforce

the tension ring by resisting direct tension from the cables. Bending moments on the tension ring are thus minimized.

At the outer perimeter, the radial cables are attached to a built-up compression ring, fabricated from two I-members which provide stiffness in both vertical and horizontal axes.

Damping of the cables to prevent flutter is achieved through the additional mass of the ceiling frames as well as the continuous mass of the roofing materials. Roof loading is resisted in tension by the cables, which in turn

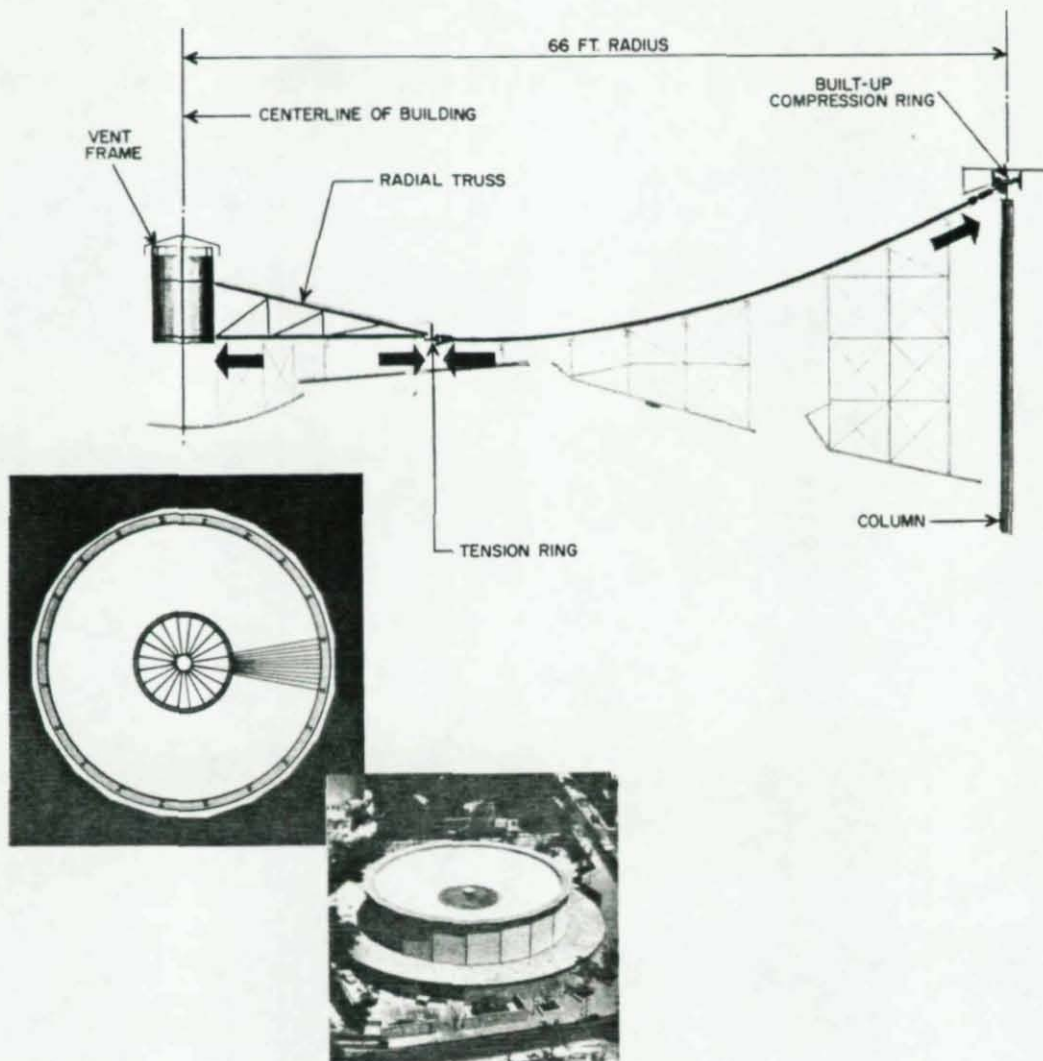


Figure 1

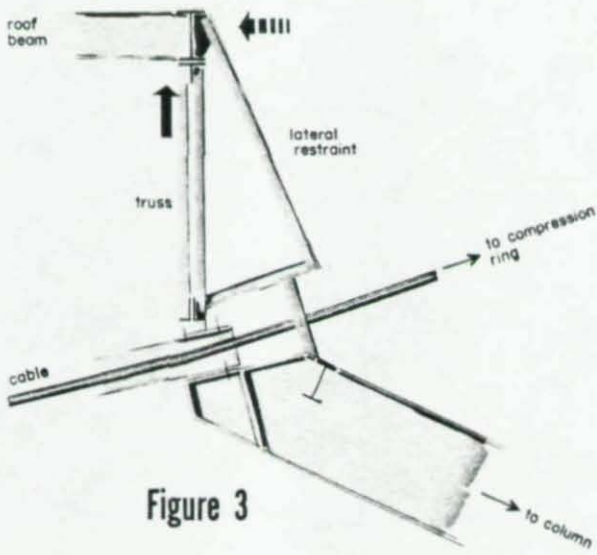


Figure 3

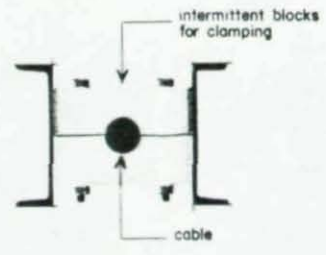


Figure 4

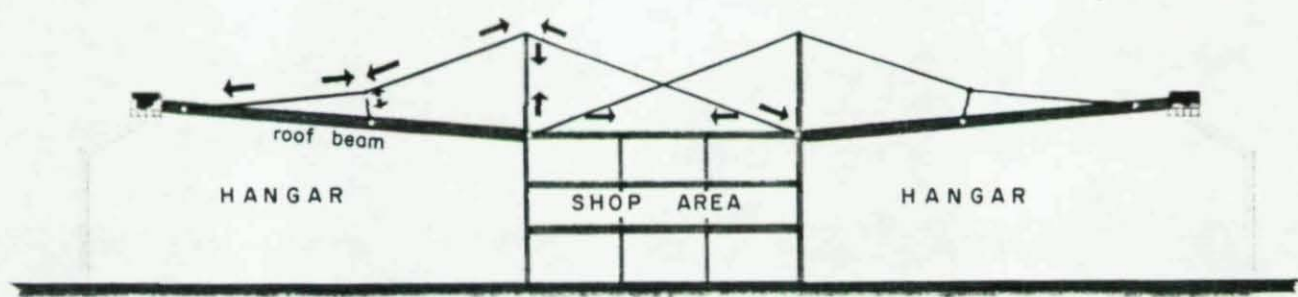
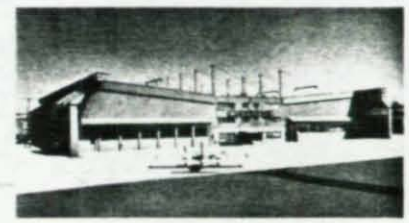


Figure 5

as a foundation for the beam-on-column system.

A beam-on-column system may be designed with or without rigid connections between beams and columns. For Madison Square, it appears that the designers chose simply supported beam spans between the columns and provided lateral supports around the periphery of the system (see detail, Figure 3).

Concentric circular trusses are provided for two purposes: First, in the case of the peripheral truss, to span large distances between the cables; secondly, in the case of the four inner trusses, to provide support for the floor beams in the heavily loaded mechanical area.

With known reactions from the beam-on-column system as loading, the cable may be designed according to classic methods. As in conventional radial cable systems, the tension ring at the center provides ample space for connection details, and the compression ring at the perimeter minimizes bending on the wall columns supporting the roof.

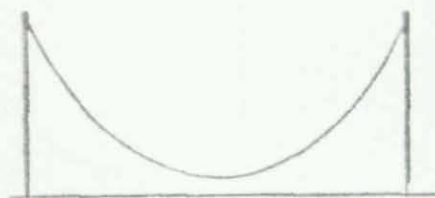
The cables will be encased in a built-up section made up of two channels to provide a means of connecting

the columns to the supporting cable (See Figure 4). Between the channels, intermittent blocks are provided for cable clamping. This technique produces a fairly rigid cable guide which can be used to advantage in predetermining the cable geometry.

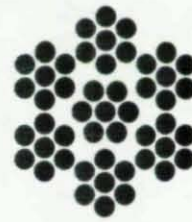
Another example of a cable-supported roof system is the Raytheon Hangar at Hanscom Air Force Base, Bedford, Massachusetts, just outside of Boston. This building demonstrates striking appearance coupled with an ingeniously uncomplicated force system. Figure 5 illustrates the force diagram for vertical loads on one half of the roof structure.

Roof loads on the stiff roof beam are transmitted as reactions on the exterior columns of the building. By simple triangulation of forces from joint to joint, the tensile forces on the main cables as well as the compressive forces on the protruding struts can be obtained directly. Thus the external reactions on the main roof beam are known. To complete the analysis, moments, shears, and axial forces on the main roof beam can then be determined.

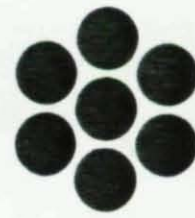
Notes



Wire Rope and Strand for Structural Applications



6-Strand
Wire Rope



7-Wire
Strand

Most manufacturers of wire rope products—including Bethlehem—have produced ample product literature over the years. But most of the available literature embraces products for a wide range of specific end uses, such as bridges, elevators, excavating and hauling machinery, radio and TV towers, tram lines and ski lifts, etc. Architects and engineers designing structural buildings, generally, have had to select the suitable cables and connections from established product lines scattered among existing multi-product literature.

To make the structural design task easier, this new Bethlehem booklet assembles in one place most of the practicable product information of interest to designers.

No new parlance or nomenclature has yet developed for this relatively new technology of cable construction for buildings, nor will it likely be developed for a while. Most terminology is identical with that of the related wire rope products. However, in the glossary on page 77, terms have been excluded which do not refer to structural applications. The term "bridge strand" as used in this booklet denotes the best available grade of strand rather than the specific use of the product.

What is "strand?"

"Strand" is an arrangement of wires helically laid around a center wire, to produce a symmetrical section.

In the steel cable industry, strand has two basic uses. First, strands are used in the manufacture of wire rope as a component part of the final product. Typical strands for this application include 7, 19, 37 and 61 wires.

Strand is also used as an individual load-carrying

tension member where flexibility or bending is not a major requirement. For any given overall diameter, strand will always be the least flexible of steel cables. Reference to the cross sectional drawings above will show why. A strand, of appropriate size for a specified load, provides the maximum strength-to-weight ratio for a given diameter of cable. It is this feature that permits successful adaptation of strand to structural applications.

Individual strands are manufactured in diameters through 4 in., and can contain as many as 300 wires.

What is "wire rope?"

"Wire rope" is a plurality of strands laid helically around a core. The core may be a fiber rope, another steel strand, or a small wire rope.

Wire rope provides increased flexibility as compared to an individual strand, and generally contains 6 or 8 strands plus the central core. For structural applications, wire rope consisting of 6 strands laid helically around a center strand is commonly used.

Wire rope is manufactured in nominal diameters through $4\frac{1}{4}$ in.

Coatings for Bethlehem Wire Rope and Strand

BETHANIZING (electrolytic zinc)

The Bethanizing process permits Bethlehem to produce five different weights of electrolytic zinc coatings to meet a wide range of corrosion-resistance requirements. As the corrosion life of a zinc coating is directly proportional to its weight, a heavier coating can be chosen for areas of

PRESTRETCHING WIRE ROPE AND STRAND

As compared with most steel products, wire rope is a relatively elastic product, and for most service requirements the normal as-manufactured condition provides safe and satisfactory service life.

For certain requirements, however, such as for main cables and suspenders of suspension bridges, guy ropes for high towers, cable-supported roof structures, and similar applications, the wire rope or strand should approach closely a condition of true elasticity. To secure this condition, stretching of the as-manufactured rope or strand is necessary.

Reasons for Prestretching

Prestretching may be defined as the application of a predetermined tension to a finished wire rope or strand for the following reasons.

1. To make the rope or strand truly elastic by removing the "constructional looseness" inherent in the product as it comes from the stranding or closing machines.

This is essential for most suspended or guyed structures, since it enables the designer to predict better the elastic behavior of the rope or strand after its erection in the structure. In a suspension bridge, for example, the elongations of the main cables under load must be nearly alike, and at a predictable rate, so that the mid-span sag may be uniform.

2. To permit measuring and marking, under prescribed loads, of the proper spacing on the rope or strand of such locations as the centers of towers and suspenders.

The elongation of a wire rope or strand under tension is due to: (1) The elastic or recoverable stretch of the steel itself. (2) The non-elastic constructional or permanent stretch, which is a variable quantity depending upon the size of the stranding and closing equipment used in manufacture, the arrangement of the wires, and the length of the lays of the rope or strand—factors which are responsible for the inherent condition sometimes described by the term "constructional looseness."

The elastic stretch of the steel permits a full recovery to the original condition and length, upon release of an applied tension, provided the tension does not exceed the elastic limit of the steel wires. Constructional stretch, on the other hand, results in a permanent set or increase in length when tension is applied and then released.

Removal of Stretch

The amount of constructional stretch in rope or strand can be minimized by the use of the proper sizes of wire and lengths of lay, and by fabrication on heavy, rugged machinery, but it cannot be entirely eliminated. If the constructional stretch must be reduced to minimum amounts, the rope or strand must be subjected to tension after fabrication.

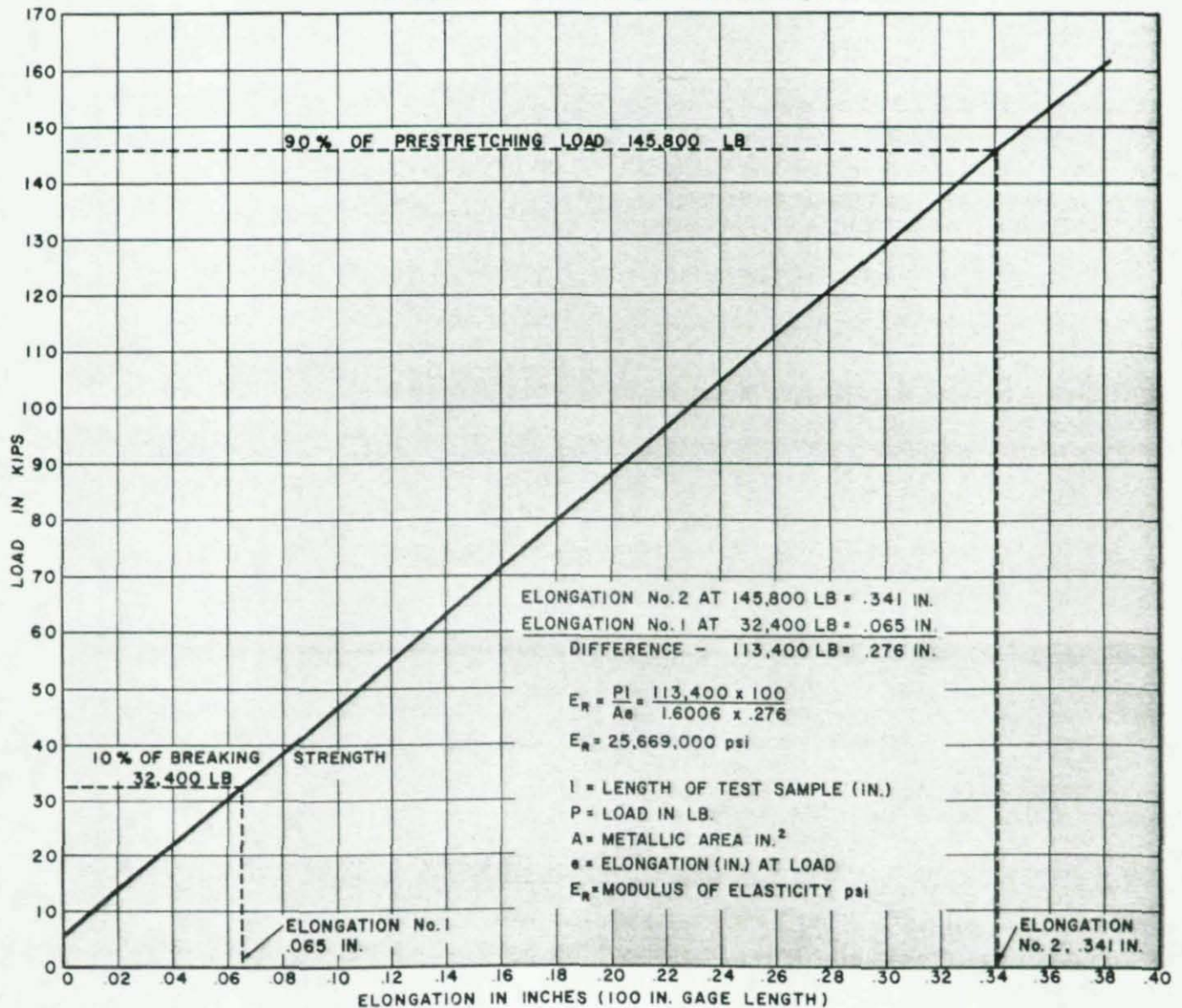
Removal of constructional stretch is effected by repeated applications of tension to the rope or strand, the number and duration of the applications depending on design factors and characteristics of the rope and strand. The first application removes nearly all of the "looseness" inherent in the rope. A second application produces only a slight additional permanent stretch, and the third loading usually proves that the second has done its job. This repeated stretching forces the component wires and strands to seat themselves in closer contact, and the rope is left with well-defined and uniform elastic properties similar to the steel itself.

With constructional stretch eliminated, any given working tension, or load of predetermined relation thereto, can be applied, and overall lengths and fitting positions can be measured and located within close tolerances. In the case of suspension bridge cables, locations for all cable-band and tower centers can be accurately measured and marked, thus facilitating erection of the bridge.

The operation of prestretching is as follows. One end of the rope or strand is fastened to a fixed crosshead, and the other end is attached to the head of a horizontal tensioning machine. The necessary tension is then applied. However, the need to stretch rope in diameters

Typical Modulus of Elasticity Chart, based upon data recorded during prestretching.

$1\frac{5}{8}$ INCH DIAM 1 x 67 GALVANIZED BRIDGE STRAND
GROSS METALLIC AREA - 1.6006 SQ. IN.



Bridge Strand

For Main, Wind, and Suspender Cables. Single Strand, Multiple Wire, Zinc-Coated

Multiple-wire bridge strand is furnished in varying numbers and layers of wires depending on the diameter, and in lengths up to approximately 5000 ft. Because of its higher unit strength, this strand can be used with smaller diameters than multiple-strand bridge rope, and its use for suspension bridge cables usually results in less costly structures.

Bridge strand of this type can be prestretched in any length that can be made or shipped.

Bridge strand can be furnished with Bethanized zinc coatings.



Single Strand, Multiple Wire

Diam in.	Weight per ft approx lb	Metallic Area approx sq in.	Breaking Strength tons	Diam in.	Weight per ft approx lb	Metallic Area approx sq in.	Breaking Strength tons
1/2	0.52	0.150	15	1 5/16	7.89	2.25	230
5/8	.66	.190	19	2	8.40	2.40	245
3/4	.82	.234	24	2 1/16	8.94	2.55	261
7/8	.99	.284	29	2 1/8	9.49	2.71	277
3/4	1.18	.338	34	2 1/16	10.1	2.87	293
1 1/8	1.39	.396	40	2 1/4	10.5	3.04	310
5/8	1.61	.459	46	2 3/16	11.2	3.21	327
1 1/16	1.85	.527	54	2 3/8	11.7	3.38	344
1	2.10	.600	61	2 7/16	12.5	3.57	360
1 1/16	2.37	.677	69	2 1/2	12.8	3.75	376
1 1/8	2.66	.759	78	2 5/8	13.6	3.94	392
1 1/16	2.96	.846	86	2 3/4	14.5	4.13	417
1 1/4	3.28	.938	96	2 11/16	15.2	4.33	432
1 3/8	3.62	1.03	106	2 3/4	15.9	4.54	452
1 3/8	3.97	1.13	116	2 7/8	17.4	4.96	494
1 7/8	4.34	1.24	126	3	18.9	5.40	538
1 1/2	4.73	1.35	138	3 1/8	20.5	5.86	584
1 5/8	5.13	1.47	150	3 1/4	22.2	6.34	625
1 3/4	5.55	1.59	162	3 3/8	23.9	6.83	673
1 11/16	5.98	1.71	176	3 1/2	25.7	7.35	724
1 3/4	6.43	1.84	188	3 5/8	27.6	7.88	768
1 7/8	6.90	1.97	202	3 3/4	29.5	8.43	822
1 7/8	7.39	2.11	216	3 7/8	31.5	9.00	878
				4	33.6	9.60	925

Minimum moduli of elasticity of the above strands, when prestretched, are as follows

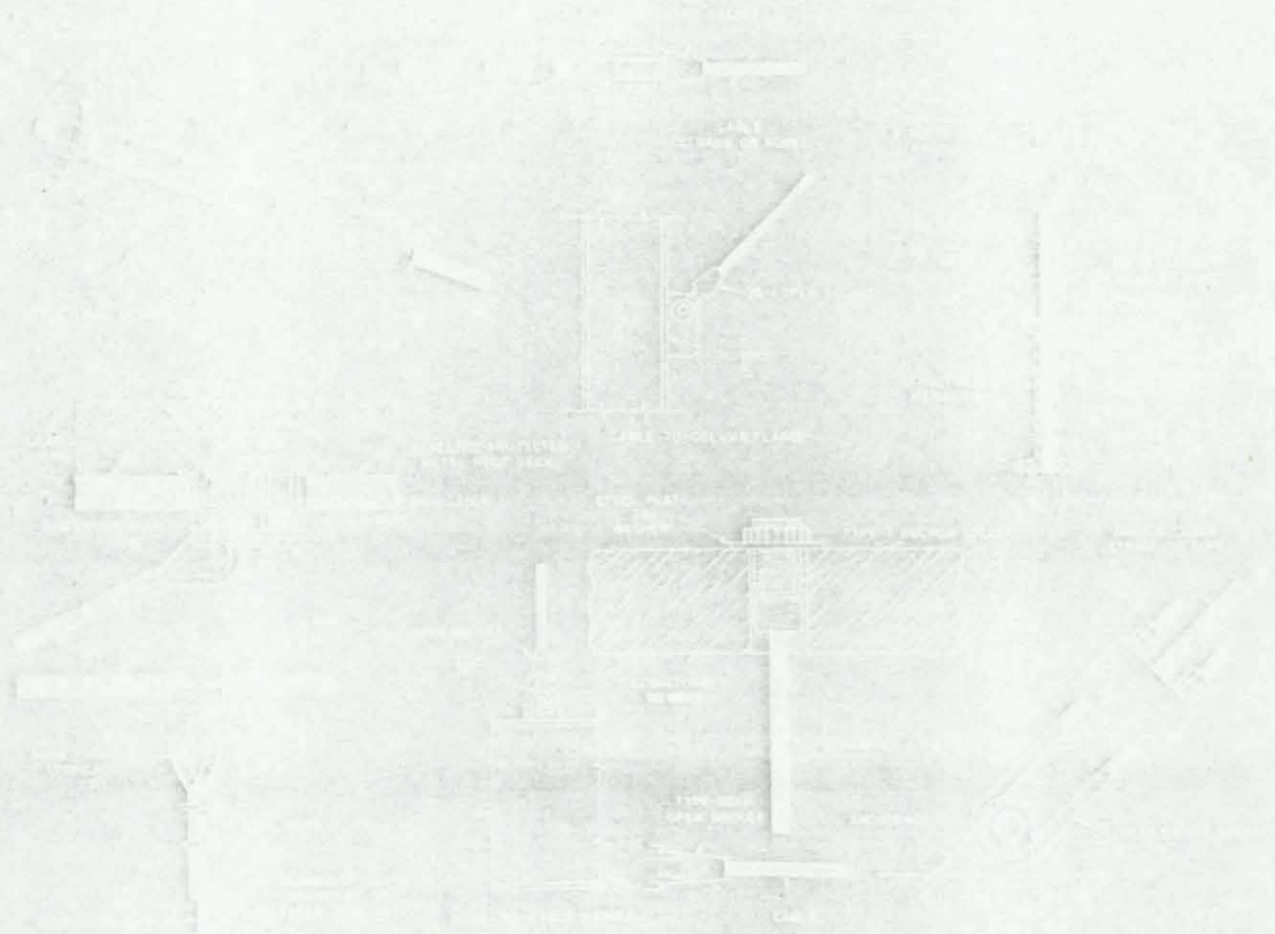
1/2-in. to 2 1/16-in. diam	24,000,000 psi
2 3/8-in. and larger.....	23,000,000 psi

Moduli are based on Class "A" coating; for heavier coatings, reduce modulus approximately 1,000,000 psi

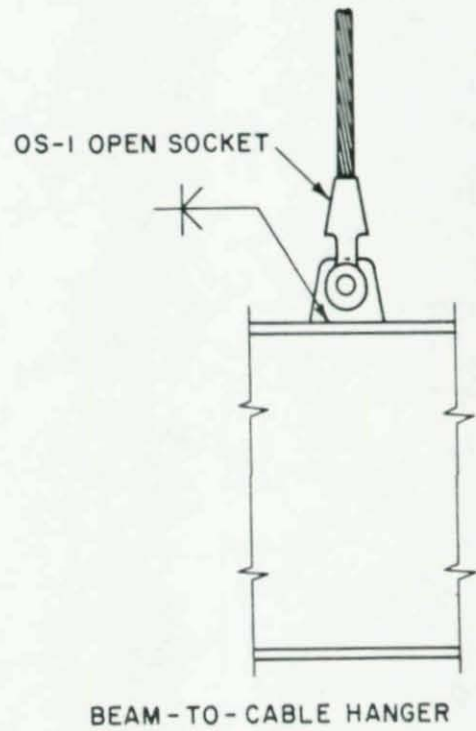
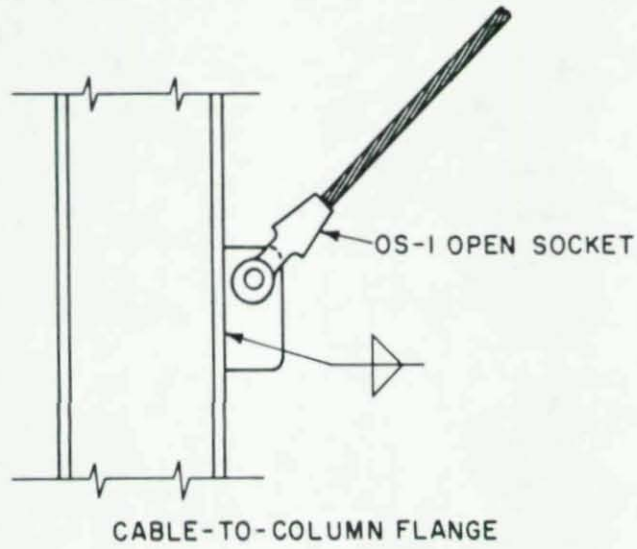
Notes



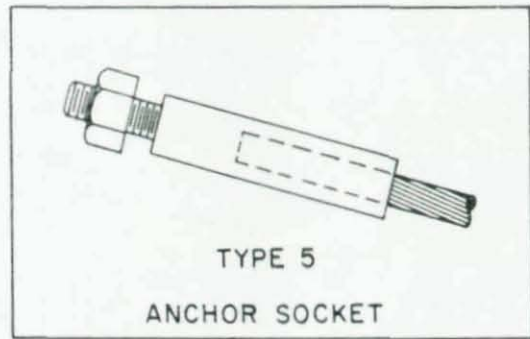
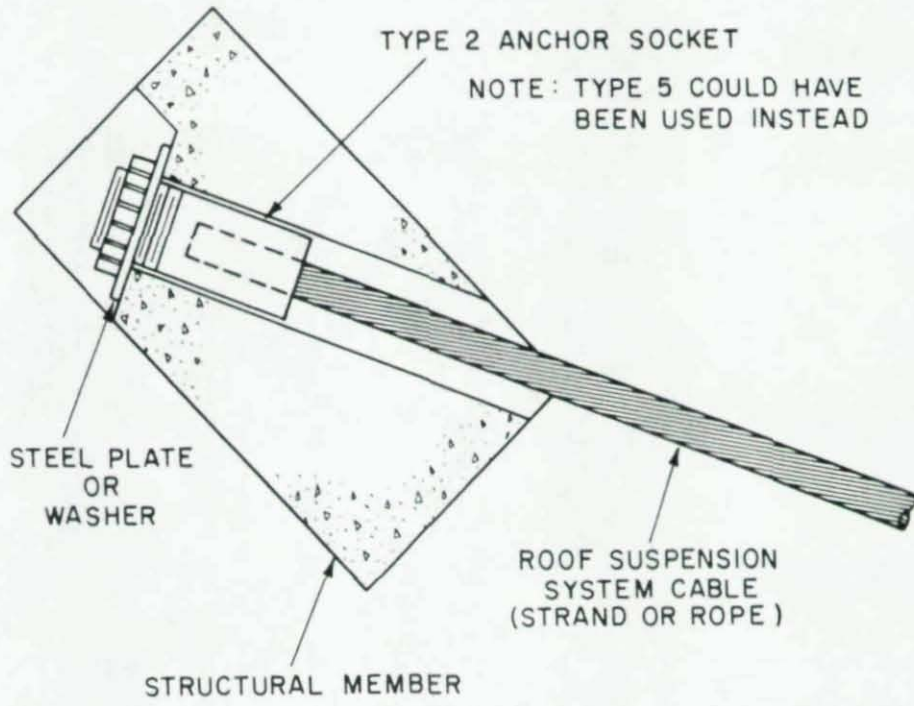
typical connections



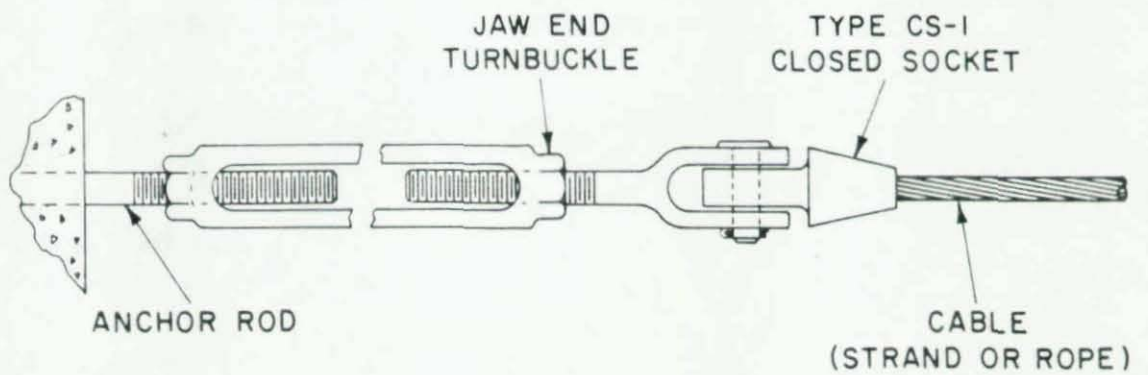
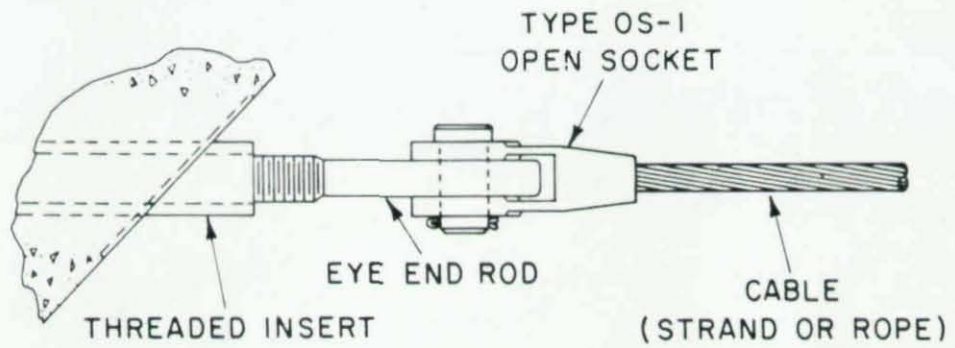
TWO OS-1 OPEN SOCKET CONNECTIONS



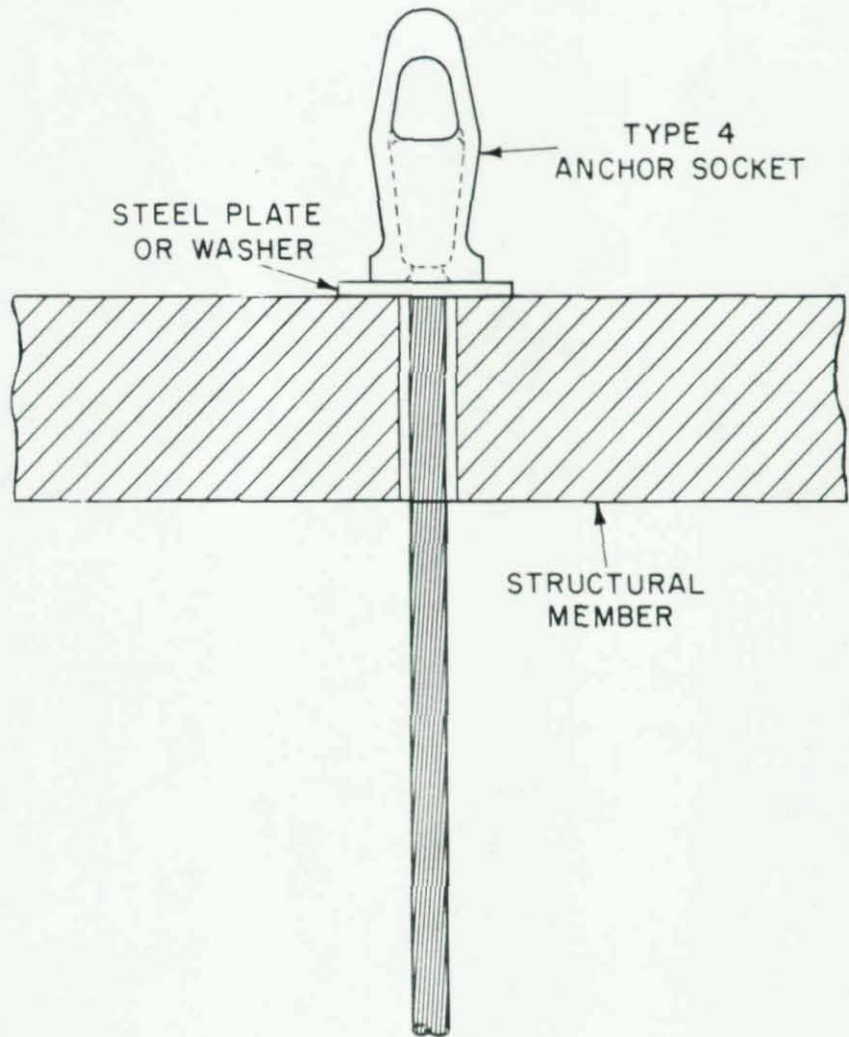
TYPE 2 OR 5 ANCHOR SOCKET APPLICATION



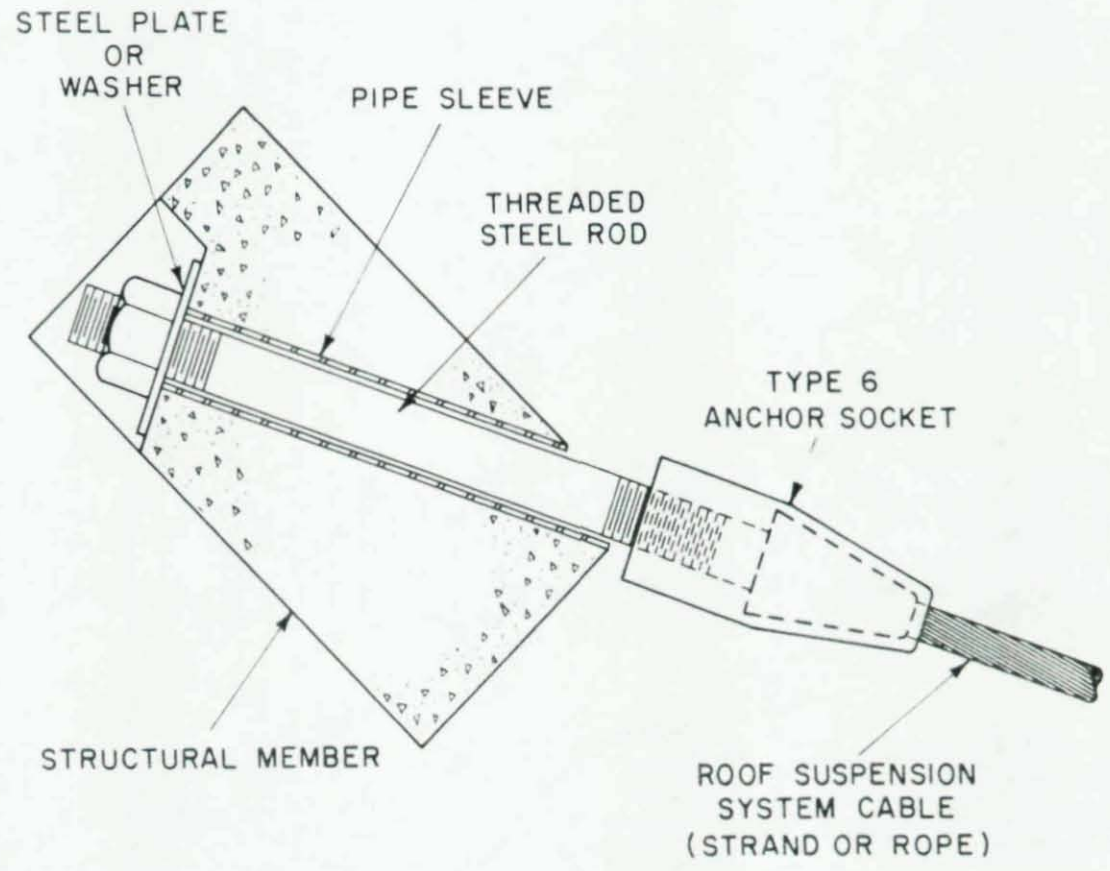
TYPES OS-1 AND CS-1 OPEN AND CLOSED SOCKET APPLICATIONS



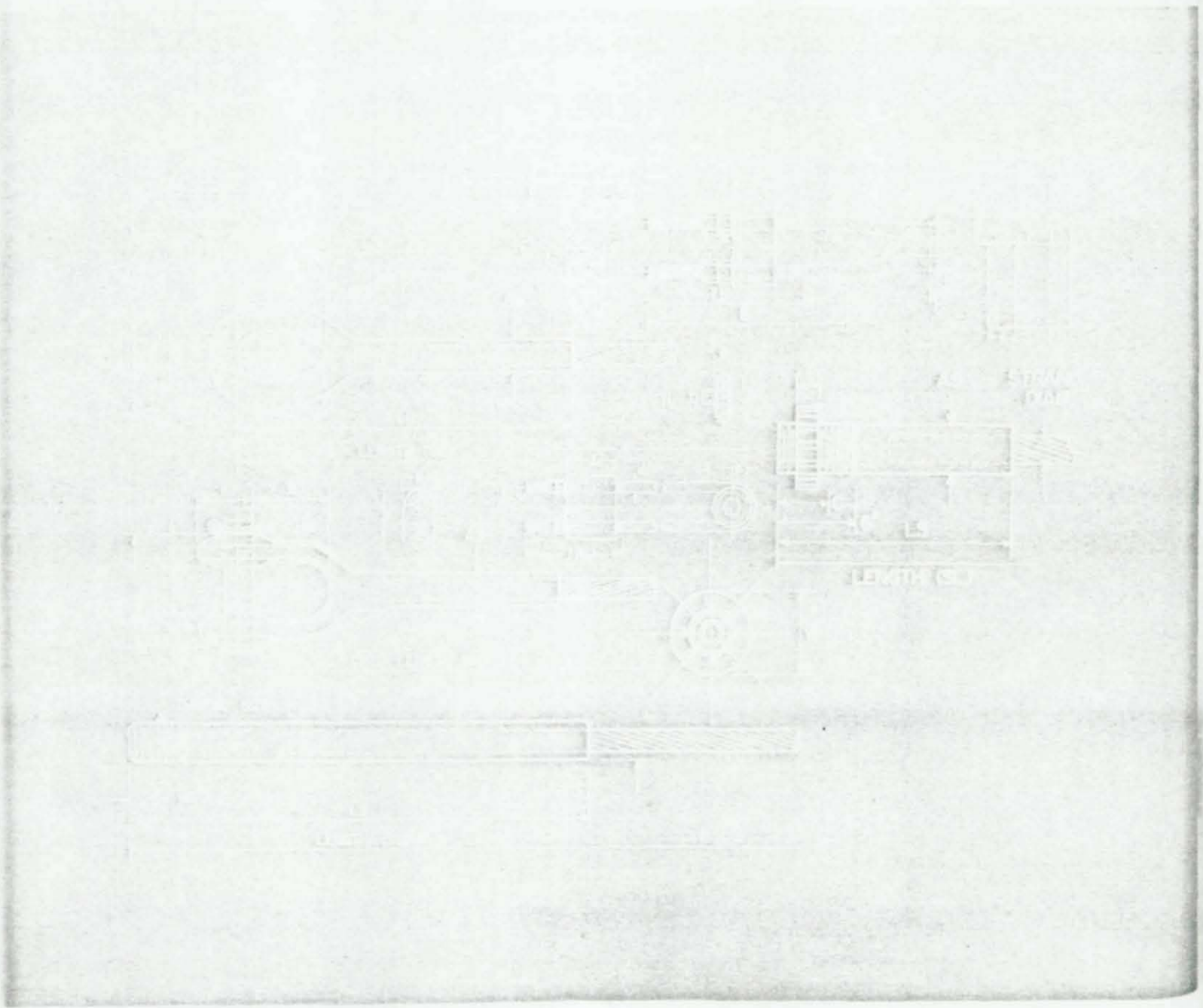
TYPE 4 ANCHOR SOCKET APPLICATION



TYPE 6 ANCHOR SOCKET APPLICATION

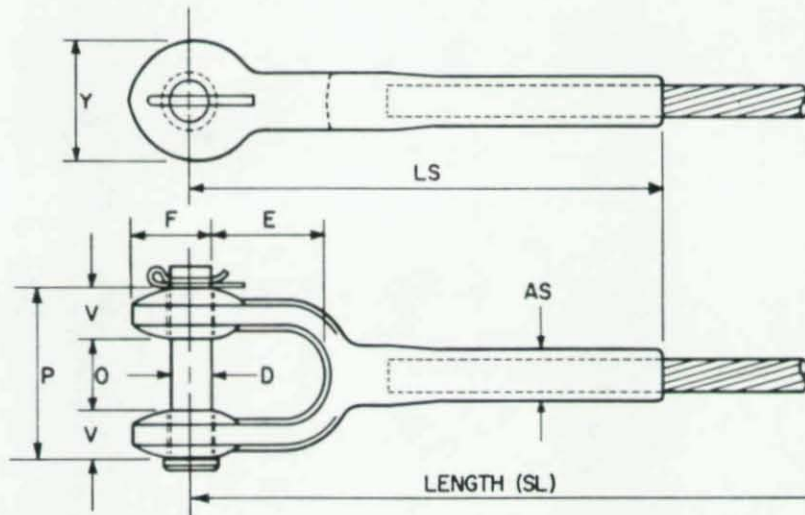


hardware for structures



Swaged Strand Clevis FS-1610

Can be used in place of Type OS-1
Open Strand Socket where strengths and
diameters are the same.

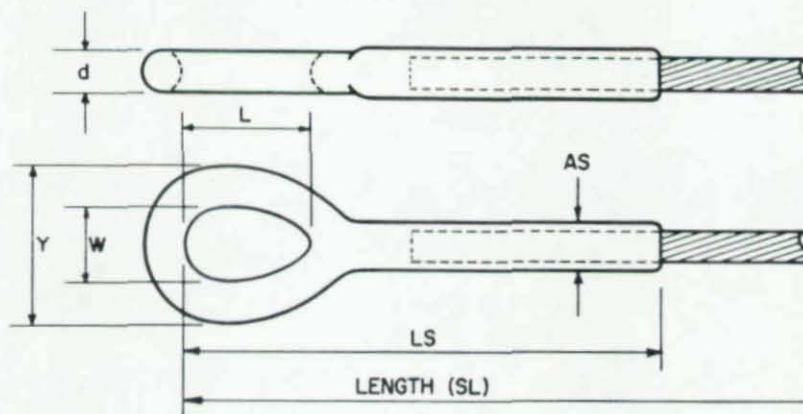


Strand Diam, in.	Breaking Strength, lb	D in.	E in.	F in.	O in.	P in.	V in.	Y in.	AS (approx), in.	LS (approx), in.
1/2	30,000	7/8	2 1/16	1 21/32	1 3/16	2 3/4	25/32	2 1/8	7/8	10
5/16	38,000	1 1/8	2 13/16	2 3/32	1 3/4	3 3/4	1	2 5/8	1 1/8	12
3/8	48,000	1 1/8	2 13/16	2 3/32	1 3/4	3 3/4	1	2 5/8	1 1/8	12 5/8
1 1/16	58,000	1 3/8	2 13/16	2 15/32	2 1/16	4 3/16	1 1/16	3 1/8	1 3/8	13 3/4
3/4	68,000	1 3/8	2 13/16	2 15/32	2 1/16	4 3/16	1 1/16	3 1/8	1 3/8	14 1/2
13/16	80,000	1 5/8	3 3/8	2 29/32	2 3/8	4 7/8	1 1/4	3 1/2	1 1/16	17
7/8	92,000	1 5/8	3 3/8	2 29/32	2 3/8	4 7/8	1 1/4	3 1/2	1 1/16	18
1 5/16	108,000	2	3 1 1/16	3 17/32	2 1/2	5 5/8	1 1/16	4 3/16	1 3/4	20 1/2
1	122,000	2	3 1 1/16	3 17/32	2 1/2	5 5/8	1 1/16	4 3/16	1 3/4	21
1 1/16	138,000	2	3 1 1/16	3 17/32	2 1/2	5 5/8	1 1/16	4 3/16	1 3/4	22
1 1/8	156,000	2 1/4	4 7/16	4 5/8	2 7/8	6	1 1/16	5 5/8	2 1/4	25
1 3/16	172,000	2 1/4	4 7/16	4 5/8	2 7/8	6	1 1/16	5 5/8	2 1/4	25 1/2
1 1/4	192,000	2 1/4	4 7/16	4 5/8	2 7/8	6	1 1/16	5 5/8	2 1/4	26 1/2

00622

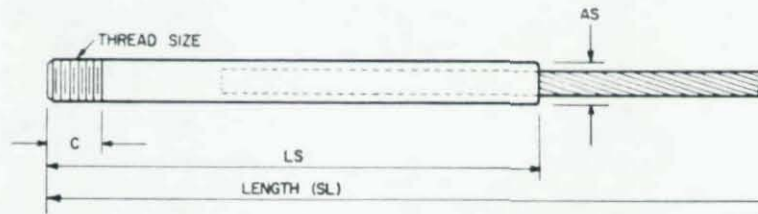
Swaged Strand Eye FS-1612

Can be used in place of Type CS-1 Closed Strand Sockets where strengths and diameters are the same.



Strand Diam, in.	Breaking Strength, lb	d in.	l in.	w in.	y in.	AS (approx), in.	LS (approx), in.
$\frac{1}{2}$	30,000	$\frac{7}{8}$	3	$1\frac{1}{16}$	$3\frac{3}{16}$	$\frac{7}{8}$	$11\frac{3}{4}$
$\frac{5}{16}$	38,000	$1\frac{1}{8}$	$3\frac{3}{16}$	$1\frac{13}{16}$	$4\frac{1}{16}$	$1\frac{1}{8}$	$13\frac{3}{4}$
$\frac{3}{8}$	48,000	$1\frac{1}{8}$	$3\frac{3}{16}$	$1\frac{13}{16}$	$4\frac{1}{16}$	$1\frac{1}{8}$	15
$1\frac{1}{16}$	58,000	$1\frac{1}{4}$	$4\frac{1}{8}$	$2\frac{1}{8}$	$4\frac{5}{8}$	$1\frac{3}{8}$	$15\frac{3}{4}$
$\frac{3}{4}$	68,000	$1\frac{1}{4}$	$4\frac{1}{8}$	$2\frac{1}{8}$	$4\frac{5}{8}$	$1\frac{3}{8}$	$16\frac{1}{2}$
$1\frac{3}{16}$	80,000	$1\frac{1}{2}$	$4\frac{1}{16}$	$2\frac{3}{8}$	$5\frac{3}{8}$	$1\frac{1}{16}$	$18\frac{1}{2}$
$\frac{7}{8}$	92,000	$1\frac{1}{2}$	$4\frac{1}{16}$	$2\frac{3}{8}$	$5\frac{3}{8}$	$1\frac{1}{16}$	$19\frac{1}{2}$
$1\frac{5}{16}$	108,000	$1\frac{3}{4}$	$5\frac{3}{4}$	$2\frac{1}{16}$	$6\frac{3}{16}$	$1\frac{3}{4}$	22
1	122,000	$1\frac{3}{4}$	$5\frac{3}{4}$	$2\frac{1}{16}$	$6\frac{3}{16}$	$1\frac{3}{4}$	$22\frac{1}{2}$
$1\frac{1}{16}$	138,000	$1\frac{3}{4}$	$5\frac{3}{4}$	$2\frac{1}{16}$	$6\frac{3}{16}$	$1\frac{3}{4}$	23
$1\frac{1}{8}$	156,000	2	$6\frac{1}{2}$	$3\frac{1}{8}$	$7\frac{1}{8}$	$2\frac{1}{4}$	$26\frac{1}{2}$
$1\frac{3}{16}$	172,000	2	$6\frac{1}{2}$	$3\frac{1}{8}$	$7\frac{1}{8}$	$2\frac{1}{4}$	27
$1\frac{1}{4}$	192,000	2	$6\frac{1}{2}$	$3\frac{1}{8}$	$7\frac{1}{8}$	$2\frac{1}{4}$	$27\frac{1}{2}$

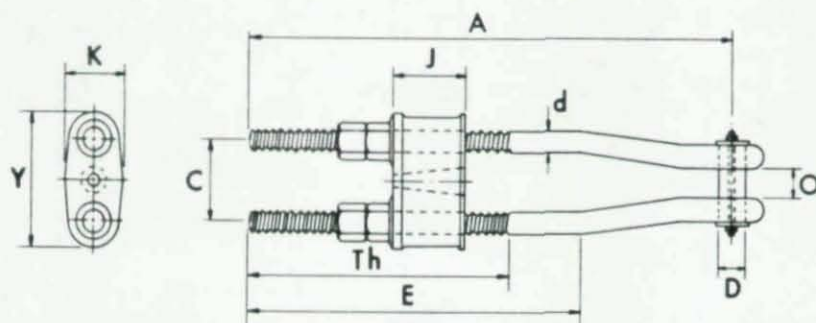
Type 5 Threaded Stud for Bridge Strand



Strand Diam, in.	LS (approx), in.	AS (approx), in.	C, Min, in.	Thread Size	Min Breaking Strength, lb
1/2	7 7/8	1	1 1/4	1-8UNC-2A	30,000
5/16	9	1 1/8	1 1/4	1-8UNC-2A	38,000
3/8	9 3/8	1 1/4	1 3/8	1 1/8 - 7UNC-2A	48,000
1 1/16	10 1/8	1 3/8	1 1/2	1 1/4 - 7UNC-2A	58,000
3/4	11 3/8	1 1/2	1 3/4	1 1/2 - 6UNC-2A	68,000
13/16	12 3/8	1 3/4	2	1 3/4 - 5UNC-2A	80,000
7/8	13 3/8	1 3/4	2	1 3/4 - 5UNC-2A	92,000
1 5/16	14 1/2	1 7/8	2	1 3/4 - 5UNC-2A	108,000
1	15 1/4	1 7/8	2	1 3/4 - 5UNC-2A	122,000
1 1/16	15 5/8	2 1/4	2 1/2	2 1/4 - 4 1/2 UNC-2A	138,000
1 1/8	16 1/2	2 1/4	2 1/2	2 1/4 - 4 1/2 UNC-2A	156,000
1 3/16	17 1/8	2 1/4	2 1/2	2 1/4 - 4 1/2 UNC-2A	172,000
1 1/4	17 1/2	2 1/4	2 1/2	2 1/4 - 4 1/2 UNC-2A	192,000
1 5/16	19 1/8	2 7/16	2 3/4	2 1/2 - 4UNC-2A	212,000
1 3/8	20 3/8	2 3/4	3	2 3/4 - 4UNC-2A	232,000
1 7/16	21 1/4	2 3/4	3	2 3/4 - 4UNC-2A	252,000
1 1/2	22 3/8	2 7/8	3 1/2	3-4UNC-2A	276,000
1 9/16	24	3 3/8	3 1/2	3-4UNC-2A	300,000
1 5/8	24 1/2	3 3/8	3 1/2	3-4UNC-2A	324,000

1. Studs will be furnished zinc coated or cadmium plated unless otherwise specified.
2. Thread length "C" is minimum required to meet the minimum breaking strength of the strand, but can be furnished with lengths to suit individual customer requirements.
3. When nuts are required, studs will be supplied with regular semi-finished hex pattern, either zinc coated or cadmium plated.

Open Bridge Socket Assembly for Rope and Strand



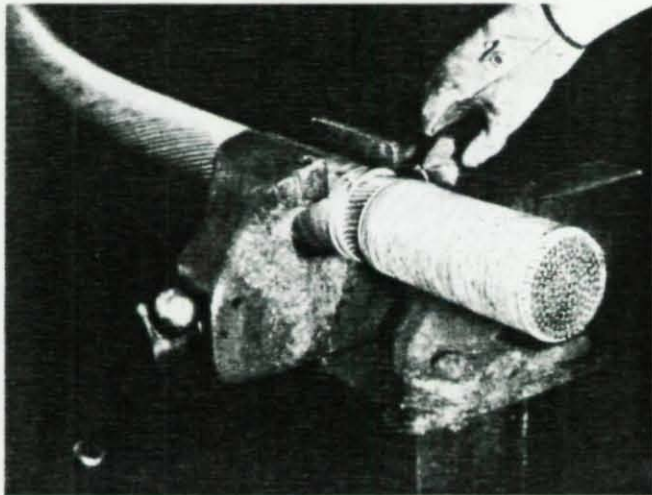
Rope Diam. in.	Strand Diam. in.	Std Take-up, in.	A for Std Take-up, in.	A for 48-in. Take-up, in.	C in.	D in.	D in.	E for Std Take-up, in.	E for 48-in. Take-up, in.	J in.	K in.	O in.	TH for Std Take-up, in.	TH for 48-in. Take-up, in.	Y in.	Weight, lb	
																Std Take-up,	48-in. Take-up,
1/2	1/2	9	20	59	3 3/8	5/8	1 3/16	14 1/2	53 1/2	3 3/8	2 1/16	1 1/4	10 1/2	49 1/2	4 5/8	9	16
3/8	5/16, 3/8	9	22	61	4 3/8	3/4	1 3/8	15	54	3 1 3/16	2 7/16	1 1/2	10 3/4	49 3/4	5 7/8	16	26
3/4, 7/8	1 1/16, 3/4	9	23	62	4 1 1/16	1	1 5/8	16 1/2	55 1/2	4 7/16	3 1/4	1 3/4	11 1/4	50 1/4	6 5/16	28	45
1	1 3/16, 7/8	9	25	64	5 5/16	1 1/8	2	17	56	5 1/16	3 1 1/16	2	11 1/2	50 1/2	7 5/16	40	62
1 1/8	1 5/16, 1	9	26	65	5 3/4	1 1/4	2 1/4	18 1/2	57 1/2	6	4 1/16	2 1/4	11 3/4	50 3/4	8 1/8	55	82
1 1/4	1 1/16, 1 1/8	12	30	66	6	1 3/8	2 1/2	21 1/2	57 1/2	5 1 3/16	4 1/2	2 1/2	15	51	8 5/8	68	98
1 3/8	1 3/16, 1 1/4	12	33	69	6 3/4	1 5/8	2 3/4	22 1/2	58 1/2	6 3/8	4 7/8	3	15 1/2	51 1/2	9 3/4	100	143
1 1/2	1 5/16, 1 3/8	12	34	70	7 3/16	1 3/4	3	23 1/2	59 1/2	6 1 5/16	5 5/16	3	15 3/4	51 3/4	10 7/16	124	173
1 5/8, 1 3/4	1 7/16, 1 1/2	15	39	72	8 1/8	2	3 1/2	27	60	7 5/16	6 1/2	3 1/2	19 1/4	52 1/4	11 3/4	180	239
1 7/8, 2	1 9/16, 1 3/4	15	42	75	9	2 1/4	3 3/4	28 1/2	61 1/2	8 1/8	7 5/16	4	19 3/4	52 3/4	13 3/8	249	323
2 1/8, 2 1/4	1 1 3/16, 2	18	50	80	10 1/4	2 1/2	4 1/4	33	63	9 5/16	8 1/8	4 1/2	23 1/4	53 1/4	14 3/4	356	439
2 3/8, 2 1/2	2 1/16, 2 1/4	18	52	82	11 1/2	2 3/4	4 3/4	35 1/2	65 1/2	10 7/8	8 1 5/16	5	23 3/4	53 3/4	16 1/2	485	586
2 5/8, 2 3/4	2 5/16, 2 3/8	18	54	84	12 1 1/16	3	5	36 1/2	66 1/2	11 1 3/16	9 3/4	5 5/8	24 1/4	54 1/4	18 1/16	610	730
2 7/8, 3	2 7/16, 2 5/8	21	59	86	13 3/8	3 3/4	5 3/4	41	68	12 1 3/16	10 9/16	6	27 3/4	54 3/4	19 1/4	776	903
3 1/4	2 1 1/16, 2 3/4	21	61	88	14 1/16	3 1/2	5 3/4	42 1/2	69 1/2	13 3/16	11 3/8	6 1/4	28 3/4	55 1/4	20 5/16	920	1068
3 1/2	2 7/8, 3	21	63	90	15 1/4	3 3/4	6 3/4	45	72	15 1/2	12 3/16	7 1/2	28 3/4	55 3/4	22	1180	1349
3 3/4	3 1/8, 3 1/4	24	70	94	17 1/4	4	7	50	74	17 1/8	13	7 3/4	32 1/4	56 1/4	24 1/2	1519	1690

Socketing

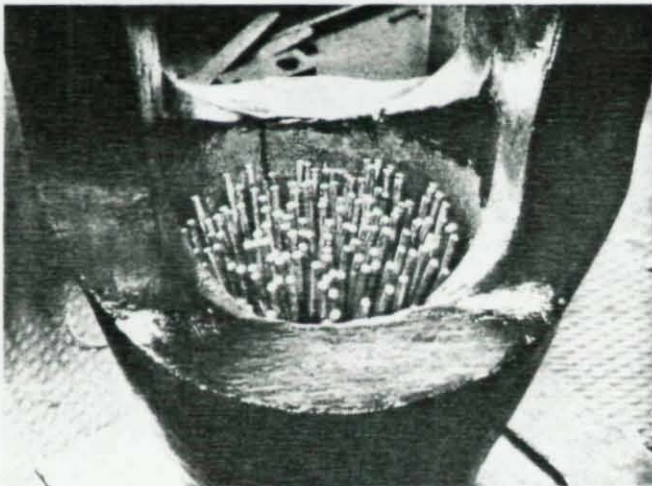
Socketing is one method of attaching an end fitting to a piece of wire rope or strand.

The other method is swaging, or pressing. In socketing, the first step, seizing (winding a wire about the end), is performed before the wire rope or strand is cut.

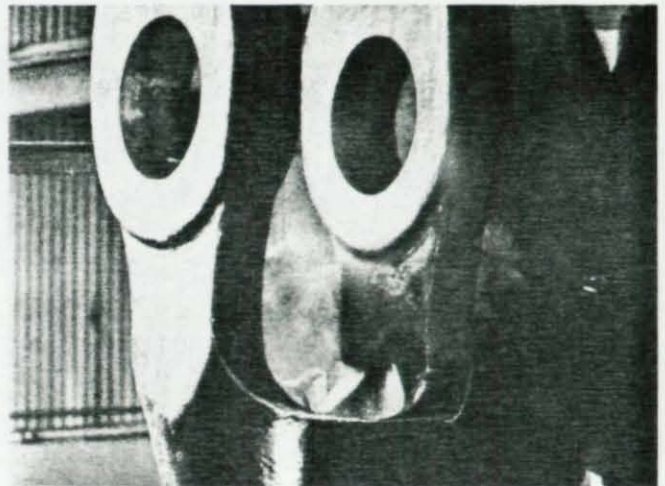
The height of the socket basket is measured from the end of the wire rope or strand, and seizing is applied to where the bottom of the socket will be. The seizing will hold the wires of the strand or rope during cutting, and will prevent its losing its lay or becoming unraveled.



Next, the top seizing is removed and the ends are broomed out to insure that all wires will be properly cleaned. When broomed, the wires are ultrasonically cleaned to remove lubricants and any foreign matter. Now surgically clean and ready for the final operation, the wires are immersed in a flux solution.



The socket is then installed and the wires are broomed out.

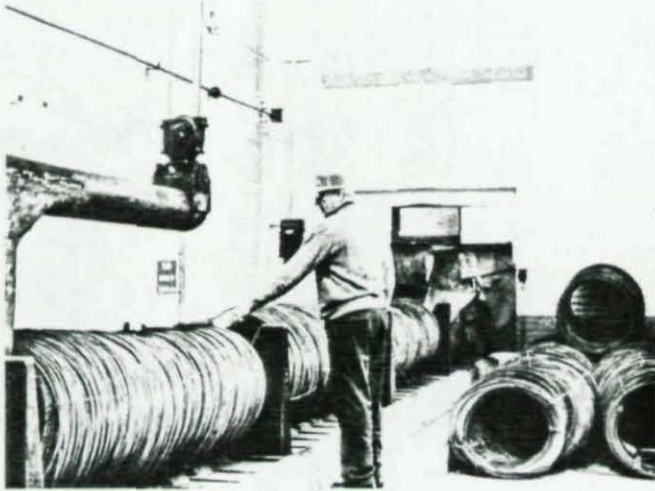


Pure, molten zinc is poured into the socket, completing the operation.

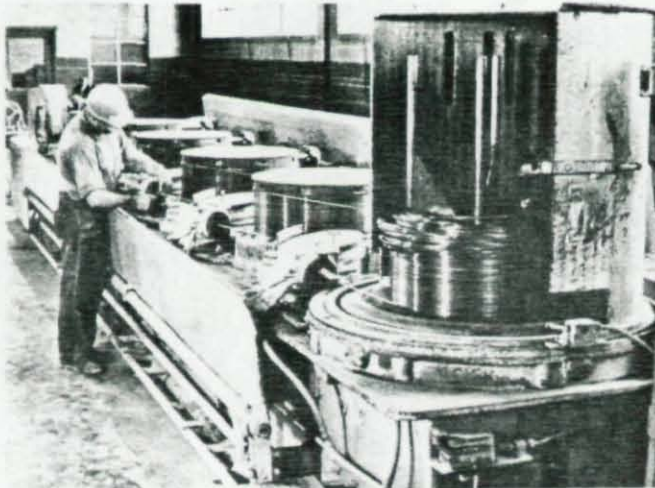
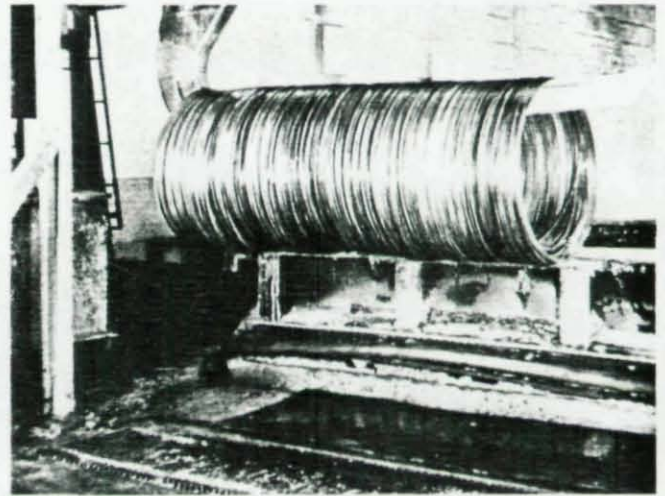
Bethlehem engineers are available to give assistance in material, specifications, and connector selection, as well as in the application of erection and handling techniques learned through many years of experience.

How We Make Bethlehem Wire Rope and Strand

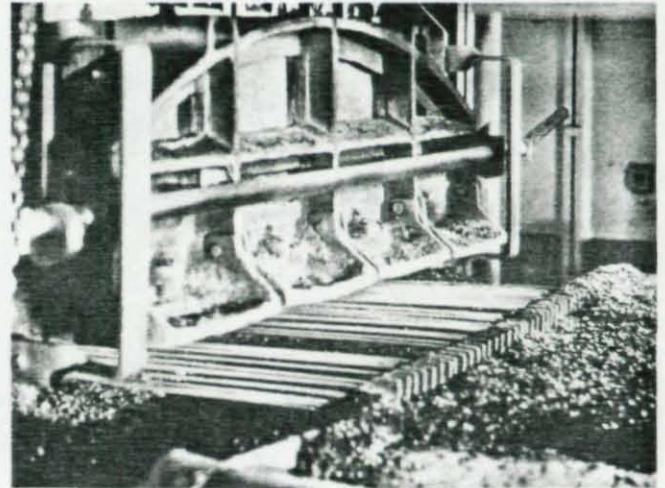
The "raw material" of wire rope and strand is rod. Steel rod is a hot-rolled product, produced in much the same way as the familiar wide-flange H-beam. The first step in the process of manufacturing wire rope and strand is inspection of the rod to insure that all quality standards—physical and chemical—are met.



After inspection, and assuming acceptance by the inspectors, the rod is cleaned. All mill scale is removed by acid-dipping; the acid is neutralized in a second bath series, which also serves to apply a lubricant beneficial to the subsequent drawing operation.

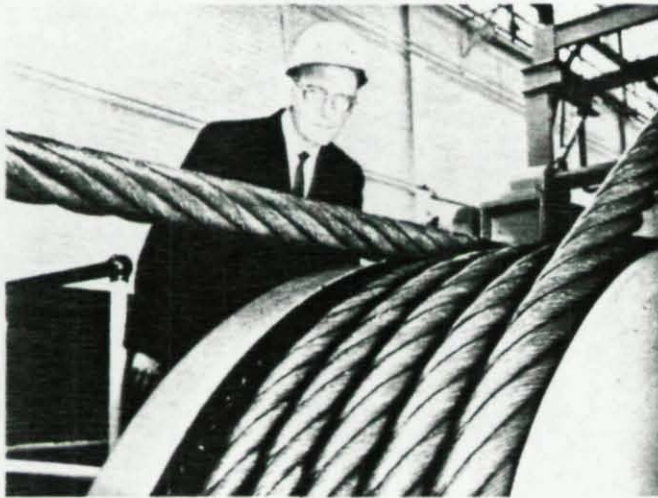


After thorough cleaning, the rod is made into wire on a multi-stage dry drawing machine. Here, the rod is pulled through successively smaller dies, each time reducing the wire in diameter while improving its mechanical properties. This drawing operation is either the final one or the prelude to additional work. After this stage, the wire will be heat-treated if it is to undergo additional drawing.



In the wire rope industry, heat-treating is known as "patenting." After being reduced to approximately 75 per cent of its original cross sectional area, the wire must be patented to enable further reduction in size. Essentially, patenting consists of passing wire through a furnace and quenching it in lead or air, depending upon the desired final results.

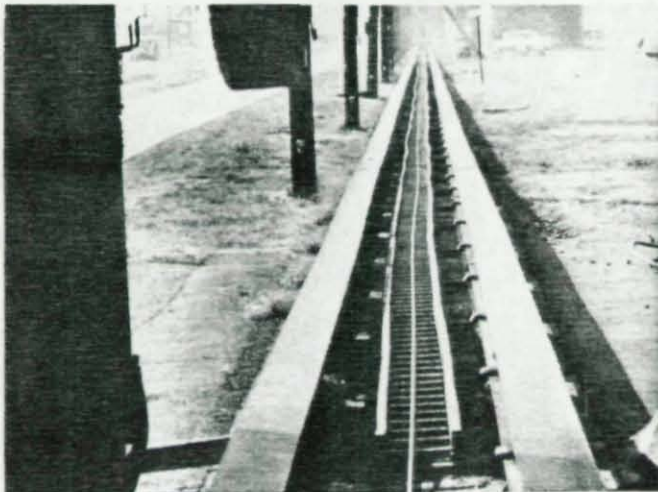
With its passage through the closing die of the closing machine, the wire rope becomes a finished product, ready for use.



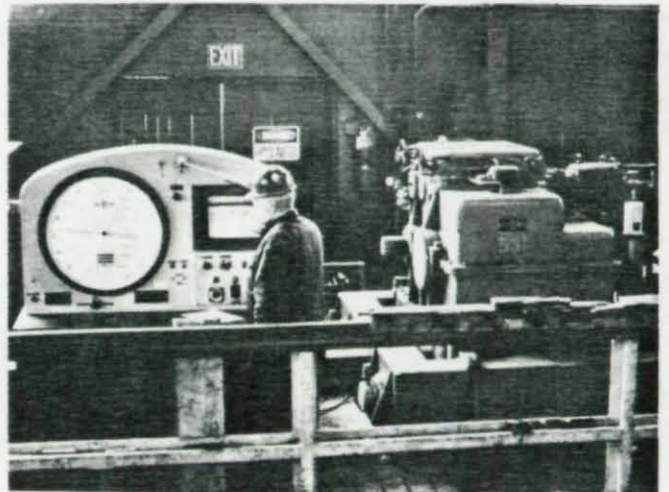
Here are some of the many end connectors used with wire rope and strand for structural applications. They have one thing in common: they are all designed to exceed the breaking strength of the rope or strand to which they will be attached. They come in many sizes, and take a wide variety of configuration. The ones shown are standard types. Frequently, a connector is designed for one specific application, although this is not the usual case. As weight reduction is important for suspended structures, the use of modern alloy steels is growing.



Prestretching is done on a 1600-ft long track. It is accomplished by anchoring the rope or strand at one end and loading at the opposite end to a certain percentage of the calculated breaking strength. This prestretching eliminates the constructional stretch that occurs during manufacture. It also increases the modulus of elasticity of the member. Also, on this machine it is possible to give cables the exact loading they will receive in the structure. The length can thus be measured very accurately, so as to insure proper sag and tension when in place on any suspended or other type of structure.



The prestretching track, looking out toward the dead end.



The "live" end of the prestretching facility, showing the tensioning machine and gage.